ISCTE IUL
Instituto Universitário de Lisboa

DEPARTMENT OF INFORMATION SCIENCE AND TECHNOLOGY

Impact of In-Band Crosstalk in an Optical Network Based on Multi-Degree CDC ROADMs

Dissertation presented in partial fulfillment of the requirements for the Master's Degree on Telecommunications and Information Science

by

Diogo Gonçalo Sequeira

Supervisors:

Dr. Luís Cancela, Assistant Professor, ISCTE-IUL

Dr. João Rebola, Assistant Professor, ISCTE-IUL

October 2017

Acknowledgements

I am thankful for having Prof. Luís Cancela and Prof. João Rebola as my supervisors in this work. Their availability and continuous support were very important throughout this work and they were fundamental to conclude this dissertation. I would also like to thank Instituto de Telecomunicações (IT) – ISCTE-IUL, for providing access to their installation and the material support.

I want to thank my family, in particular my parents, for their unconditional support and encouragement and my girlfriend, for the motivation given during these last years.

Finally, thanks to all my friends and colleagues, specially to my colleagues Bruno Pinheiro, for his help in this work, and Ruben Vales, for his companionship during these two long years.

Thank you all!

Resumo

Os nós das redes de comunicação ótica mais comuns são os multiplexadores óticos de inserção/extração reconfiguráveis (ROADMs – acrónimo anglo-saxónico de reconfigurable optical add/drop multiplexers). A arquitetura e componentes destes nós têm evoluído ao longo do tempo no sentido de se tornarem mais flexíveis e dinâmicos. Em particular, as estruturas de adição/extração destes nós, tornaram-se mais complexas e detêm novas características que oferecem as funcionalidades CDC (acrónimo anglo--saxónico de colorless, directionless e contentionless). Uma das principais limitações do nível físico das redes óticas, o crosstalk homódino, deve-se principalmente ao isolamento imperfeito dos componentes presentes dentro destes nós. Este tipo de crosstalk tem um impacto ainda mais significativo quando o sinal ótico atravessa uma cadeia de nós baseados em ROADMs.

Nesta dissertação, o impacto do crosstalk homódino, filtragem ótica e ruído ASE (acrónimo anglo-saxónico de amplified spontaneous emission) no desempenho de uma rede de comunicação ótica baseada numa cadeia de CDC ROADMs com deteção coerente e usando o formato de modulação PDM-QPSK (acrónimo anglo-saxónico de polarization-division multiplexing quadrature phase-shift keying) a um ritmo binário de 100-Gb/s é investigado através de simulação Monte-Carlo. Consideraram-se duas arquiteturas, B&S e R&S (acrónimos anglo-saxónicos para broadcast and select e route and select), e duas possíveis implementações para a estruturas de inserção/extração, os MCSs e os WSSs (acrónimos anglo-saxónicos de multicast switches e wavelengh selective switches).

A degradação do desempenho da rede ótica devido ao crosstalk homódino foi obtida através do cálculo da relação sinal-ruído ótica. Em particular, obteve-se uma penalidade de 1 dB para esta relação devido ao crosstalk homódino quando o sinal percorre uma cadeia de 19 CDC ROADMs com grau 16, uma arquitetura R&S e estruturas de inserção/extração baseadas em WSSs.

Palavras-chave: CDC ROADMs, crosstalk homódino, deteção coerente, filtragem ótica, ruído ASE, simulação de Monte-Carlo

Abstract

The most common optical networks nodes are known as reconfigurable optical add/drop multiplexers (ROADMs). The architecture and components of these nodes have evolved over the time to become more flexible and dynamic. Particularly, the wavelength add/drop structures of these nodes have become more complex and with new features such as colorless, directionless and contentionless (CDC). One of the main limitations of the optical networks physical layer, the in-band crosstalk, is mainly due to the imperfect isolation of the components inside these nodes. This crosstalk is enhanced, when an optical signal traverses a cascade of ROADM nodes.

In this work, the impact of in-band crosstalk, optical filtering and amplified spontaneous emission (ASE) noise on the performance of an optical communication network based on a cascade of CDC ROADMs with coherent detection and the modulation format quadrature phase-shift keying with polarization-division multiplexing (PDM-QPSK) at 100-Gb/s is studied through Monte-Carlo simulation. Two architectures, broadcast and select (B&S) and route and select (R&S), and two possible implementations for the add/drop structures, the multicast switches (MCSs) and the wavelength selective switches (WSSs), were considered.

The degradation of the optical communication network performance due to in-band crosstalk is assessed through the optical-signal-to-noise ratio (OSNR) calculation. In particular, an OSNR penalty of 1 dB due to in-band crosstalk is observed when the signal passes through a cascade of 19 CDC ROADMs with 16-degree, based on a R&S architecture and with add/drop structures implemented with WSSs.

Keywords: ASE noise, CDC ROADMs, coherent detection, in-band crosstalk, Monte-Carlo simulation, optical filtering

Contents

List of Figures

List of Tables

List of Acronyms

ASE	Amplified Spontaneous Emission
AWG	Arrayed-Waveguide Gratings
AWGN	Additive White Gaussian Noise
B&S	Broadcast and Select
BER	Bit Error Rate
CDC	Colorless, Directionless and Contentionless
DEC	Direct Error Counting
DSP	Digital Signal Processing
DWDM	Dense Wavelength-Division Multiplexing
EDFA	Erbium-Doped Fiber Amplifier
FEC	Forward Error Correction
GF	Galois Fields
IP	Internet Protocol
IQ	In-phase and Quadrature
ISI	Inter-Symbolic Interference
ITU	International Telecommunications Union
LCoS	Liquid Crystal on Silicon
LO	Local Oscillator
MC	Monte-Carlo
MCS	Multicast Switch
MEMS	Micro-Electro-Mechanical Systems
***M*-QAM**	*M*-ary Quadrature Amplitude Modulation
NRZ	Nonreturn-to-Zero
O/E/O	Optic-Electric-Optic conversion
OA	Optical Amplifier
OADM	Optical Add/Drop Multiplexers
OSA	Optical Spectrum Analyzer
OSNR	Optical-Signal-to-Noise Ratio
OSSM	Optical Spatial Switching Matrix
OTH	Optical Transport Hierarchy

OXC	Optical Cross-Connects
PDM	Polarization-Division Multiplexing
PSD	Power Spectrum Density
QPSK	Quadrature Phase-Shift Keying
R&S	Route and Select
ROADM	Reconfigurable Optical Add/Drop Multiplexer
SDH	Synchronous Digital Hierarchy
SONET	Synchronous Optical Network
WDM	Wavelength-Division Multiplexing
WSS	Wavelength Selective Switch

List of Symbols

B_0	–3 dB bandwidth of the optical filters
A	Blocking amplitude of stopband optical filter
$X_{M,add}$	Crosstalk generated at add section of the M^{th} ROADM
$X_{M,in}$	Crosstalk generated at inputs of the M^{th} ROADM
X_c	Crosstalk level
$I_p(t)$	Current produced by the received optical signal
$I_i(t)$	Detected signal in-phase component
$I_q(t)$	Detected signal quadrature component
$E_{in}(t)$	Electrical field incident on the photodetector
δ_{XT}	In-band crosstalk penalty
$E_{LO}(t)$	Local oscillator electric field
P_{LO}	Local oscillator power
N_e	Number of counted bits errors
N_{MC}	Number of generated sample functions
M	Number of ROADMs cascade
N_a	Number of samples per symbol
N_s	Number of simulated symbols
N_b	Number of transmitted bits
δ_F	Optical filtering penalty
R_x	Optical receiver
B_{OSA}	Optical spectrum analyzer bandwidth
R_x	Optical transmitter
$S_{o,M}$	Output optical signal of the M^{th} ROADM
R_λ	Photodetector responsivity
P_{in}	Power of the amplified signal
P_{ASE}	Power of the ASE noise
P_x	Power of the interfering signals
P_0	Power of the primary signal
N_{ASE}	PSD of ASE noise

$S_{in,f}(f)$	PSD of the filtered primary optical signal
$S_{in}(f)$	PSD of the primary optical signal
$S_{out}(f)$	PSD of the signal at the optical receiver input
$P_{in}(t)$	Received optical power
$E_r(t)$	Received signal electric field
N	ROADM degree
B_{sim}	Simulation bandwidth
$H_{Demux}(f)$	Transfer function of optical demultiplexer
$H_{Mux}(f)$	Transfer function of optical multiplexer
$H_p(f)$	Transfer function of optical passband filter
$H_b(f)$	Transfer function of optical stopband filter

Chapter 1

Introduction

The exponential growth of internet data traffic due to the increase of the number of devices (millions of connected devices are expected in the coming years), cloud services (lots of network functionalities are being put in the cloud) or video-on-demand [1], have been putting fiber optic network technologies in a continuous development in order to be able to support all the data traffic generated. Technologies, such as dense wavelength-division multiplexing (DWDM) [2], flexible grid [3], high order modulation formats [4], coherent detection and advanced digital signal processing techniques (DSP) [5] are now fundamental and mandatory to achieve the huge transport capacities required by the overall telecommunications infrastructure.

In addition to these technologies, the evolution of the optical network nodes is also very important to support this growth. In the past, these nodes were static and manual configuration was needed, nowadays, with the technology evolution, these nodes are becoming more reconfigurable [6]. This reconfigurability improves the routing and switching functionalities in the optical nodes, making them faster, dynamic and more reliable. Currently, these optical nodes are implemented with reconfigurable optical add/drop multiplexers (ROADMs).

On the other hand, the optical network physical layer limitations require a deeper study because the optical signal along its light-path, passes through optical fiber links as well as many network components inside the ROADMs, such as optical switches, (de)multiplexers or splitters/couplers. Consequently, the losses, noises and interferences accumulated along the light-path will degrade the optical signal transmission along the optical network. One of the optical network physical layer impairments that becomes enhanced along the optical signal light-path and degrades the optical network performance is the in-band crosstalk [7].

1.1 Road to Flexible Optical Networks Based on ROADMs

Fiber optics communications continue to evolve in order to support all the traffic that is being thrown to the network. Most of this traffic is, nowadays, based on the Internet Protocol (IP) which requires an optical network more flexible and dynamic [6].

The growing traffic demand leads also to the need of higher bit rates per optical channel. The well-known fixed grid, with an optical channel spacing of 50 GHz, even with sophisticated modulation schemes, no longer works for 400 Gb/s and above. Therefore, many efforts have been made to standardize a new grid, the flexible grid [3]. In this scenario, the optical channel spacing can be adjusted accordingly to the network needs, leading to optical channels with a larger space and high granularity, consequently, they are able to carry higher bit rates than with a fixed grid. Currently, the international telecommunication union (ITU) recommends a grid granularity of 6.25 GHz with a minimum frequency slot of 12.5 GHz [8], [9]. For example, we can have an optical channel with 37.5 GHz or 75 GHz instead of the most commons with 50 GHz and 100 GHz spacings. Recent studies demonstrated that a grid granularity of 6.25 GHz gives more freedom to adjust the spacing between the optical channels and avoid portions of unused spectrum [10], [11].

Consequently, given the change of traffic type and the implementation of a more flexible optical network, the ROADM nodes and all optical network components must be developed with new characteristics. In the ROADM nodes, the main changes are found in the add/drop structures, with the implementation of the colorless, directionless and contentionless features [6].

1.2 Coherent Detection and Modulation Formats

One of the techniques that leads to a great improvement of the optical networks performance is the coherent detection alongside with advanced DSP. Systems with coherent detection allow that the information carried in the optical signal can be coded in amplitude, frequency, phase and polarization, allowing the use of higher modulation formats. Furthermore, with coherent detection, polarization-division multiplexing (PDM) is typically used [12], [13]. The PDM technique allows transmitting two modulated optical signals in both signal polarizations, hence, doubling the spectral efficiency [4].

Another advantage of coherent detection is the possibility of using advanced DSP hardware at the optical receivers to compensate any linear impairments occurring during transmission [14]. Linear impairments, such as the chromatic and polarization mode dispersions, are compensated by the DSPs and this compensation is fundamental to achieve such high data rates. Some of the non-linear impairments can be also compensated with the use of DSPs [14]. On the other hand, coherent detection requires optical receiver structures more complex and expensive than in direct detection receivers.

In 2010, the optical coherent receivers were commercial available and the optical channel capacity increased to 100 Gb/s with the use of advanced modulation formats, such as the quadrature phase-shift keying (QPSK), in addition to PDM and advanced DSPs [15].

In the future, and possibly with the introduction of the flexible grid and the superchannel concept, the optical channel capacity will go to 400 Gb/s and 1 Tb/s, using higher order modulation formats than the QPSK, such as PDM-8 quadrature amplitude modulation (QAM) and PDM-16-QAM [16], [17].

1.3 In-Band Crosstalk

The crosstalk is a physical layer impairment which is mainly caused by the imperfect isolation of the optical components inside a ROADM node [7]. The imperfect isolation leads to optical signal leakages that are added to the desired (primary) signal along the light-path and lead to system performance degradation. The in-band crosstalk is worse than other types or crosstalk, such as out-of-band crosstalk, for the network performance since it cannot be removed by optical filtering at the receiver [18]. It occurs when the interfering signals have the same nominal wavelength as the desired signal, but are originated from different laser sources. In-band crosstalk can lead to a serious network performance degradation [7].

In an optical network based on ROADMs, the in-band crosstalk will accumulate over the ROADM cascade and can limit the number of nodes that the signal pass in the network [19]. In this work, our main focus is to study exhaustively the impact of in-band crosstalk generated inside of ROADMs nodes on the network performance. This study is performed by properly modeling the ROADM node, with different architectures and add/drop structures types, and the in-band crosstalk generated inside them.

In the literature, some studies were performed to address the impact of the in-band crosstalk due to cascaded ROADMs on the network performance, however with a simple ROADM model [20] or not considering the add/drop structures [21]. In this work, we model more rigorously the multi-degree colorless, directionless and contentionless (CDC) ROADMs considering the ROADM components: type of add/drop structures and respective architectures.

1.4 Dissertation Organization

This dissertation is organized as follows. In Chapter 2, we describe how we simulate the optical communication network to transmit and receive *M*-QAM signals, explaining the important aspects of this implementation and the modeling of the optical components.

The third chapter focuses on the study of the ROADMs nodes and its components. A summary about the evolution, main characteristics and architectures of the ROADMs is presented. We discuss the properties of ROADM add/drop structures, namely CDC structures. The advantages and disadvantages of ROADMs broadcast and select (B&S) and route and select (R&S) architectures are also discussed in this chapter.

In the fourth chapter, the crosstalk generated inside the ROADMs nodes is studied considering a start topology network with 4 and 5 ROADMs. The number of in-band crosstalk terms that are generated inside a multi-degree CDC ROADM is quantified.

In the fifth chapter, the performance of an optical network impaired by in-band crosstalk, optical filtering and amplified spontaneous emission (ASE) noise based on CDC ROADMs, implemented with multicast switches (MCSs) and wavelength selective switches (WSSs), is evaluated. The network simulation model is presented as well as the in-band crosstalk signals generated through the optical signal path.

Finally, the sixth chapter summarizes the main conclusions of this dissertation and provides some ideas for possible future work.

1.5 Dissertation Main Contributions

The main contributions of this work to the research topics studied are the following:

1. CDC ROADM model, for B&S and R&S architectures, that takes into account the in-band crosstalk generated inside these nodes. Two add/drop structures were considered, MCS-based and WSS-based;
2. Assessment of the impact of the in-band crosstalk, optical filtering and ASE noise in an optical network composed by multi-degree CDC ROADMs, considering QPSK signals and assuming a fixed grid.

References

[1] Cisco Systems, “Cisco Visual Networking Index: Forecast and methodology, 2016-2021,” White Paper. San Jose, CA, USA, 2016.

[2] J. Kahn and K. Ho, "Spectral efficiency limits and modulation/detection techniques for DWDM systems," in *IEEE Journal of Selected Topics in Quantum Electronics*, vol. 10, no. 2, pp. 259-272, April 2004.

[3] O. Gerstel, M. Jinno, A. Lord and S. Yoo, "Elastic optical networking: a new dawn for the optical layer?," in *IEEE Communications Magazine*, vol. 50, no. 2, pp. s12-s20, February 2012.

[4] P. Winzer, "High-Spectral-Efficiency Optical Modulation Formats," in *Journal of Lightwave Technology*, vol. 30, no. 24, pp. 3824-3835, December 2012.

[5] E. Ip, A. Lau, D. Barros, and J. Kahn, “Coherent detection in optical fiber systems,” *Optics Express*, vol. 16, no. 2, pp. 753–791, January 2008.

[6] S. Gringeri, B. Basch, V. Shukla, R. Egorov and T. Xia, "Flexible architectures for optical transport nodes and networks," in *IEEE Communications Magazine*, vol. 48, no. 7, pp. 40-50, July 2010.

[7] I. Monroy and E. Tangdiongga, *Crosstalk in WDM Communication Networks*. Norwell, MA: Springer, 2002.

[8] “Spectral Grids for WDM Applications: DWDM Frequency Grid,” ITU-T Recommendation G.694.1, 2012 [Online].
Available: https://www.itu.int/rec/T-REC-G.694.1/en.

[9] M. Jinno, "Elastic Optical Networking: Roles and Benefits in Beyond 100-Gb/s Era," in *Journal of Lightwave Technology*, vol. 35, no. 5, pp. 1116-1124, March 2017.

[10] D. Xie *et al.*, "LCoS-Based Wavelength-Selective Switch for Future Finer-Grid Elastic Optical Networks Capable of All-Optical Wavelength Conversion," in *IEEE Photonics Journal*, vol. 9, no. 2, pp. 1-12, April 2017.

[11] J. Pedro, "Designing transparent flexible-grid optical networks for maximum spectral efficiency [Invited]," in *IEEE/OSA Journal of Optical Communications and Networking*, vol. 9, no. 4, pp. C35-C44, April 2017.

[12] C. Fludger *et al.*, "Coherent Equalization and POLMUX-RZ-DQPSK for Robust 100-GE Transmission," in *Journal of Lightwave Technology*, vol. 26, no. 1, pp. 64-72, January 2008.

[13] P. Winzer, A. Gnauck, C. Doerr, M. Magarini and L. Buhl, "Spectrally Efficient Long-Haul Optical Networking Using 112-Gb/s Polarization-Multiplexed 16-QAM," in *Journal of Lightwave Technology*, vol. 28, no. 4, pp. 547-556, February 2010.
[14] J. Zhang, J. Yu and H. Chien, "Linear and Nonlinear Compensation for 8-QAM SC-400G Long-Haul Transmission System," in *Journal of Lightwave Technology*, vol. PP, no. 99, pp. 1-1, September 2017.
[15] L. Nelson *et al*., "WDM performance and multiple-path interference tolerance of a real-time 120 Gbps Pol-Mux QPSK transceiver with soft decision FEC," *2012 Optical Fiber Communication Conference and Exposition and the National Fiber Optic Engineers Conference (OFC/NFOEC)*, Los Angeles, CA, 2012, pp. 1-3, March 2012.
[16] P. Winzer, "Beyond 100G Ethernet," in *IEEE Communications Magazine*, vol. 48, no. 7, pp. 26-30, July 2010.
[17] P. Winzer, “Scaling optical fiber networks: Challenges and solutions.” *Optics and Photonics News*, vol. 26, no. 3, pp. 28-35, March 2015.
[18] P. Legg, M. Tur and I. Andonovic, "Solution paths to limit interferometric noise induced performance degradation in ASK/direct detection lightwave networks," in *Journal of Lightwave Technology*, vol. 14, no. 9, pp. 1943-1954, September 1996.
[19] S. Tibuleac and M. Filer, "Transmission Impairments in DWDM Networks With Reconfigurable Optical Add-Drop Multiplexers," in *Journal of Lightwave Technology*, vol. 28, no. 4, pp. 557-598, February 2010.
[20] M. Filer and S. Tibuleac, "Generalized weighted crosstalk for DWDM systems with cascaded wavelength-selective switches," *2012 Conference on Optical Fiber Communication and the National Fiber Optic Engineers Conference (OFC/NFOEC)*, Los Angeles, CA, pp. 1-3, March 2012.
[21] M. Filer and S. Tibuleac, "N-degree ROADM architecture comparison: Broadcast-and-select versus route-and-select in 120 Gb/s DP-QPSK transmission systems," *2014 Optical Fiber Communication Conference and Exhibitions (OFC)*, San Francisco, CA, pp. 1-3, March 2014.

Chapter 2

Simulation Model of an Optical Communication Network

2.1 Introduction

In this chapter, a generic simulation model of an optical communication network is presented, and some important aspects for its implementation using computer simulation are described.

In section 2.2, we explain with some detail the existing optical components in an optical network and how they are modeled in the Matlab software. The optical transmitter and its main characteristics are presented in subsection 2.2.1. The signal modulation formats studied in this dissertation are also presented. The power spectrum density (PSD) functions, constellations and eye diagrams obtained by simulation are shown for QPSK and 16-QAM modulation formats. Subsection 2.2.2 is reserved for presenting the optical fiber. In subsection 2.2.3, the optical coherent receiver structure is presented and explained. The optical amplifier is characterized in subsection 2.2.4.

The Monte Carlo (MC) simulator developed to assess the performance of the optical communication networks described in previous section, and implemented in Matlab, is described by a flow-chart in section 2.3.

In section 2.4, the metrics used in this work to evaluate the performance of an optical communication network using MC simulation, the direct error counting (DEC) and optical-signal-to-noise ratio (OSNR) penalty, are presented.

The conclusions of this chapter are given in section 2.5.

2.2 Generic Model of the Optical Network

In this section, a generic simulation model of an optical communication network is presented and explained, as well as four of its main components: the optical transmitter, the optical fiber, the optical coherent receiver and the optical amplifier. As in this work the focus is about the impairments in the optical nodes, we reserve chapters 3 and 4 to present all characteristics and technological evolution of the ROADMs network nodes.

Figure 2.1 depicts a generic simulation model of the optical communication network. The optical signals are generated by an optical transmitter, which will be described in subsection 2.2.1. Subsequently, the transmitted signal enters the optical network, it passes through the optical links (which are composed by the optical fiber, optical amplifiers and optical nodes) until it reaches the optical receiver. The characteristics of the optical fiber are described in subsection 2.2.2 and the model considered for the amplifiers is described in subsection 2.2.4. Along its optical path in the network, ASE noise from amplification and the interfering signals from imperfect isolation of the optical components inside the nodes are generated and added to desired (primary) signal. At the optical network output, the signal impaired by ASE noise and interfering signals reaches the optical receiver. In this work, we consider a coherent detection receiver, which will be described with detail in subsection 2.2.3. When the signal is detected in the optical receiver, the optical network performance is evaluated through the bit error rate (BER) estimation.

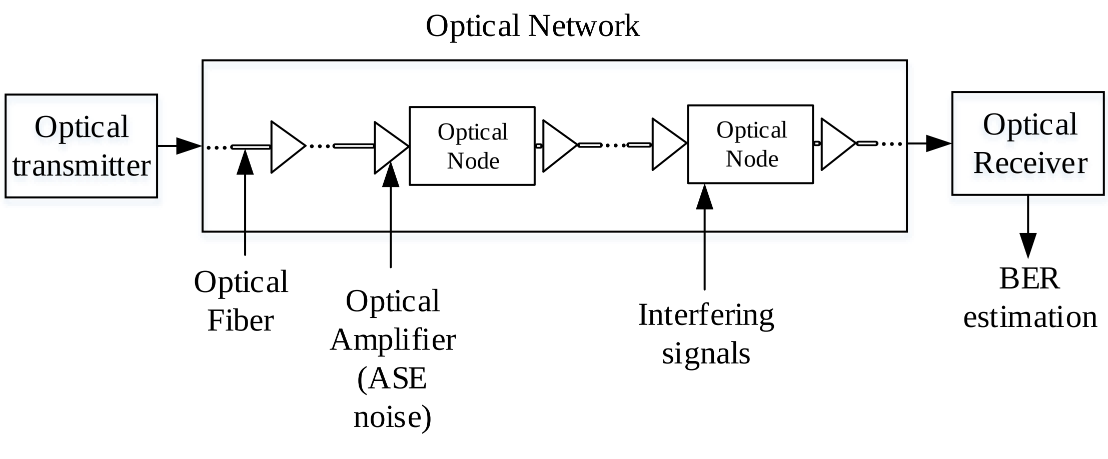

Figure 2.1 - Generic simulation model of the optical communication network.

2.2.1 Optical Transmitter

Regarding the data sequence, in computer simulations, it is important to choose a suitable symbols sequence for obtaining reliable results. Typically, pseudo-random binary sequences are used to represent the data sequence [1]. Since in this work, we simulate M-QAM signals (QPSK/4-QAM and 16-QAM), the symbols sequence was generated using Galois Fields (GF) arithmetic [1]. In our simulations, this method produces a sequence of 256 symbols for QPSK signals and of 512 symbols for 16-QAM signals. These sequences lengths are chosen to take into account accurately the effect of inter-symbolic interference (ISI) on the signal.

In Matlab software, the symbols sequences are represented by discrete vectors in the time or in the frequency domains. The time vector has N_sN_a positions, where N_s is the number of simulated symbols and N_a is the number of samples per symbol. We assume $N_a = 64$ which gives us a good definition of the sequence generated. The frequency vector, which has the same number of positions as the time vector, is obtained by computing the *Fast Fourier Transform* of the time vector.

After generating the symbols sequence, the next step performed is the mapping. The main function of the mapping is to assign amplitude levels corresponding to the in-phase and quadrature components of the input sequence of symbols. Generally, the generation of an optical signal in an optical communication network is accomplished using a laser followed by an in-phase/quadrature (IQ) modulator [2]. In this work, we assume an ideal optical transmitter. Tables 2.1 and 2.2 represent the mapping used for QPSK and 16-QAM signals, respectively, where a Gray mapping is assumed. The constellations for these modulation formats at the optical transmitter output are shown in figure 2.2. The bits represented in both figures correspond to the mapping shown in Tables 2.1 and 2.2.

Table 2.1 - QPSK mapping

Symbol	Bits	Symbol mapped
1	00	$-1-j$
2	01	$-1+j$
3	11	$1+j$
4	10	$1-j$

Table 2.2 - 16-QAM mapping

Symbol	Bits	Symbol mapped	Symbol	Bits	Symbol mapped
1	0000	$-3-3j$	9	1000	$3-3j$
2	0001	$-3-j$	10	1001	$3-j$
3	0010	$-3+3j$	11	1010	$3+3j$
4	0011	$-3+j$	12	1011	$3+j$
5	0100	$-1-3j$	13	1100	$1-3j$
6	0101	$-1-j$	14	1101	$1-j$
7	0110	$-1+3j$	15	1110	$1+3j$
8	0111	$-1+j$	16	1111	$1+j$

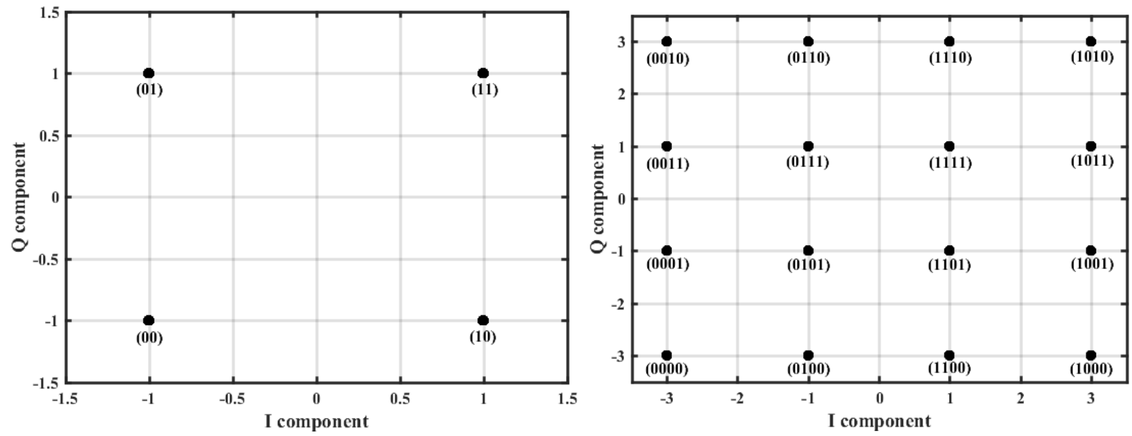

(a) **(b)**

Figure 2.2 - Constellations for (a) QPSK and (b) 16-QAM modulation formats with the respective mappings.

The focus of this work is mainly on the QPSK modulation format, since it is the most common modulation format, in links with 100-Gb/s data rates and coherent detection. Although, we also present some studies regarding the 16-QAM modulation format. For example, in chapter 5, the validation of our simulation model will be made for both modulation formats. In the following, we present the optical signals and PSDs obtained for both modulation formats, QPSK and 16-QAM, at the output of the optical transmitter.

In this work, we generate the optical signals with rectangular shape and with a bit rate of 50-Gb/s. This bit rate corresponds to a single polarization of the optical signal. Figure 2.3 shows a sequence of rectangular pulses for a nonreturn-to-zero (NRZ) QPSK signal, figure 2.3 (a), and for a NRZ 16-QAM signal, figure 2.3 (b).

Figure 2.4 depicts the PSD of a 50-Gb/s NRZ rectangular (a) QPSK and (b) 16-QAM signals. By observing this figure, for the QPSK modulation format (Figure 2.4 (a)) the bandwidth of the main lobe is 50 GHz, while for 16-QAM (Figure 2.4 (b)) is 25 GHz.

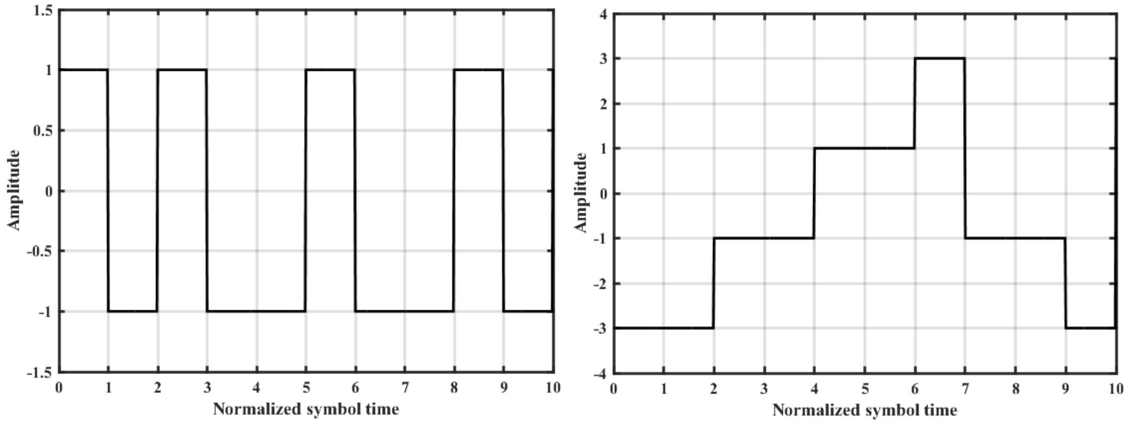

(a) **(b)**

Figure 2.3 - (a) QPSK and (b) 16-QAM signals generated with rectangular pulses.

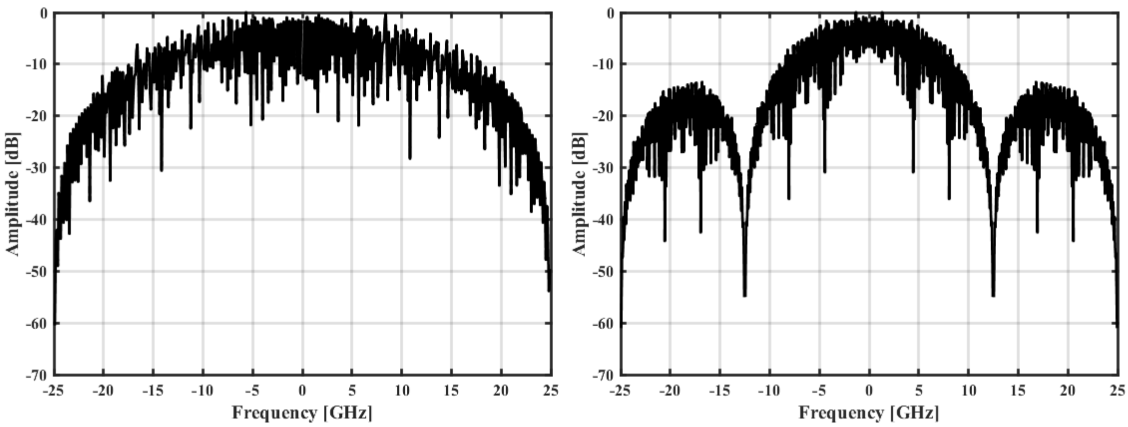

(a) **(b)**

Figure 2.4 - PSDs of a 50-Gb/s NRZ rectangular (a) QPSK and (b) 16-QAM signals.

Notice that the interfering signals, which arise along the optical network are assume as being generated by identical optical transmitters. Throughout this work, we assume always that the interfering signals have the same attributes as the transmitted signal: same modulation format, baud rate, and OSNR level, but with arbitrary different transmitted symbols, different phase and with a time misalignment between the desired signal and the interfering signal. The phase difference is modeled as a uniform distributed random variable between 0 and 2π. The time misalignment is modeled as a uniform distributed random variable between 0 and the symbol time [3].

2.2.2 Optical Fiber

Another important component of the optical network is the optical fiber. Besides other advantages, the optical fiber extremely large bandwidth and low attenuation, about 0.2 dB/km, allows very high capacity transmission with very long reach. Hence, optical fiber is the selected guided media that supports the overall telecommunications infrastructure and its increasing demand for data traffic. It is responsible for carrying the optical signal along the optical network.

However, the optical fiber introduces impairments that degrade the transmission performance: attenuation, dispersion and fiber nonlinearities [4]. The optical signal attenuation can be compensated by the optical amplification in the network. The optical dispersion, either chromatic dispersion or polarization mode dispersion, are nowadays compensated by the DSPs present in the coherent detectors [5]. The optical fiber nonlinearities occur for high launched powers at the fiber input, and its effect is reduced in presence of high accumulated dispersion along the optical network. Furthermore, the DSPs of the coherent receiver can also compensate some of the nonlinearities impact [6].

In this work, the main focus is to study the impact of the in-band crosstalk in the optical network. As other effects that impair the optical signal can mask the impact of the in-band crosstalk on the network performance, we assume an ideal fiber transmission in an optical network simulation model, and neglect the optical fiber impairments.

2.2.3 Optical Coherent Receiver

In this subsection, the model used for the optical coherent receiver is described. As we mentioned in the previous chapter, the coherent detection is nowadays the most used detection technology in long-haul networks with high capacity per optical channel (100-Gb/s and above). Figure 2.5 depicts the block diagram of the optical coherent receiver for a single polarization of the signal, as considered in this work. Since, in this work we assume that these components are ideal, the receiver performance can be assessed considering only the structure of figure 2.5 for a single polarization of the signal [7]. The coherent receiver with dual polarization consists of two polarization beam splitters connected with two structures identical to the one depicted in figure 2.5.

The structure of the optical coherent receiver is formed by a 2×4 90º hybrid followed by two balanced photodetectors. There are many possibilities for implementation of the hybrid. We have chosen the most commonly and commercially available implementation. The hybrid, shown in figure 2.5, is composed by four 3 dB couplers and a 90º phase shift in the lower branch, which allows the receiver to decode the in-phase and quadrature signal components of the received current, $I_i(t)$ and $I_q(t)$, respectively.

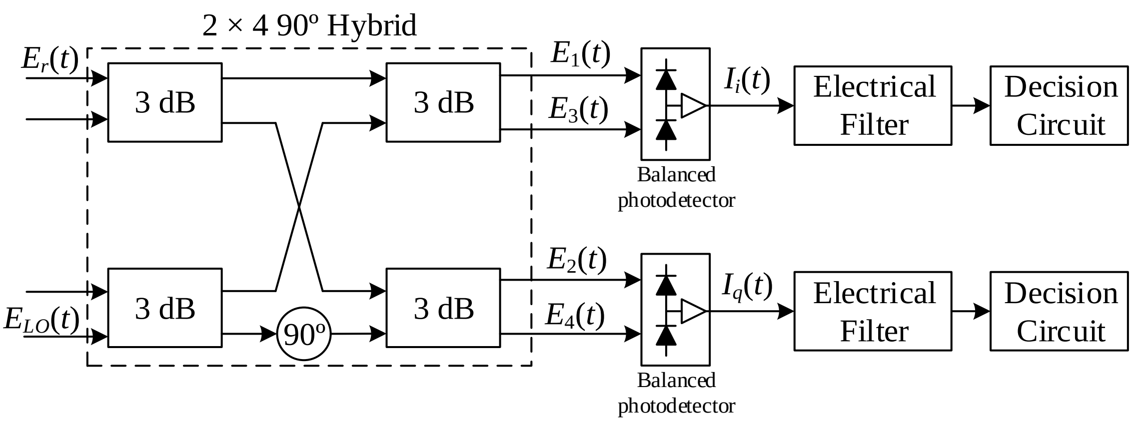

Figure 2.5 - Block diagram of the model used for the optical coherent receiver for a single polarization of the signal.

In figure 2.5 $E_r(t)$ and $E_{LO}(t)$ denote the complex envelope of received signal (at the output of the optical network) and local oscillator (LO) field. The 2×4 90º Hybrid is described by the following input/output relationship [7]

$$\begin{bmatrix} E_1(t) \\ E_2(t) \\ E_3(t) \\ E_4(t) \end{bmatrix} = \frac{1}{2} \cdot \begin{bmatrix} 1 & 1 \\ 1 & j \\ 1 & -1 \\ 1 & -j \end{bmatrix} \cdot \begin{bmatrix} E_r(t) \\ E_{LO}(t) \end{bmatrix} \tag{2.1}$$

The LO is an essential component of a coherent receiver. It allows the coherent receiver to decode the signal information in both in-phase and quadrature components. To maximize the coherent receiver performance, the LO frequency must be as close as possible to the optical carrier frequency [8]. In this work, the LO is considered synchronized with the optical carrier frequency and noises generated in this component are neglected. Hence, the LO can be defined as $E_{LO} = \sqrt{P_{LO}}$, where P_{LO} is the power of LO.

Each balanced photodetector, depicted in figure 2.5, converts the optical signal to an electrical signal. The operation of a photodetector can be described by its responsivity defined by [9]

$$R_\lambda = \frac{I_p(t)}{P_{in}(t)} \tag{2.2}$$

where $I_p(t)$ is the current produced at the output of the photodetector by the incident optical power $P_{in}(t)$ at the photodetector input. In this work, for simplification, we will consider that the photodetector responsivity is $R_\lambda = 1$ [A/W]. Hence $P_{in}(t) = |E_{in}(t)|^2$, where $E_{in}(t)$ is the electrical field incident on the photodetector.

All optical receivers have a low pass filter after the photodetection and before the decision circuit, as represented in figure 2.5, to reduce the ISI and the noise, consequently improve the OSNR [10]. Ideally, the shape of this filter must be the same of the incoming signal. Theses filters are known as matched filters [11]. In this work, we used a 5*th* order Bessel filter as the received electrical filter, which is a typical model used in several studies [12], [13]. The –3 dB bandwidth of this electrical filter is equal to the symbol rate. Figure 2.6 illustrates the eye diagrams of a received electrical signal without physical impairments for both modulation formats, QPSK and 16-QAM. As we can see by these figures, at the optical receiver, after passing through the 5*th* order Bessel electrical filter, the eye diagrams are completely open at the optimum sampling time instant.

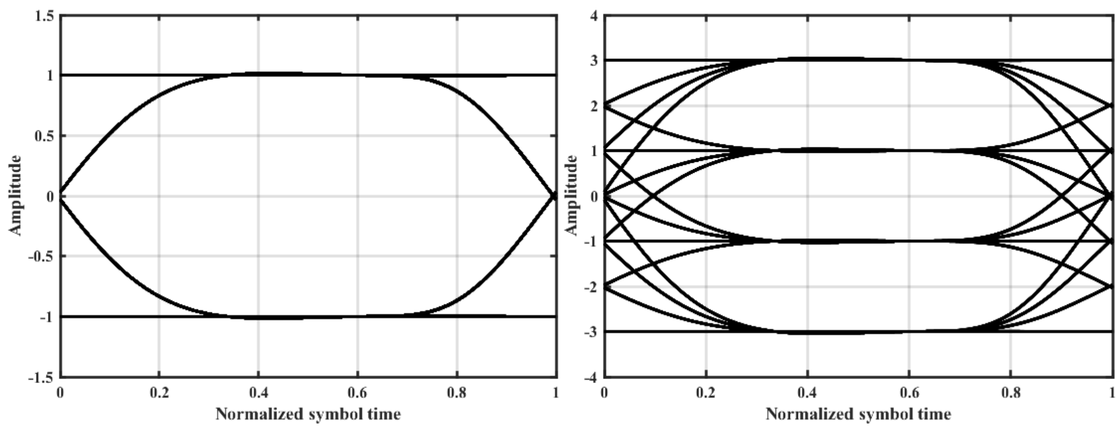

(a) **(b)**

Figure 2.6 - Eye diagrams of a received electrical signal without physical impairments for (a) QPSK and (b) 16-QAM modulation formats.

2.2.4 Optical Amplifier

In an optical network, the optical signal suffers attenuation which is introduced mainly by the optical fiber, but also by the several components that the signal passes until it reaches its destination. To compensate the path losses, in-line optical amplification is essential [9]. In addition to in-line amplification, i.e., between the optical fibers links, normally, we find optical amplifiers (OA) also at all ROADM inputs/outputs [14]. The optical amplification in the ROADMs inputs is mainly to compensate the path losses, while in the ROADMs outputs is to compensate the power losses inside the nodes.

There are three main types of OA: Erbium-Doped Fiber Amplifiers (EDFAs), semiconductor optical amplifiers and Raman Amplifiers. The most commonly used in the optical nodes and the one considered in this work is the EDFA. This type of OA can achieve a high gain, about 30 dB, and operates in the C band (1530 – 1565 nm), the band commonly used in optical communications [15].

However, optical amplification also adds ASE noise to the signal, which degrades the system performance [9]. In this work, we assume that the AOs compensate exactly the network losses, and only add ASE noise to the signal. The ASE noise power is defined by setting the OSNR, which can be defined by

$$OSNR = \frac{P_{in}}{P_{ASE}} \tag{2.3}$$

where P_{in} is the average power of the signal at the OA output, and the P_{ASE} is the average power of the ASE noise added to the signal by the OA, which is defined by

$$P_{ASE} = N_{ASE} B_{OSA} \tag{2.4}$$

where B_{OSA} is the optical spectrum analyzer (OSA) bandwidth with the typical value of 12.5 GHz and is related to the simulation bandwidth B_{sim} by [16]

$$B_{OSA} = \frac{B_{sim} N_{ASE}}{P_{ASE}} \tag{2.5}$$

In equations 2.4 and 2.5, the N_{ASE} is the PSD of the generated ASE noise. In this work, the ASE noise is considered to be an Additive White Gaussian Noise (AWGN).

2.3 Monte-Carlo Simulation Flow-Chart

In this section, we explain the MC simulation with the support of the flow-chart depicted in figure 2.7 [17]. The flow-chart represents the simulator implemented in the Matlab software to evaluate the performance of the optical communication network that will be studied in this work. The MC method is a well-known technique for statistical simulation in several scientific areas, where there is the need to describe and characterize the influence of a stochastic process in a specific system.

The flow-chart in figure 2.7 works as follow. The first iteration of the MC simulation is to save the reference signal (the transmitted signal), without the addition of any statistical sample function. With this reference signal, the receiver knows the transmitted symbols, can obtain the propagation delay of the optical network and also the optimum sampling time from the eye diagram of the received signal. From the propagation delay, we can perform exactly the synchronism between the received (impaired by any statistical effect) and transmitted signals.

On the following MC iterations, the statistical sample functions are added to the signal transmitted along the simulated optical communication network. The received signal is compared with the reference signal to check if the received signal has errors. This process is known as DEC. When a specific number of errors is achieved, the MC simulator stops and the BER is estimated.

The main cause of errors in our network simulation model will be the ASE noise and the interfering in-band signals that are generated along the optical network. The statistical sample functions generated in the simulator correspond to those two impairments. In this work, the stopping criteria is considered for a total of 1000 symbols errors in all MC iterations [17].

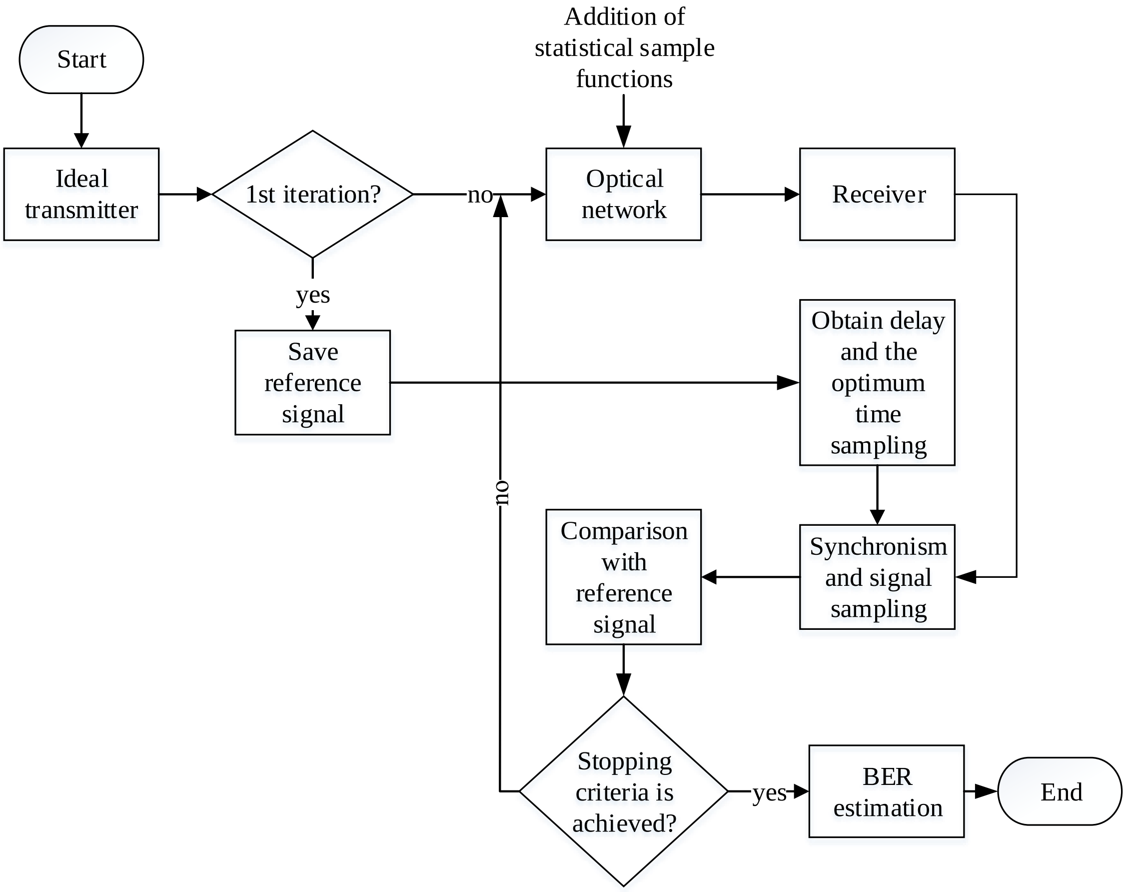

Figure 2.7 - Flow-chart of the MC simulation to obtain the BER of the optical communication network.

2.4 Performance Evaluation Methods

In this work, we use the most common metric for the performance evaluation of optical communication systems, the BER, which is estimated by DEC. The BER is essentially the ratio between the number of bits errors and the total number of transmitted bits. By assuming Gray mapping, the BER is defined by [1], [17]

$$BER = \frac{N_e}{N_{MC}N_b(log_2 M)} \tag{2.7}$$

where N_e is the number of counted bit errors, N_{MC} is the number of generated sample functions, N_b is the number of transmitted bits in one MC iteration and M is the modulation order format. In this work, we evaluate the system performance for a BER equal to 10^{-3}, because after the use of the forward error correction (FEC), the optical communication systems can achieve a lower BER, in the order of the 10^{-15} [18]. In typical optical receivers with coherent detection, FEC techniques are implemented in the DSPs.

Another metric used in this work to evaluate the performance of the optical communication systems is the OSNR penalty. It consists of measuring the required OSNR at a desired BER, of the optical network without a specific impairment and then add the desired impairment to the optical network and obtain the required OSNR with that impairment. From the difference between the required OSNRs with and without impairments, the OSNR penalty due to that physical impairment can be estimated. This technique can be applied to the several impairments in an optical network. In this study, we will evaluate the OSNR penalty at a BER of 10^{-3}, due to the in-band crosstalk, the optical filtering and the ASE noise.

2.5 Conclusions

In this chapter, a generic model of an optical communication network has been described, and the model used in Matlab software to simulate the optical network has also been presented.

We presented with more detail several optical components and their simulation model: the optical transmitter, the optical fiber, the optical coherent receiver, the optical amplifier and the respective modulation formats generated, the QPSK and 16-QAM.

Finally, the MC simulation has been explained through the use of a flow-chart, and the performance evaluation methods of the optical communication network, the BER, estimated by DEC, and the OSNR penalty have been also presented.

References

[1] M. Jeruchim, P. Balaban, and K. Shanmugan, *Simulation of Communication Systems: Modeling, Methodology, and Techniques*, 2nd ed. New York: Kluwer, 2000.
[2] G. Agrawal, *Lightwave Technology: Telecommunication Systems*. New York: Wiley, 2005.
[3] L. Cancela, D. Sequeira, B. Pinheiro, J. Rebola and J. Pires, "Analytical tools for evaluating the impact of in-band crosstalk in DP-QPSK signals," *2016 21st European Conference on Networks and Optical Communications (NOC)*, Lisbon, pp. 6-11, June 2016.
[4] A. Chraplyvy, "Limitations on lightwave communications imposed by optical-fiber nonlinearities," in *Journal of Lightwave Technology*, vol. 8, no. 10, pp. 1548-1557, October 1990.
[5] E. M. Ip and J. M. Kahn, "Fiber Impairment Compensation Using Coherent Detection and Digital Signal Processing," in *Journal of Lightwave Technology*, vol. 28, no. 4, pp. 502-519, February 2010.
[6] X. Zhou and C. Xie, *Enabling Technologies High Spectral-efficiency Coherent Optical Communication Networks*. New Jersey: John Wiley & Sons, 2016.
[7] M. Seimetz and C. Weinert, "Options, Feasibility, and Availability of 2 × 4 90º Hybrids for Coherent Optical Systems," in *Journal of Lightwave Technology*, vol. 24, no. 3, pp. 1317-1322, March 2006.
[8] L. Binh, *Digital processing: optical transmission and coherent receiving techniques*. Taylor and Francis, 2013.
[9] G. Agrawal, *Fiber-Optic Communication Systems*, 4th ed., New York: Wiley, 2010.
[10] M. Seimetz, *High-Order Modulations for Optical Fiber Transmission*, T. Rhodes, Ed. Atlanta, GA:Springer, 2009.
[11] J. Proakis and M. Salehi, *Digital Communications*, 5th ed. McGraw-Hill, 2008.
[12] S. Yao, S. Fu, H. Wang, M. Tang, P. Shum and D. Liu, "Performance comparison for NRZ, RZ, and CSRZ modulation formats in RS-DBS Nyquist WDM system," in *IEEE/OSA Journal of Optical Communications and Networking*, vol. 6, no. 4, pp. 355-361, April 2014.
[13] G. Bosco, V. Curri, A. Carena, P. Poggiolini and F. Forghieri, "On the Performance of Nyquist-WDM Terabit Superchannels Based on PM-BPSK, PM-QPSK, PM-8QAM or PM-16QAM Subcarriers," in *Journal of Lightwave Technology*, vol. 29, no. 1, pp. 53-61, January 2011.
[14] T. Zami, "Current and future flexible wavelength routing cross-connects," in *Bell Labs Technical Journal*, vol. 18, no. 3, pp. 23-38, December 2013.
[15] R. Ramaswami, K. Sivarajan, and G. Sasaki, *Optical Networks: A Practical Perspective*, 3rd ed. San Francisco, CA: Morgan Kaufmann, 2009.
[16] R. Hui and M. O'Sullivan, *Fiber Optic Measurement Techniques*. Burlington, MA: Academic, 2009
[17] B. Pinheiro, "Impact of In-Band Crosstalk on the Performance of Optical Coherent Detection Communication Systems", Dissertation presented for the Masters Degree on Telecommunications and Information Science, ISCTE-IUL, 2015.
[18] F. Chang, K. Onohara and T. Mizuochi, "Forward error correction for 100 G transport networks," in *IEEE Communications Magazine*, vol. 48, no. 3, pp. S48-S55, March 2010.

Chapter 3

ROADMs – Evolution, Characteristics, Components and Architectures

3.1 Introduction

In this chapter, we present the optical network nodes, currently known as ROADMs. In section 3.2, a summary about the ROADMs evolution is presented, since the first generation until the current generation mainly based on WSSs.

Section 3.3 presents the main ROADM characteristics.

In section 3.4, the ROADM components are presented.

Next, in section 3.5, the properties and implementation of the ROADM add/drop structures are explained.

In section 3.6 the ROADMs architectures are presented and, its advantages and disadvantages are discussed.

Finally, in section 3.7, the conclusions of this chapter are presented.

3.2 Evolution of ROADMs

When the wavelength division multiplexing (WDM) technology was introduced in the 90’s into transport networks, synchronous digital hierarchy (SDH) network and synchronous optical network (SONET), its main function was to increase the network capacity. The WDM technology was implemented in these networks, mainly in networks with ring topology, as point-to-point connections between the nodes where all the wavelengths were multiplexed/demultiplexed [1]. Consequently, in these first WDM networks, the signal transmission was done at the optical domain and the signal processing (routing and switching) was done in the electrical domain, i.e., there was O/E/O conversion of the signals in the network nodes, as depicted in figure 3.1. These networks are called opaque networks [2]. Opaque networks started having limitations in both the signal processing time and bit rate. Since then, there has been a great evolution in the type and amount of traffic handled by these networks. The traffic type changed from voice signals into data, particularly IP traffic, which demanded more flexibility and capacity in the network nodes. This high flexibility and capacity is also achieved in the optical networks by using nodes working totally in the optical domain.

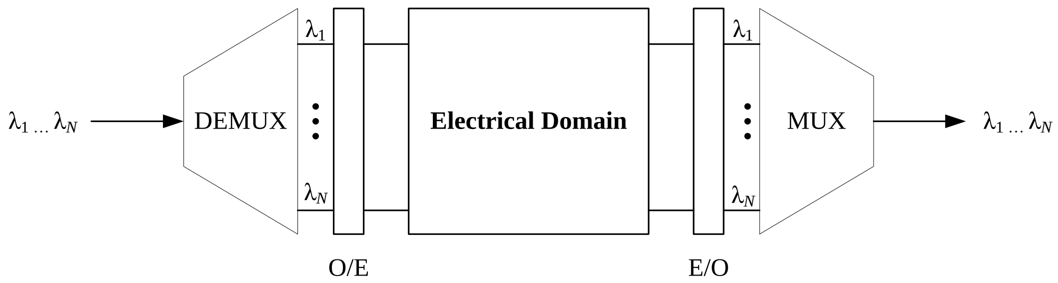

Figure 3.1 - Node of the opaque optical network with O/E/O conversion.

With the technology evolution, the term “transparent” was introduced into the optical networks. Unlike opaque networks, in transparent optical networks, the signals do not need O/E/O conversion in the network nodes in order to be switched and routed. Based on the concept of transparency, second generation WDM networks emerged. In these networks, the signal routing and switching are done in the optical domain [3], as illustrated in figure 3.2. Therefore, the pre-planning of the network became possible, i.e., to define which wavelengths to add/drop in each node, and which wavelengths go through the node – express signals [1]. With this possibility, the network nodes were named optical add/drop multiplexers (OADMs). These nodes are like the add/drop multiplexers in the SDH or SONET networks, but work in the optical domain.

The next step arises with the possibility of add/drop any wavelength in any node, to increase the network dynamism. By allowing the change of which wavelengths were added/dropped in each node in a dynamic way, brought the possibility of reconfiguring the pre-planned network. Consequently, the network nodes became reconfigurable and they are known as ROADMs.

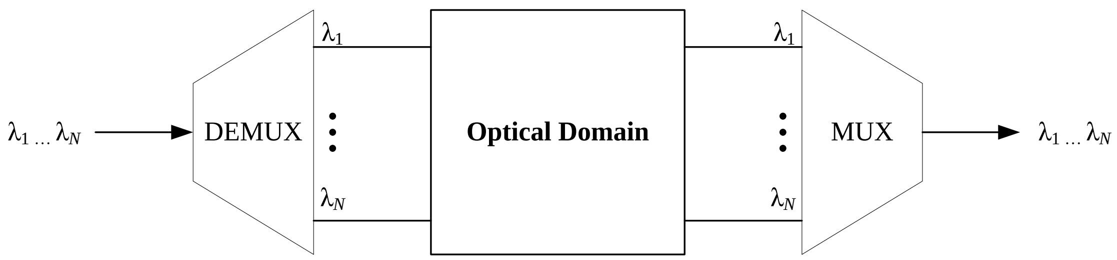

Figure 3.2 - Node of the transparent optical network without O/E/O conversion.

In the beginning of the ROADMs implementation, the ring topology was the most used in transport networks (SDH/SONET). In this topology, the nodes were only served by two pairs of optical fiber, and they were known as 2-degree ROADMs [4]. The degree of the ROADMs is associated with the number of fiber pairs that are serving the node. These degrees are also named directions. The need to establish connections between several rings to increase the network connectivity caused the increase of the number of fiber pairs serving a ROADM, leading to the ROADMs with multiple degrees, i.e., *N*-degree ROADM [4]. We can see in Figure 3.3 (a), that the central ROADM is connecting four rings and has an 8-degree. This multi-ring topology is typically used in metropolitan networks [4]. In backbone and regional networks, in order to increase the connectivity between the nodes, the common topology is the mesh topology. In this case there is a higher number of multi-degree ROADMs, as we can see in figure 3.3 (b).

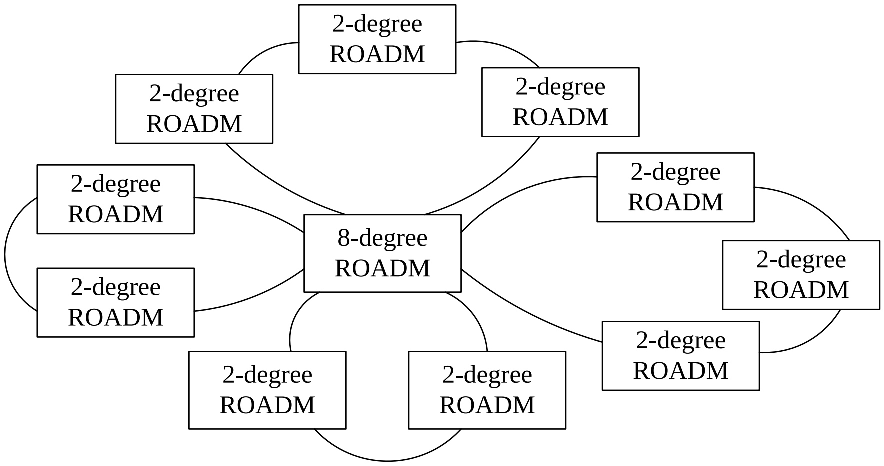

(a) Multi-ring topology

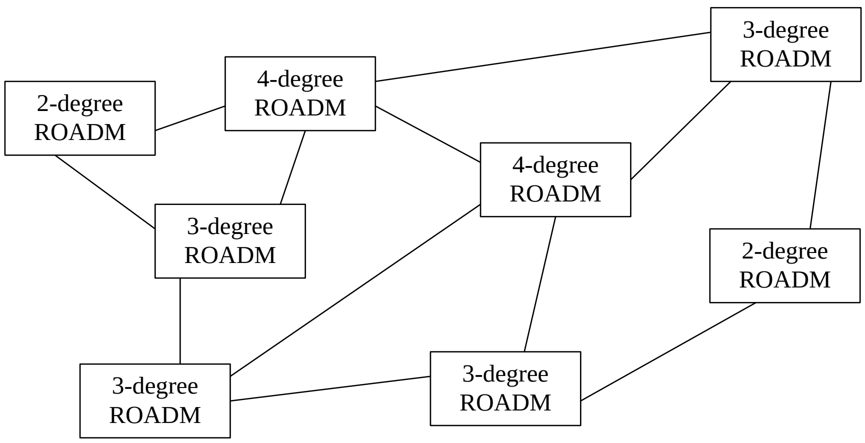

(b) Mesh topology

Figure 3.3 - Optical network with (a) multi-ring and (b) mesh topologies.

3.3 ROADM Characteristics

In this section, we will present the ROADMs main features [5]:

- Connectivity: the basic function of ROADMs is to provide connectivity between the network nodes:
  - Full-ROADM: there are no wavelengths restrictions, these ROADMs can (de)multiplex any optical signal at any wavelength;
  - Partial-ROADM: there are wavelengths restrictions, these ROADMs can process only some wavelengths.
- Cascadeability: when an optical signal passes through one ROADM it can suffer ISI from optical filtering, interference from signal leakage and corruption by noise. These impairments become larger when the number of ROADMs nodes that the signal passes increases. Consequently, these impairments limit the number of cascaded ROADMs. This feature is the main reason for metropolitan and long-haul networks being constituted by a few number of nodes. The main focus of this work is to quantify the limitation in the number of ROADMs that the optical signals can pass imposed by the physical impairments, such as the optical filtering, ASE noise and in-band crosstalk.
- Channel monitoring: the components inside the ROADMs can generate a feedback signal. This signal can be used, for example, to equalize the channel, by adjusting the channel amplitude (power) or phase.
- Scalability: ability to make the ROADM node grow, increase their degree/direction. This feature avoids bottlenecks in the networks. The optical networks with ROADMs based on WSSs have the advantage of being easily scalable than the optical cross connects (OXCs).
- Add/drop capability: one ROADM is 100% add/drop capable, if it can (de)multiplex any wavelengths arising from any direction.

The technology developments have been gradually increasing the reconfigurability and flexibility of the optical network [6]. The following features are related with the future flexible all-optical networks:

- Spectral flexibility: nowadays the WDM networks mainly utilize a standardized frequency fixed grid with channel spacing of 50 GHz. In the near future, it will be possible to adjust the frequency spacing between the channels by using the flexible grid. In order to have channels with high bit rates, the concept of superchannels was also introduced [6], [7]. In figure 3.4, we can observe the differences between the fixed and the flexible grids. A superchannel allows the inner wavelengths to be grouped closer together instead of transporting each wavelength in an individual 50 GHz channel. As we can see in figure 3.4, we can save spectrum with the use of the superchannels.

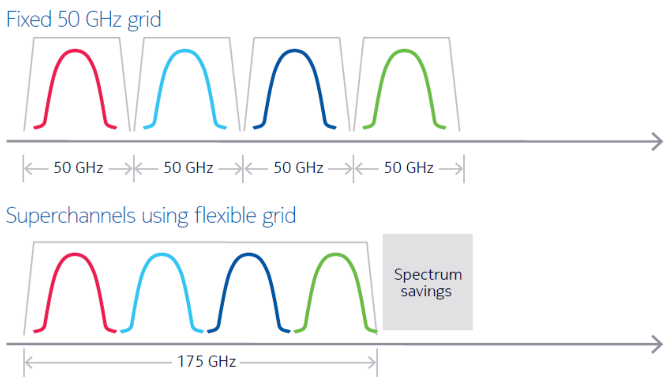

Figure 3.4 - Fixed grid with channel spacing of 50 GHz and flexible grid with superchannels and spectrum saving [7].

- Flexible transponders: these components increase the spectral efficiency. The transponders should be able to support any traffic type (e.g. Ethernet, optical transport hierarchy (OTH) and SDH/SONET), bit rate and modulation format (e.g. *M*-QAM).
- Switching speed: it is the time that a 2×2 switching element takes to change from bar state to cross state and vice versa. Figure 3.5 depicts these states, (a) bar state and (b) cross state. Nowadays, the technology most widely used to fabricate optical switches is the micro-electro-mechanical systems (MEMS) [8]. This technology has a switching speed in the order of milliseconds. Nevertheless, another technology is entering the market, the liquid crystal on silicon (LCoS) technology, which has a switching speed in the order of microseconds [9]. More flexibility and reconfigurability in optical networks require fast switching speed, since this feature directly influences the time that an optical signal goes from the input to an output port in a ROADM node, and consequently affects the network latency.

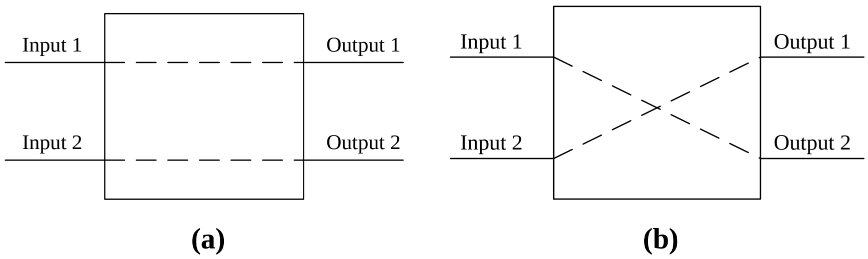

Figure 3.5 - 2×2 switching element in the (a) bar and (b) cross states.

3.4 ROADM Components

In the last years, the ROADMs components evolution has been important to support the increase of data traffic and the change of traffic type, from voice to IP traffic. In this context, we will present the ROADMs main components [5] and the technologies used to fabricate these components [8]:

- Optical splitter/coupler: 1×*N* optical splitter receives an optical signal at its input and splits the signal power equally by the *N* outputs, as shown in figure 3.6 (a). The *N*×1 optical coupler is one 1×*N* splitter used in opposite direction, as shown the figure 3.6 (b). Thus, one *N*×1 optical coupler receives *N* optical signals and joins all signals into one output. There is the possibility of an *N*×*N* optical splitter/coupler, as depicted in figure 3.6 (c). This component results from the combination of one *N*×1 optical coupler with one 1×*N* optical splitter. Thereby, we can have many inputs signals routed to many outputs.

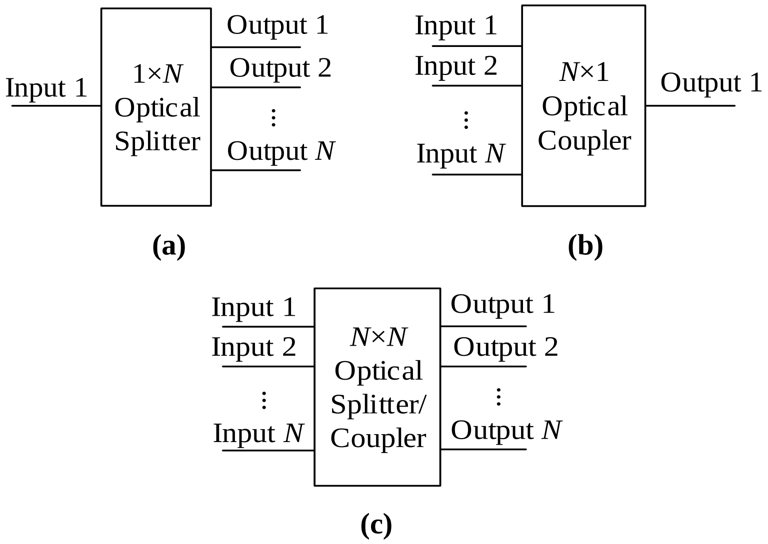

Figure 3.6 - Optical splitters and couplers: (a) 1×*N* optical splitter (b) *N*×1 optical coupler and (c) *N*×*N* optical splitter/coupler.

- Wavelength splitter/coupler: also denominated wavelength (de)multiplexer. One 1×*N* wavelength splitter is like one 1×*N* optical splitter but the split is made depending on the signal wavelength instead of the signal power. One 1×*N* wavelength splitter receives a WDM signal at the input and splits each wavelength to one specific output, as depicted the figure 3.7. The most common technology to implement this component is the array waveguide grating (AWG). The utilization of one 1×*N* wavelength splitter in the opposite direction origins one *N*×1 wavelength coupler.

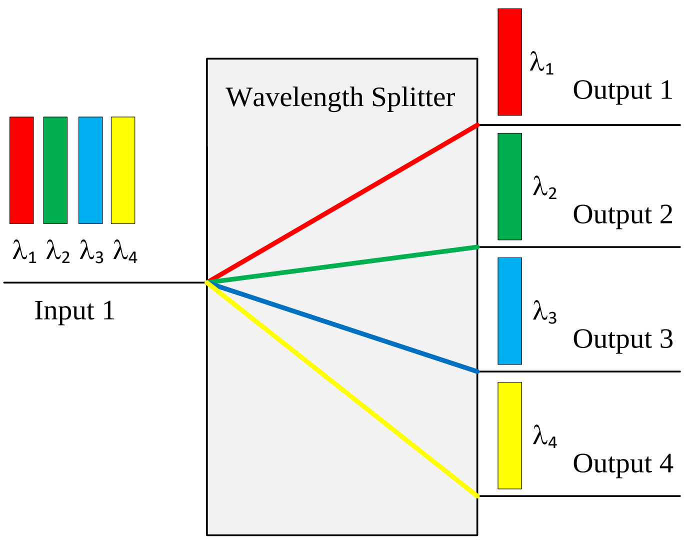

Figure 3.7 - Example of a 1×4 wavelength splitter.

- Optical switch: this is the most important component for routing and switching the signal over the network in the optical domain, i.e. without O/E/O conversion. The dimension of the switching element is 2×2, as previous illustrated in figure 3.5. These can also be used as 2×1 or 1×2 switching elements. Based on this element is possible to build *N*×*N* optical switches. As we saw in last section, nowadays the most common technology to fabricate these switches is the MEMS. This technology consists in flexible micro mirrors with very small dimensions, and some examples of MEMS technology can be found in [8], [10]. This component is responsible for the optical signal power leakages within the ROADMs, because the isolation between ports is not perfect.

- Wavelength selective switch (WSS): nowadays is the most important ROADM component. The WSS results from the combination between optical switches and wavelength (de)multiplexers. Nowadays, the technology chosen for its implementation is the LCoS [11], [12]. There are three types of WSSs:
    - 1×*N* WSS: one optical input signal with multiple wavelengths and each wavelength can be selected for the desired output. Figure 3.8 depicts an example of a 1×4 WSS implementation.
    - *N*×1 WSS: *N* optical input signals with multiple wavelengths and the desired wavelengths are selected for the output. This type of WSS is the most used in the ROADM outputs.
    - *N*×*M* WSS: *N* optical input signals with multiple wavelengths are selected for the desired *M* outputs. Normally, *N* represents the number associated with the ROADM degree and *M* is the number of connections with the add/drop ports. This type of WSSs has high manufacturing costs, but avoids wavelength contention, minimizes interferences, as reported in [13], such as the crosstalk.

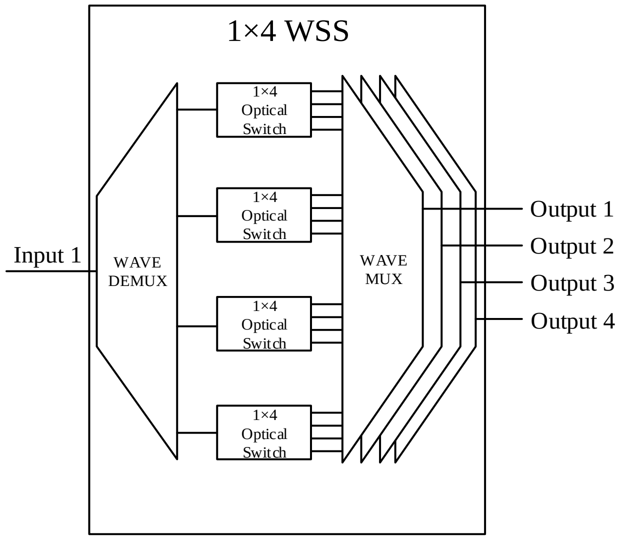

Figure 3.8 - Inside of a 1×4 WSS.

- Multicast switches (MCSs): as the *N*×*M* WSSs have high manufacturing cost, nowadays, the most common alternative is the MCSs [14]. This component is made from optical splitters/couplers and switches. Consequently, it is not as wavelength selective as the *N*×*M* WSS, this means that the optical signals are only selected once instead of twice as happens in *N*×*M* WSSs [11].

3.5 Properties of ROADM Add/Drop Structures

One of the main functions of the ROADMs nodes, besides routing the wavelengths from the inputs to the outputs, is to add and drop wavelengths. This functionality not only helps traffic monitoring by remote changes of the wavelengths that are added/dropped in the ROADM node, as well as network failures correction or simpler optical network planning [15]. The properties of ROADM add/drop structures have evolved with the technology developments and also with the need of a more flexible and dynamic optical network.

In the first generation of ROADM add/drop structures, the drop section was implemented with wavelength (de)multiplexers and the add section with optical couplers, as illustrated figure 3.9. Each add/drop port was configured only to operate at a specific wavelength, these structures were called colored [1]. For this reason, in these structures, the transponders (transmitters and receivers) were fixed, only transmitting and receiving a specific wavelength.

Note that the components A and B mentioned in the following figures are going to be discussed in section 3.6 and we consider that each fiber transports 4 wavelengths.

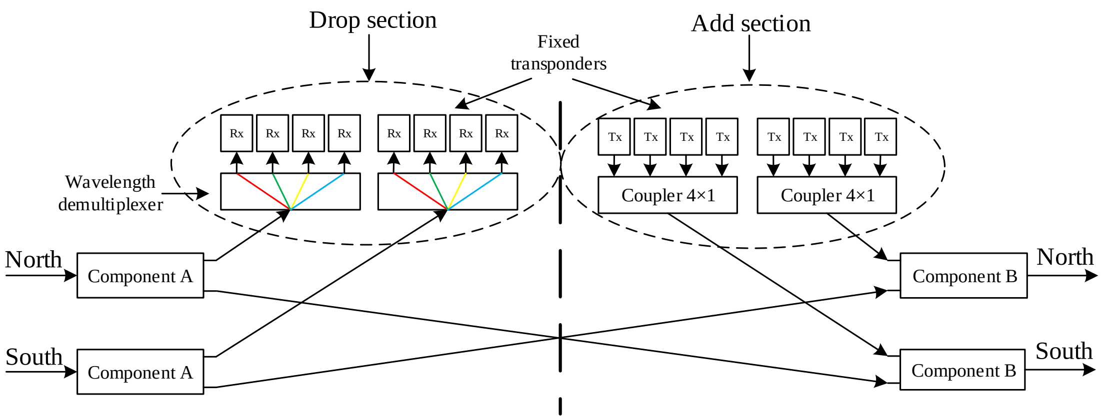

Figure 3.9 - 2-degree colored ROADM.

3.5.1 Colorless Add/Drop Structures

With the technology advances, the transponders became tunable and the first WSSs were developed. Using these two components in add/drop structures, the limitation imposed by wavelength demultiplexers and fixed transponders on colored ROADM is solved. Consequently, it became possible to add/drop any wavelength in any port of ROADM add/drop structures. The ROADMs nodes that have this property are known as colorless – C ROADMs. In this type of ROADMs, depicted in figure 3.10, the add section is implemented with tunable transponders followed by optical couplers and the drop section with 1×*N* WSSs. Note that the add section can be also implemented with WSSs, replacing the optical coupler, for example, to minimize the impact of crosstalk. But, on the other hand, WSSs have high manufacturing costs.

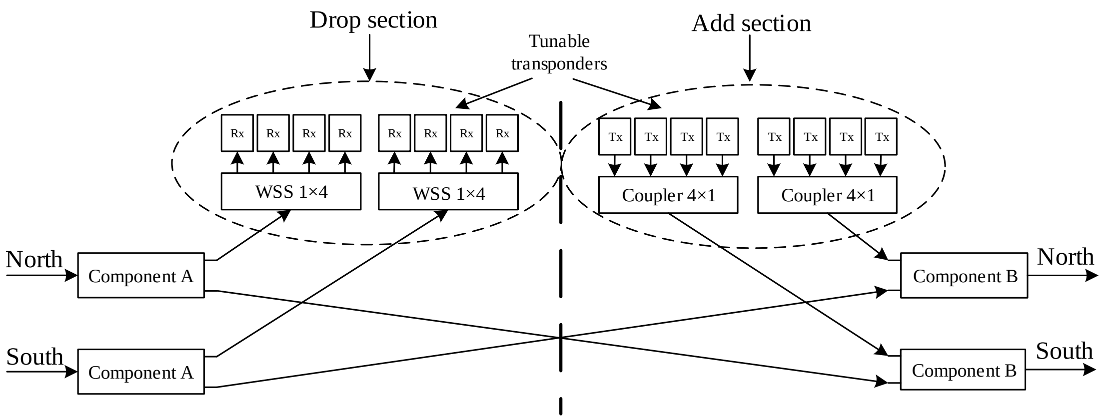

Figure 3.10 - 2-degree colorless ROADM.

3.5.2 Colorless and Directionless Add/Drop Structures

Another property of ROADM add/drop structures is the ability to redirect the input or add signals to all ROADM directions. The ROADMs with this add/drop property are called directionless – D ROADMs, and one possible implementation of these ROADMs is depicted in figure 3.11. Often in the literature this property is referred as nondirectional. The implementation of this property led to more robust components in both ROADM inputs/outputs and add/drop structures. For example, considering an 8-degree directionless ROADM (D ROADM, *N*=8), with add/drop structures in all degrees/directions: the component at each ROADM input will have a dimension of 1×15 (1×2*N*–1), and can be an optical splitter or a WSS, depending on the ROADM configuration [15]. In the add section, the component, normally, an optical coupler will have a dimension of 1×8 (1×*N*). In this example, we considered that the ROADM has add/drop structures in all directions, but there may be cases where this is not necessary. One D ROADM only needs more than one add/drop structure if there is the need to add/drop two or more optical signals with the same wavelength. The maximum number of add/drop structures is given by the ROADM degree. Thus, if we need to drop three optical signals with the same wavelength on one 3-degree ROADM with two add/drop structures, wavelength contention will arise inside the ROADM [16]. The wavelength contention also can occur, for example on the ROADM depicted in figure 3.11, when two signals with the same wavelength are dropped in the same drop structure.

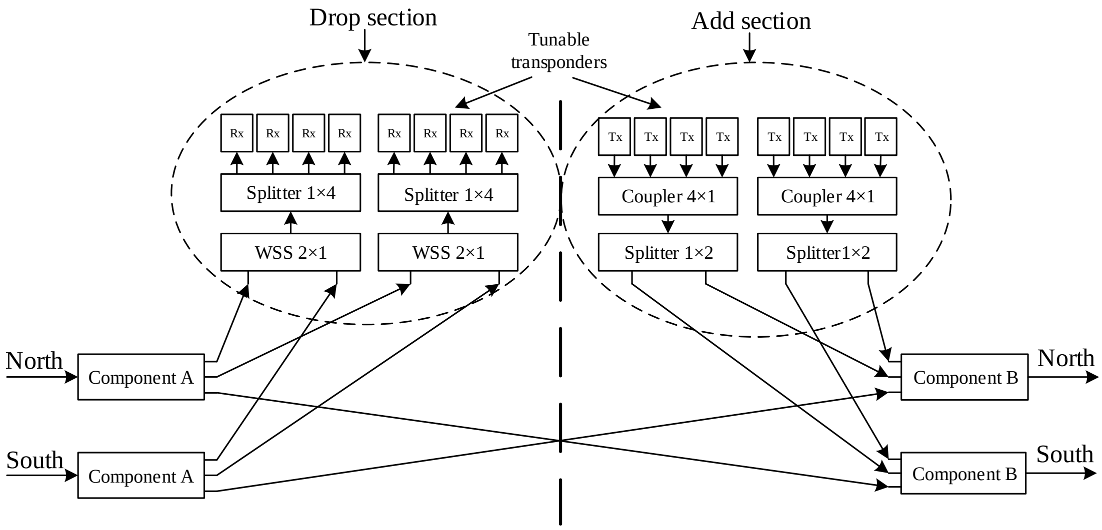

Figure 3.11 - 2-degree colorless and directionless ROADM.

3.5.3 Colorless, Directionless and Contentionless Add/Drop Structures

To avoid the wavelength contention inside the ROADMs, the add/drop structures must be contentionless. In a 100% contentionless ROADM, there are no restrictions of wavelength, the add/drop structures are able to add or drop the same wavelengths in different ports. Then a full-ROADM, defined in section 3.3, must be colorless, directionless and contentionless – CDC ROADM. At the beginning of the implementation of these ROADMs add/drop structures, an optical spatial switching matrix (OSSM) was used [17]. This implementation became limited because it is not modular, represents a single point of failure and when the ROADM degree increases, i.e., the optical network increases, the number of OSSM ports grows and becomes more difficult to control the OSSM.

Nowadays, the most common way to build the CDC ROADMs add/drop structures is with MCS [14], as depicted in figure 3.12 (a), or with $N\times M$ WSSs [18], [19], as depicted in figure 3.12 (b). As we saw in the last section, the MCSs are not as selective in wavelength as the WSSs. That is the main reason why CDC ROADMs implemented with MCSs are more vulnerable to crosstalk.

Another property of ROADMs add/drop structures, that is being implemented nowadays in ROADMs, based on the flexible grid, is the gridless property [20], [21]. The ROADMs with this property are able to adapt to traffic based on the flexible grid and add/drop, routing and switching all traffic type that reaches the node.

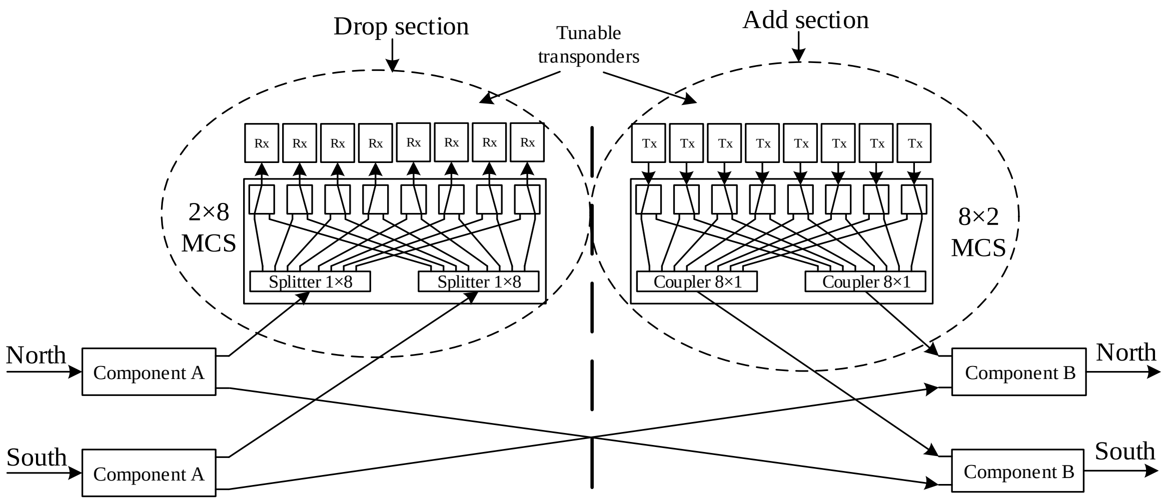

(a)

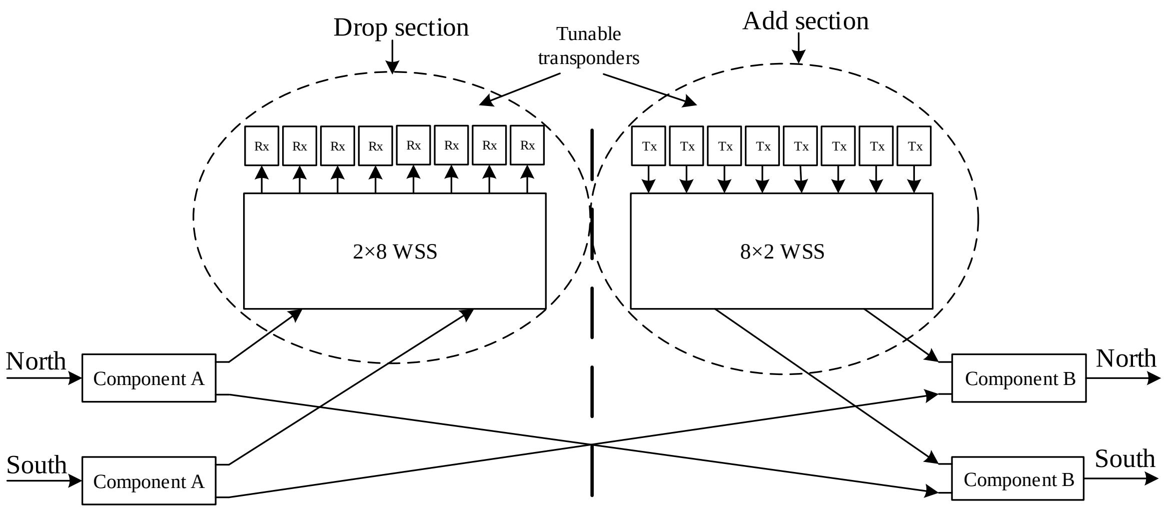

(b)

Figure 3.12 - 2-degree colorless, directionless and contentionless (CDC) ROADM implemented with (a) MCSs and (b) $N\times M$ WSS.

3.6 ROADM Architectures

The ROADM main architectures are the B&S, R&S and wavelength-selective architecture [4]. In this work, we will only focus on two of these architectures, B&S and R&S. The wavelength-selective ROADM architecture is not very scalable and has higher costs [4]. The ROADMs architectures have great influence on the components used in the ROADMs inputs and outputs, represented by components A and B in the previous figures of the section 3.5.

In the ROADMs based on a B&S architecture, at the ROADM inputs, the broadcast of the optical input signal is made to all ROADM degrees, through an optical splitter. Then, at the ROADM outputs the optical signal is selected by a WSS.

The difference in the ROADMs based on a R&S architecture, is that instead of broadcasting the optical input signal at the ROADM inputs, the optical input signal is selected by a WSS. As a result, with this architecture, we have two stages of wavelength selection, at the inputs and outputs of the ROADM. Consequently, the optical signal passes through one more filtering stage in this architecture than with a B&S architecture. Table 3.1 shows the differences between these two architectures, its advantages and disadvantages.

Table 3.1 - Difference between the components used, advantages and disadvantages of the B&S and R&S ROADMs architectures.

Architecture name	**Input component**	**Output component**	**Advantages**	**Disadvantages**
Broadcast & Select (B&S)	Optical splitter	WSS	Filtering, costs and possibility of broadcast	Impossible to make direct selection, splitting losses
Route & Select (R&S)	WSS	WSS	Low insertion losses, possibility of direct selection and reduced crosstalk	Costs and filtering

The architecture B&S is more suitable for networks where the optical signal passes several nodes [22]. As we mentioned in table 3.1, one of advantages of the B&S architecture is the filtering. As the optical signal passes through less filters than in a R&S architecture, the penalty due to a filter cascade is lower. Less impact of cascaded filtering is then an advantage of the architecture B&S and an important disadvantage of the architecture R&S.

Since, the architecture R&S is based on WSSs, the cost of R&S implementation is higher than B&S implementation. Also, due to the fact that the implementation of the R&S architecture is with WSS, the penalties due the crosstalk are smaller in this architecture. The optical signal undergoes two stages of wavelength selection, therefore the crosstalk signals that appears at the ROADM outputs have a smaller power when compared to the optical signal that undergoes only one stage of wavelength selection, as in the case of the B&S architecture.

3.7 Conclusions

In this chapter, we have studied the ROADMs evolution, its main characteristics, as well as the characteristics and evolution of the ROADM add/drop structures.

With the technology evolution, the type of traffic requires a network more flexible, dynamic and reconfigurable. Consequently, the networks went from a ring to a mesh topology with a high number of ROADMs nodes with multi-degree. Since one optical signal must go through more ROADM nodes until reach its destination, the cascadeability and scalability of ROADMs are, nowadays, important characteristics.

A full-ROADM must be a CDC ROADM. To implement these add/drop structures characteristics, the most important component is the $N\times M$ WSS. Although, this component has high cost and a high optical filtering penalty, it avoids the contention inside the add/drop structures and minimizes the crosstalk. A good alternative to this component is the MCS. With this component, the optical filtering penalty and the cost is lower, but the crosstalk penalty is higher.

Two different ROADM node architectures were described and studied, the B&S and R&S. The advantages and the disadvantages of both architectures were discussed.

References

[1] S. Gringeri, B. Basch, V. Shukla, R. Egorov and T. J. Xia, "Flexible architectures for optical transport nodes and networks," in *IEEE Communications Magazine,* vol. 48, no. 7, pp. 40-50, July 2010.
[2] B. Ramamurthy, H. Feng, D. Datta, J. Heritage and B. Mukherjee, "Transparent vs. opaque vs. translucent wavelength-routed optical networks," *1999 Optical Fiber Communication Conference and the International Conference on Integrated Optics and Optical Fiber Communication (OFC/IOOC),* San Diego, CA, USA, vol. 1, pp. 59-61, February 1999.
[3] A. Nag and M. Tornatore, "Transparent optical network design with mixed line rates," *2008 2nd International Symposium on Advanced Networks and Telecommunication Systems*, Mumbai, pp. 1-3, December 2008.
[4] J. Simmons, *Optical Network Design and Planning*, Springer, 2ª ed., 2014.
[5] S. Woodward *et al.* "ROADM-Node Architectures for Reconfigurable Photonic Networks", *Optical Fiber Telecommunications VIB*, I. Kaminov, T. Li, and A. Willner, eds., Academic Press, 2013.
[6] O. Gerstel, M. Jinno, A. Lord and S. J. B. Yoo, "Elastic optical networking: a new dawn for the optical layer?," in *IEEE Communications Magazine*, vol. 50, no. 2, pp. s12-s20, February 2012.
[7] Nokia, "Maximize networks capacity with Nokia super coherent technologies", 2016 Available: https://resources.ext.nokia.com/asset/195753.
[8] G. Papadimitriou, C. Papazoglou and A. Pomportsis, "Optical switching: switch fabrics, techniques, and architectures," in *Journal of Lightwave Technology,* vol. 21, no. 2, pp. 384-405, February 2003.
[9] G. Baxter *et al*., "Highly programmable wavelength selective switch based on liquid crystal on silicon switching elements," *2006 Optical Fiber Communication Conference and the National Fiber Optic Engineers Conference (OFC/NFOEC),* pp. 1-3, March 2006.
[10] S. Han, T. Seok, N. Quack, B. Yoo and M. Wu, "Monolithic 50×50 MEMS silicon photonic switches with microsecond response time," *2014 Optical Fiber Communication Conference and Exhibition (OFC),* San Francisco, CA, pp. 1-3, March 2014.
[11] N. Fontaine, R. Ryf and D. Neilson, "N×M wavelength selective crossconnect with flexible passbands," *2012 Optical Fiber Communication Conference and the National Fiber Optic Engineers Conference (OFC/NFOEC),* Los Angeles, CA, pp. 1-3, March 2012
[12] H. Yang, B. Robertson, P. Wilkinson and D. Chu, "Low-cost CDC ROADM architecture based on stacked wavelength selective switches," in *IEEE/OSA Journal of Optical Communications and Networking*, vol. 9, no. 5, pp. 375-384, May 2017. [14] S.
[13] Tibuleac and M. Filer, "Transmission Impairments in DWDM Networks With Reconfigurable Optical Add-Drop Multiplexers," in *Journal of Lightwave Technology*, vol. 28, no. 4, pp. 557-598, February 2010.
[14] T. Zami, "High degree optical cross-connect based on multicast switch," *2014 Optical Fiber Communication Conference and Exhibition (OFC),* San Francisco, CA, pp. 1-3, March 2014.
[15] B. C. Collings, "Advanced ROADM technologies and architectures," *2015 Optical Fiber Communications Conference and Exhibition (OFC),* Los Angeles, CA, pp. 1-3, March 2015.

[16] M. Feuer, S. Woodward, P. Palacharla, X. Wang, I. Kim and D. Bihon, "Intra-Node Contention in Dynamic Photonic Networks," in *Journal of Lightwave Technology*, vol. 29, no. 4, pp. 529-535, February 2011.
[17] T. Zami, "Current and future flexible wavelength routing cross-connects," in *Bell Labs Technical Journal*, vol. 18, no. 3, pp. 23-38, December 2013.
[18] R. Shankar *et al.* "Multi-degree ROADM based on wavelength selective switches: Architectures and scalability." *Optics Communications*, vol. 279 no.1, pp. 94-100, November 2007.
[19] L. Zong, H. Zhao, Z. Feng and Y. Yan, "Low-cost, degree-expandable and contention-free ROADM architecture based on M×N WSS," *2016 Optical Fiber Communications Conference and Exhibition (OFC)*, Anaheim, CA, pp. 1-3, March 2016.
[20] M. Feuer and S. Woodward, "Advanced ROADM networks," *2012 Conference on Optical Fiber Communication and the National Fiber Optic Engineers Conference (OFC/NFOEC)*, Los Angeles, CA, pp. 1-3, March 2012
[21] W. Wei, C. Wang and J. Yu, "Cognitive optical networks: key drivers, enabling techniques, and adaptive bandwidth services," in *IEEE Communications Magazine*, vol. 50, no. 1, pp. 106-113, January 2012.
[22] A. Boskovic, M. Sharma, N. Antoniades and M. Lee, "Broadcast and select OADM nodes application and performance trade-offs," *2002 Optical Fiber Communication Conference and Exhibit (OFC)*, pp. 158-159, March 2002.

Chapter 4

In-Band Crosstalk Generated Inside Multi-Degree ROADMs

4.1 Introduction

In this chapter, the in-band crosstalk generated inside multi-degree ROADMs is analyzed. Firstly, in section 4.2, we describe the different crosstalk types and how they occur in an optical network with CDC ROADM based nodes.

In section 4.3, we investigate the in-band crosstalk generated inside a 3-degree C, CD and CDC ROADMs based on two architectures, B&S and R&S.

Thereafter, in section 4.4, we will increase the ROADM degree in order to understand the impact of the in-band crosstalk in a 4-degree C, CD and CDC ROADMs.

Section 4.5 resumes the number of in-band crosstalk terms generated inside multi-degree C, CD and CDC ROADMs.

Lastly, in section 4.6, the conclusions of this chapter are provided.

4.2 Crosstalk in an Optical Network Based on ROADM Nodes

The optical crosstalk is a physical layer impairment of optical networks [1], such as the optical fiber linear and nonlinear effects. In optical networks, the cause of these crosstalk signals is mainly due to the finite isolation of optical components inside the ROADMs nodes [1], [2]. The imperfect isolation of these components, such as the optical switches, originates signal power leakages that accumulates through the optical network and causes optical signal degradation at the optical receiver.

There are two types of crosstalk signals: in-band and out-of-band [1]. The out-of-band or heterodyne crosstalk in optical networks appears when the interfering signals have different wavelengths than the selected signal. This type of crosstalk is not very harmful because it can be removed at the receiver by proper filtering.

The in-band or homodyne crosstalk occurs when the interfering signals have a similar or equal wavelength than the selected (primary) signal and it is originated from a different source than the one that originates the selected signal. In-band crosstalk originates interference that cannot be removed at the receiver, and this interference accumulates along the signal path while the optical signal passes through multiple ROADMs nodes [1]. This type of crosstalk is one of the responsible for the optical signal degradation.

In figure 4.1, it is illustrated how these two types of crosstalk are generated inside a ROADM node. At the ROADM input, we have four optical signals with wavelengths λ_1, λ_2, λ_3 and λ_4. These input signals pass through component A, which can be an optical splitter or a WSS depending on the architecture used [3], [4]. The optical signals with wavelengths λ_1 and λ_2 are dropped in the drop section and a new signal with wavelength λ_1 is added in the add section, situation normally known as wavelength reuse [3]. The optical signals with wavelengths λ_3 and λ_4 are express signals. At the ROADM output, the optical signals pass through component B, usually a WSS [4]. Therefore, in the example depicted in figure 4.1, regarding the crosstalk generation, at the ROADM output, the optical signal at λ_1 is impaired by one in-band crosstalk signal and one out-of-band crosstalk signal with wavelength λ_2. At the drop section, two out-of-band crosstalk signals appear, with wavelengths λ_3 and λ_4. All these crosstalk signals appear due to imperfect isolation of the components A, B and the components in the add/drop sections.

The ROADMs components are determined by the characteristics of the add/drop ports and by the architecture used [4]. In this chapter, we investigate the impact of in-band crosstalk in multi-degree C, CD and CDC ROADMs based on the architectures B&S and R&S. For this study, is important to understand the concept of first and second order in-band crosstalk. Therefore, when an optical signal beats the isolation of one optical component (e.g. WSS), the in-band crosstalk is of first order. When it beats the isolation of two optical components, it is known as second order in-band crosstalk [5]. In the following figures, the second order in-band crosstalk signals are identified with the number 2. We do not consider crosstalk signals with higher order than 2.

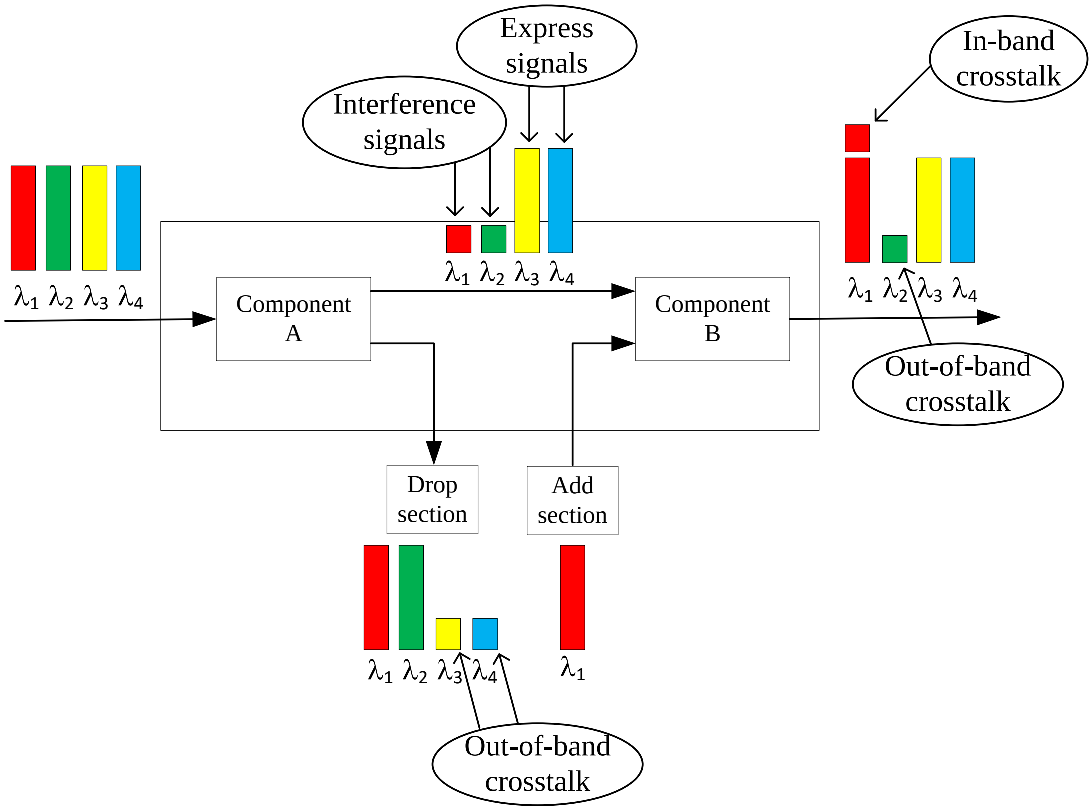

Figure 4.1 - Generation of both types of crosstalk, in-band and out-of-band, inside of ROADMs nodes.

4.3 In-Band Crosstalk Generated Inside a 3-Degree ROADM

In this section, we investigate the number of in-band crosstalk signals that will arise in a 3-degree ROADM, implemented with B&S and R&S architectures with different add/drop ports characteristics, as was done in [6] for the B&S architecture. The network topology used for this study is a four-node star network with wavelength assignment that allows a full-mesh logical topology [7] and that is depicted in figure 4.2. Note that, for the wavelength assignment is not used any specific routing and wavelength assignment algorithm, thus, the node 2 uses the same red wavelength λ_1 to communicate with other nodes. All optical signals inputs in node 2 with wavelength λ_1, are dropped and new optical signals with wavelength λ_1 are added and directed to the node outputs. Therefore, this situation is considered as the worst case in terms of crosstalk generation, because we reuse in all directions the wavelength λ_1. In this worst-case scenario, the ROADM in node 2 should have add/drop structures in all directions because all structures must be able to add/drop the same wavelength λ_1. The other optical signals, with wavelengths λ_2, λ_3 and λ_4, are considered express signals.

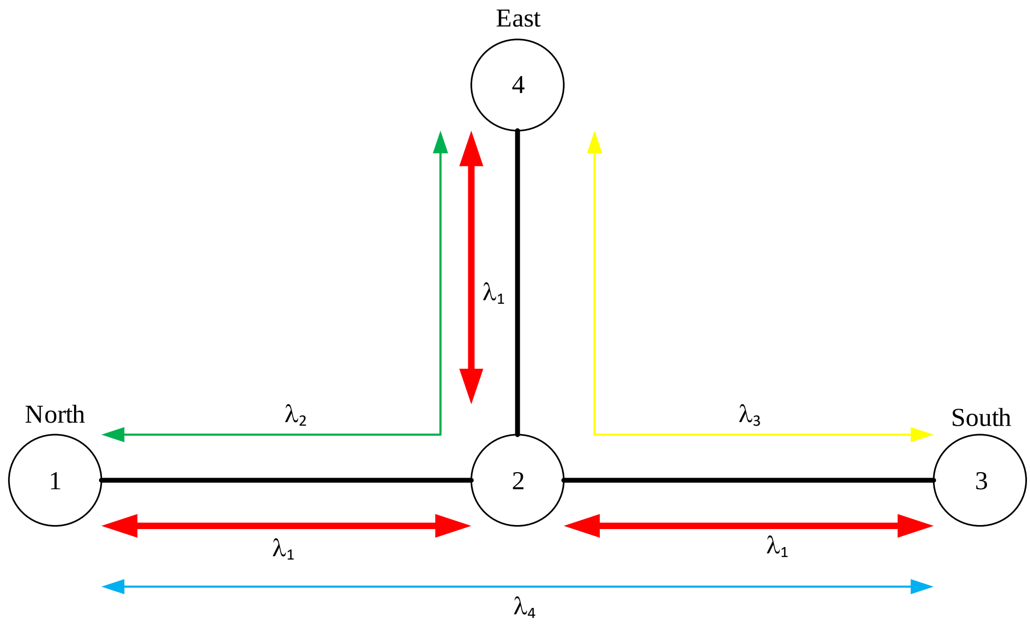

Figure 4.2 - Four-node star network with a full-mesh logical topology [6].

First, we analyze the impact of in-band crosstalk considering a 3-degree C ROADM. The structure of this ROADM is shown in figures 4.3 (a) implemented with an architecture B&S and in figure 4.3 (b) with an architecture R&S.

As we can see in both figures 4.3 (a) and (b), the number of in-band crosstalk terms that arises is the same. The difference is that, when the ROADM node is implemented with a B&S architecture, the in-band crosstalk terms are all of first order. While, with a R&S architecture, the terms at the ROADM output are second order terms (identified with number 2). In this case, at each ROADM output, the optical signal with wavelength λ_1 is impaired by two terms of in-band crosstalk, each derived from the others ROADM inputs where the signals with wavelength λ_1 come from. At each drop port, the dropped optical signal with wavelength λ_1 is not impaired by any in-band crosstalk terms.

In the following, we add the property directionless to the add/drop structures of the ROADM in node 2, thus becoming a 3-degree CD ROADM. We will analyze the impact of in-band crosstalk in this case.

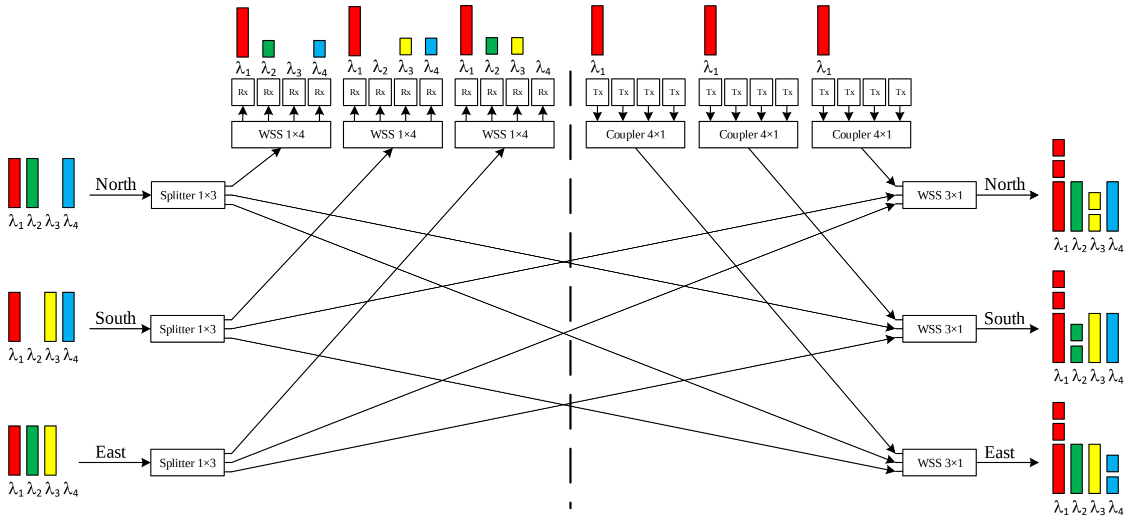

(a) Broadcast & Select

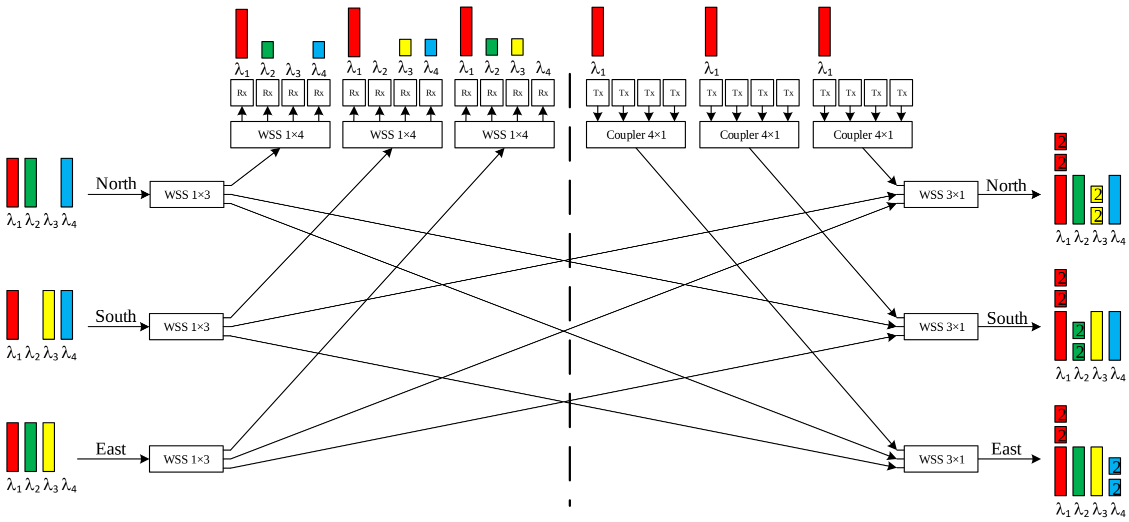

(b) Route & Select

Figure 4.3 - A 3-degree C ROADM implementation based on a (a) B&S and (b) R&S architecture with the crosstalk generation inside this structure.

Figure 4.4 depicts the structure of a 3-degree CD ROADM with an architecture B&S, in figure 4.4 (a), and with an architecture R&S, in figure 4.4 (b). With the B&S architecture, the signal with wavelength λ_1, at each ROADM output, is impaired by four first order in-band crosstalk terms. Two of these terms, are originated from the other two ROADM inputs where the wavelength λ_1 is present. The optical signals enter the ROADM, pass through an optical splitter and then, at the ROADM outputs, are selected by a WSS, just one wavelength selective stage. The others two in-band terms arise when the optical signals with wavelength λ_1 are added in the different add ports. Since the

ROADM is directionless, when an optical signal is added, the optical splitter directs it to all ROADM outputs.

This is a worst case in terms of in-band crosstalk generation, since we have an add/drop structure connected to each ROADM degree/direction. As we can see in figure 4.4, there is one in-band crosstalk term for each add signal with the wavelength λ_1 at each ROADM output. Therefore, with more add structures, the impact of in-band crosstalk at the ROADMs outputs is higher. Regarding the drop section, we can also observe in figure 4.4, that two in-band crosstalk terms with wavelength λ_1 appear at the drop sections outputs. These are generated from inputs signals with wavelength λ_1 that are directed to the other ROADM drop structures.

The improvement of using an architecture R&S, illustrated in figure 4.4 (b), is that we have two first order in-band crosstalk terms and two second order instead of four first order in-band crosstalk terms at each ROADM output. This is because the optical input signals undergo two wavelength selective stages, at the WSSs at the ROADM inputs and outputs.

In the drop section, either with a R&S or a B&S architecture, we will find only first order in-band crosstalk terms. To minimize this, we can replace the optical splitter by another WSS.

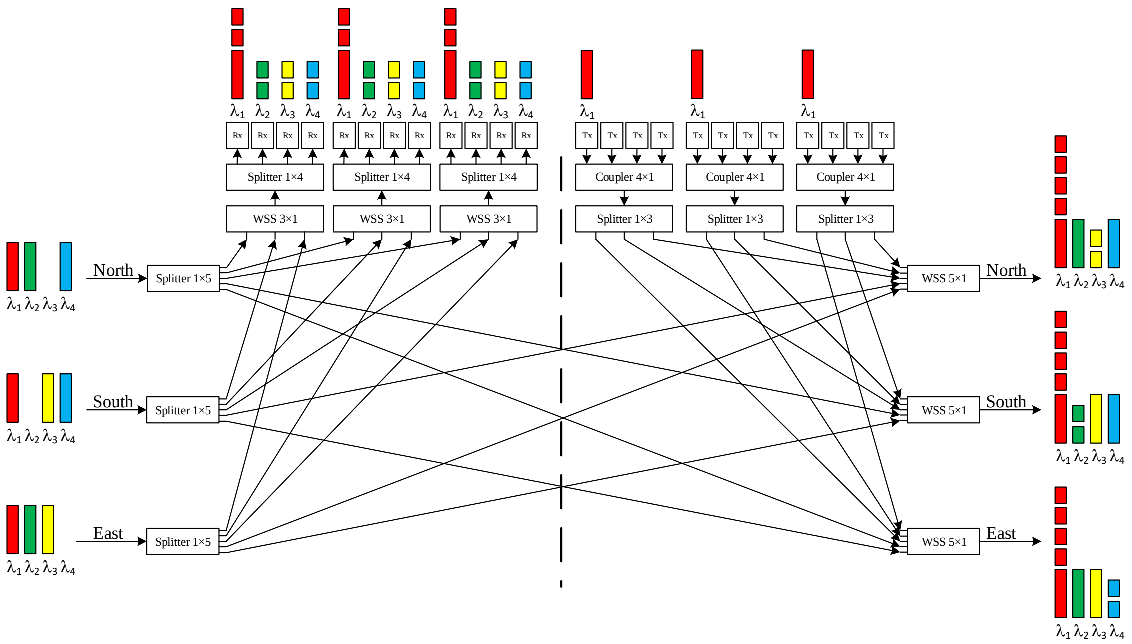

(a) Broadcast & Select

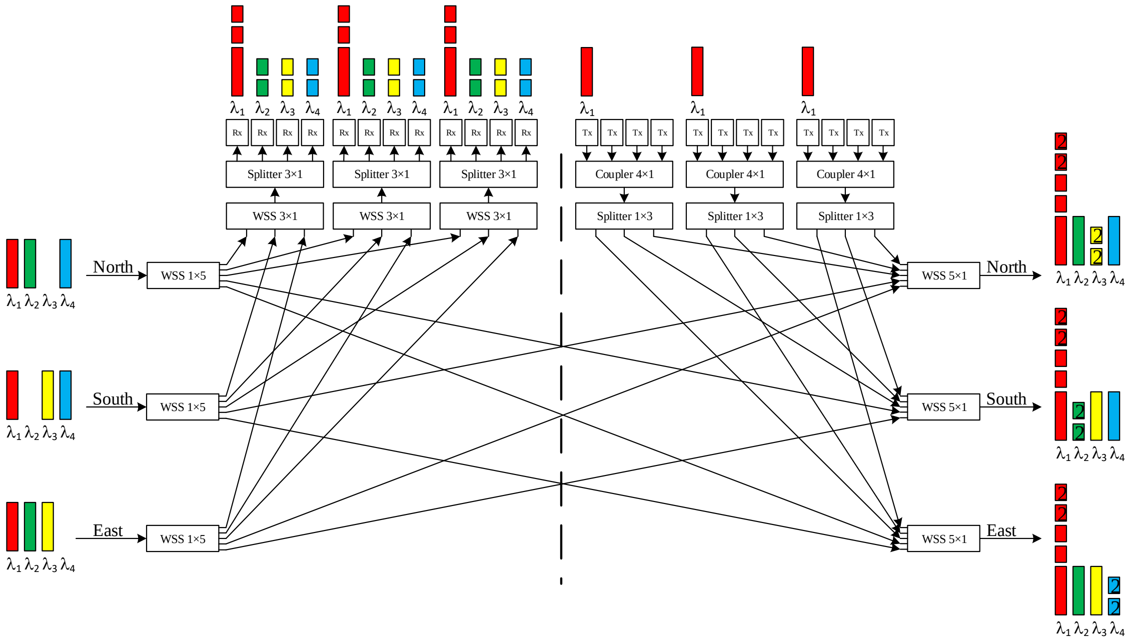

(b) Route & Select

Figure 4.4 - A 3-degree CD ROADM based on a (a) B&S and (b) R&S architecture with the crosstalk generation inside this structure.

Finally, we will study the impact of in-band crosstalk in a 3-degree CDC ROADM first with the add/drop structures implemented with MCS [8] and then with WSSs [9]. Both components are dimensioned to be 100% contentionless, i.e. the dimension of these will be $N \times M$, where N represents the ROADM degree and $M = N \times W$ where W is the number of wavelengths carried per fiber [10], [11]. In this case study, we have a 3-degree CDC ROADM and each fiber transport 4 wavelengths. Consequently, the dimension of a 100% contentionless MCS and WSS is 3×12 in the drop section and the inverse (12×3) in the add section. Note that, in a realistic scenario each fiber can carry 96 wavelengths and the ROADMs can be up to 16 degree, consequently the dimension of a MCS or a $N \times M$ WSS 100% contentionless is very large (16×96). However, many studies have shown that a contentionless percentage (also known as add/drop ratio) smaller than 100% is sufficient for a good network performance [12], [13]. For example, in [12], a typical scenario with 20% add/drop ratio is referred.

Figure 4.5 illustrates the structure of a 3-degree CDC ROADM implemented with MCSs. By comparing this implementation with the 3-degree CD ROADM, depicted in figure 4.4, we observe that the number of in-band crosstalk terms that arise at each ROADM output and drop port is the same. There is no difference between these implementations, in terms of in-band crosstalk.

Figure 4.6 depicts a 3-degree CDC ROADM implemented with WSS and based on a (a) B&S and (b) R&S architecture. In these type of ROADMs based on a B&S architecture, in the drop ports, the wavelength λ_1 is impaired by two second order in-band terms. In each ROADM output, four in-band crosstalk signals will appear, two of these are second order terms derived from the add section, and the other two are first order interferers, coming from the other ROADM directions.

To minimize the impact of in-band crosstalk, the use of $N \times M$ WSS in the add/drop structures and an architecture R&S is the right choice. In figure 4.6 (b), we can observe an implementation of this type of CDC ROADMs. In this ROADM implementation, all in-band crosstalk terms in the drop section and in the outputs are second order terms. In this specific case, as we can see in figure 4.6 and as previously mentioned, for an add/drop structure 100% contentionless, the WSSs dimension in the add/drop sections are 12×3 and 3×12, respectively. Nowadays, $N \times M$ WSSs with $N \times M \leq 36$ are commercially available [14].

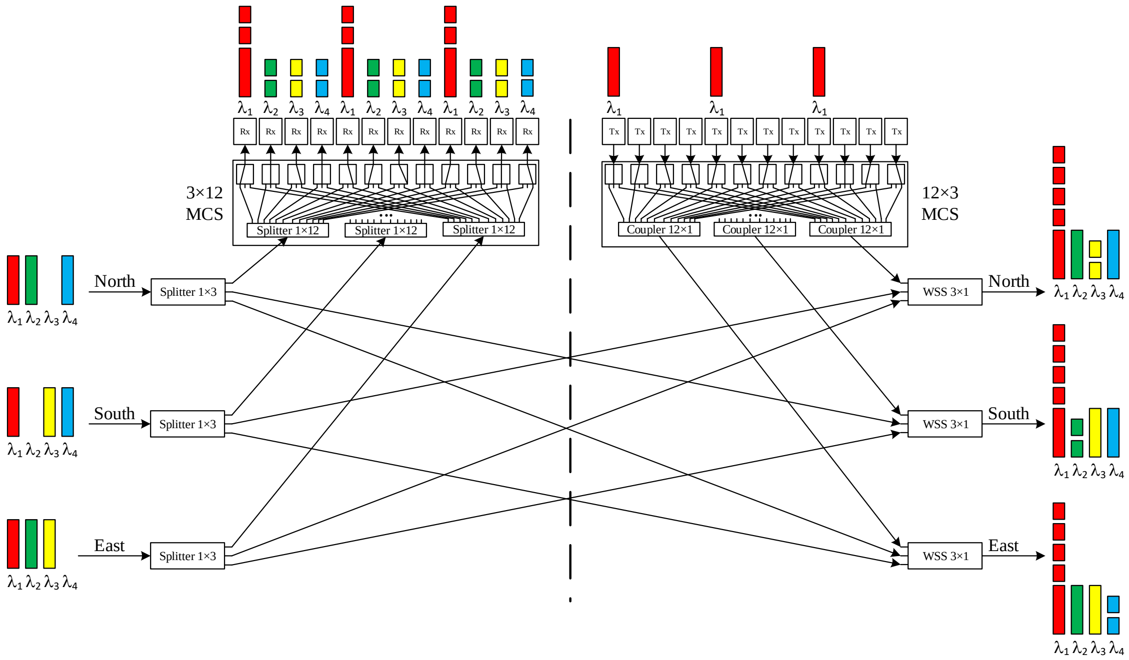

(a) Broadcast & Select

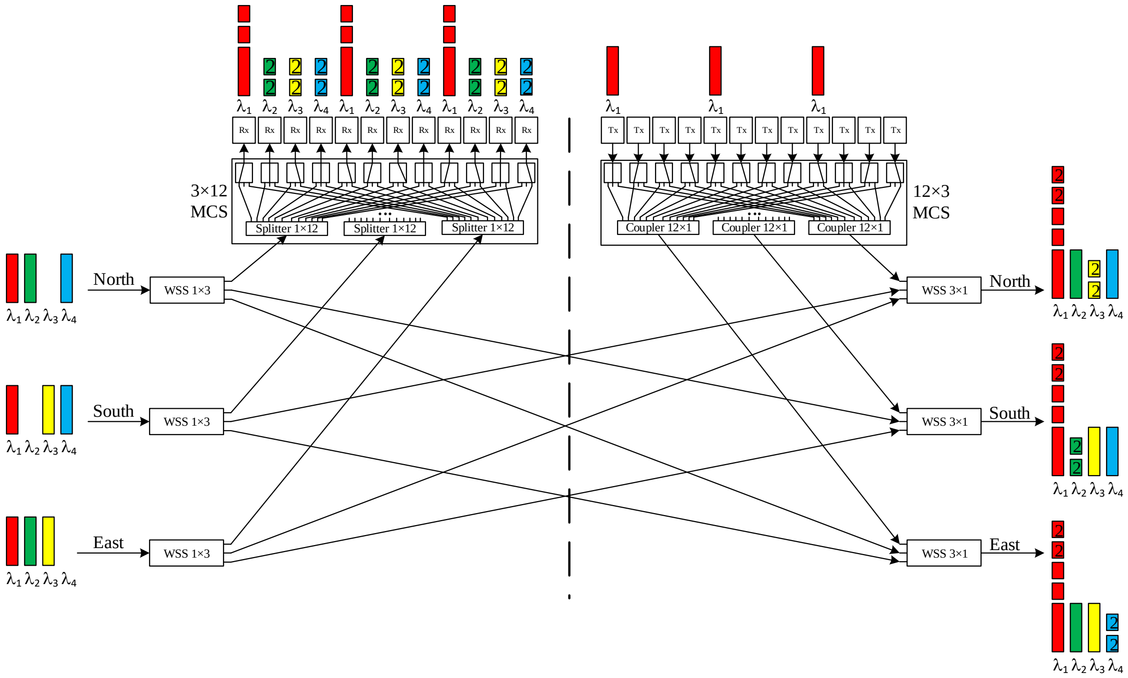

(b) Route & Select

Figure 4.5 - A 3-degree CDC ROADM implemented with MCS 100% contentionless based on a (a) B&S and (b) R&S architecture with the crosstalk generation inside this structure.

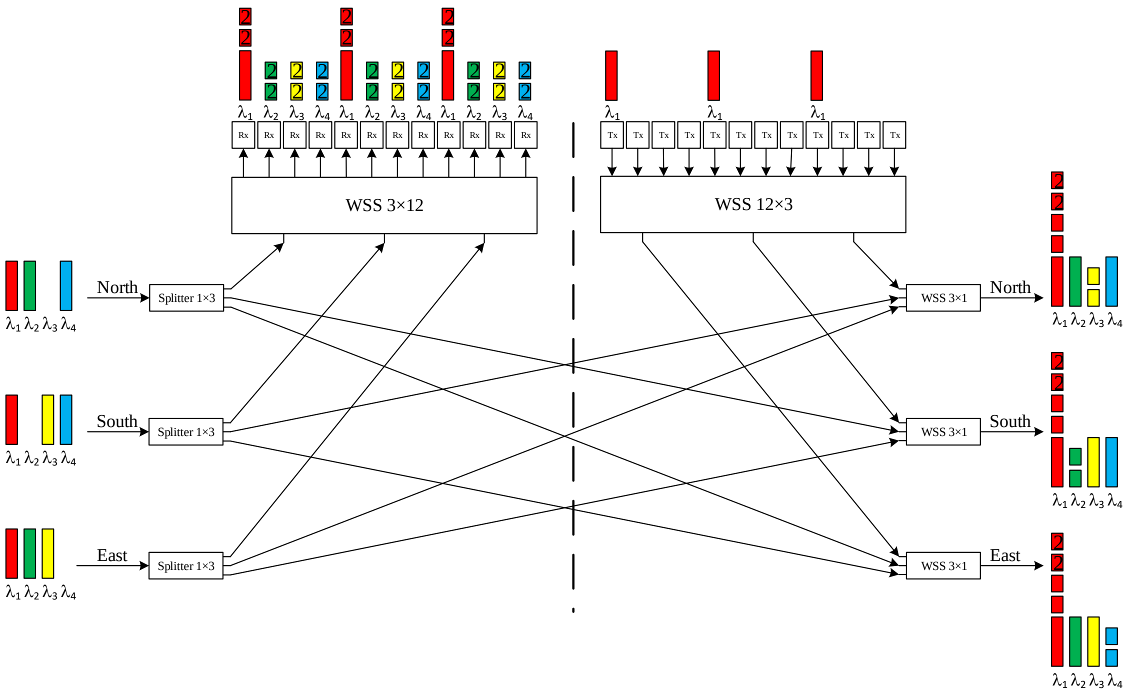

(a) Broadcast & Select

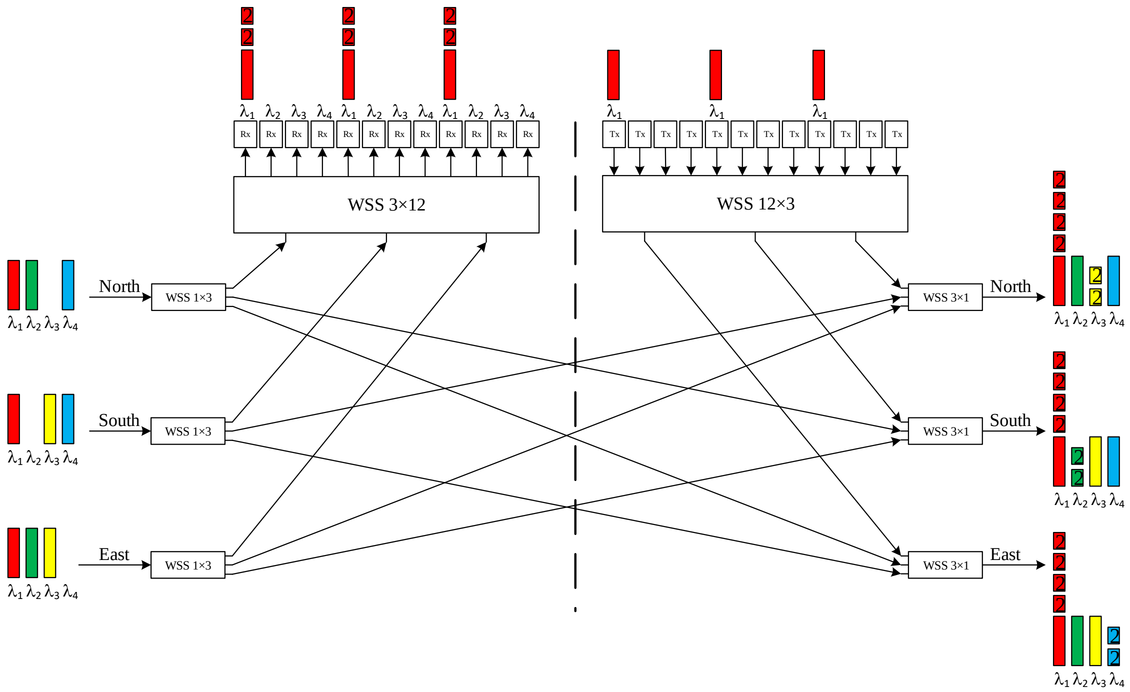

(b) Route & Select

Figure 4.6 - A 3-degree CDC ROADM implemented with WSS 100% contentionless based on a (a) B&S and (b) R&S architecture with the crosstalk generation inside this structure.

4.4 In-Band Crosstalk Generated Inside a 4-Degree ROADM

In this section, we investigate the impact of in-band crosstalk in a 4-degree ROADM based on a R&S architecture. As concluded in the previous section, the architecture R&S minimizes the impact of in-band crosstalk. For this case study, we expand the network shown in figure 4.2, but keeping the wavelength assignment. Node 2 uses the red wavelength λ_1 to communicate with all other nodes. Figure 4.7 depicts a five-node star network with full-mesh logical topology. For this case, for comparison with the four-node network depicted in figure 4.2, we continue to drop all optical signals with wavelength λ_1 and add new signals with wavelength λ_1, i.e., there is a total reuse of the red wavelength. The optical signals with wavelengths λ_2, λ_3, λ_4 and λ_5 remain express signals. Notice that with the considered wavelength assignment, new in-band crosstalk signals arise to the express signals, but our analysis is only focused on the interfering signals with wavelength λ_1.

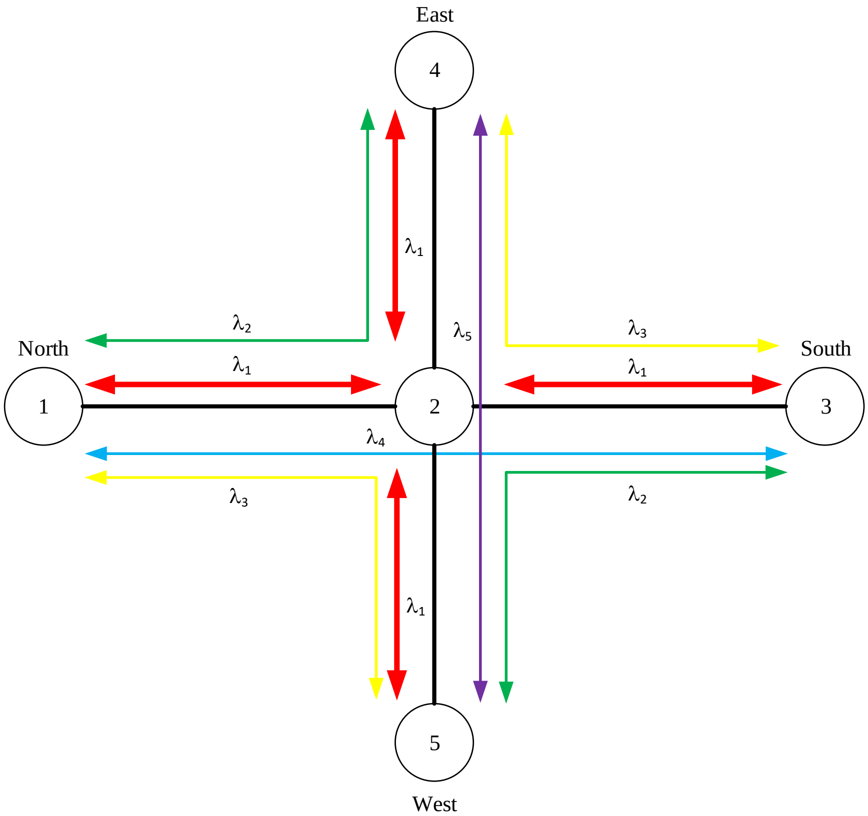

Figure 4.7 - Five-node star network with a full-mesh logical topology.

Figure 4.8 (a) depicts the structure of a 4-degree C ROADM for node 2 and the in-band and out-of-band crosstalk terms generated inside this structure. In each ROADM output, appear three in-band crosstalk terms with wavelength λ_1, two terms with wavelengths λ_2 and other two with λ_3. Comparing this case with the 3-degree C ROADM based on a R&S architecture, we have one more in-band crosstalk term at wavelength λ_1, which has origin on the node degree increase. At each drop port, the wavelength λ_1 is not impaired by any in-band crosstalk terms.

For the 4-degree CD ROADM depicted in figure 4.8 (b), in comparison with a 3-degree CD ROADM also based on a R&S architecture, at the drop ports appears one more second order in-band crosstalk term for the wavelength λ_1. This is generated also by the increase of the number of inputs signals with wavelength λ_1. In this scenario, at each ROADM output, the wavelength λ_1 is impaired by two more in-band crosstalk terms: one of second order, that is generated by the input of another signal with wavelength λ_1, and the other one of first order, that is generated when a new signal with wavelength λ_1 is added in ROADM add section.

As in 3-degree CD and CDC ROADMs implemented with MCSs studied in the previous section, in a 4-degree CD and CDC ROADMs also implemented with MCSs, the number of in-band crosstalk terms generated inside the ROADM is the same in both implementations. Consequently, the difference in terms of in-band crosstalk terms between a 3-degree and a 4-degree CDC ROADMs implemented with MCS, depicted in 4.8 (c), is the same as the difference between a 3-degree and a 4-degree CD ROADMs.

If we use $N \times M$ WSSs for the add/drop structures in the 4-degree CDC ROADM, as shown in figure 4.8 (d), the node will have just second order in-band crosstalk signals. By comparing this case with the 3-degree CDC ROADM implemented also with WSSs, we get one more in-band crosstalk term at each drop port, due to the increase of inputs signals with wavelength λ_1. At each ROADM output, two more in-band crosstalk terms appear, one due to the new input with wavelength λ_1 and the other one due to the addition of another signal with wavelength λ_1. Note that in this case, to construct a CDC ROADM 100% contentionless, it would be necessary to have WSSs with large dimensions, i.e. 4×20 and 20×4. Nowadays, there are structures with such dimensions commercially available, but not commonly used in optical networks, mainly because is a very expensive component.

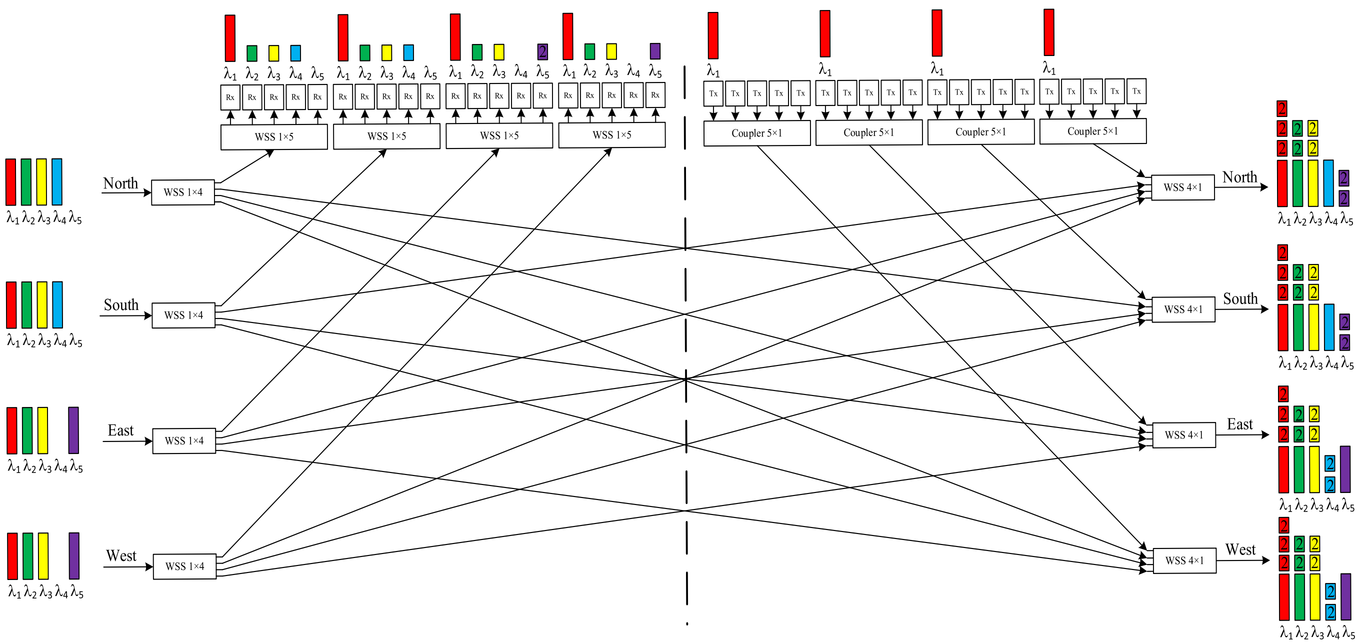

(a) Colorless

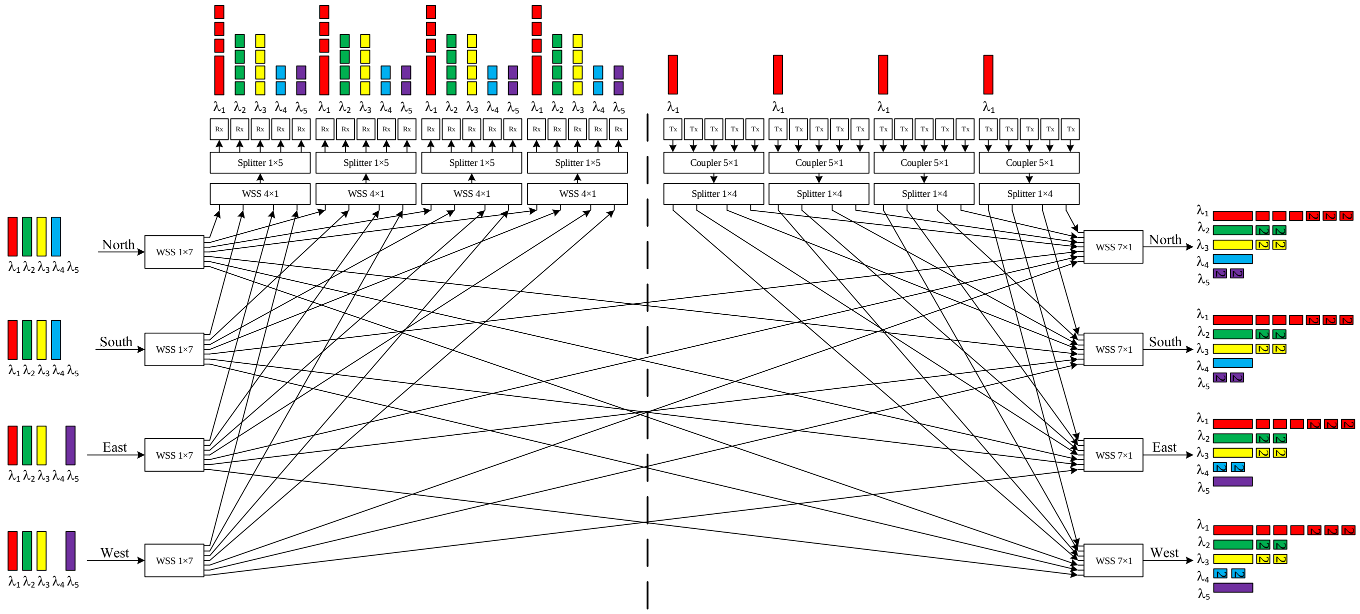

(b) Colorless and directionless

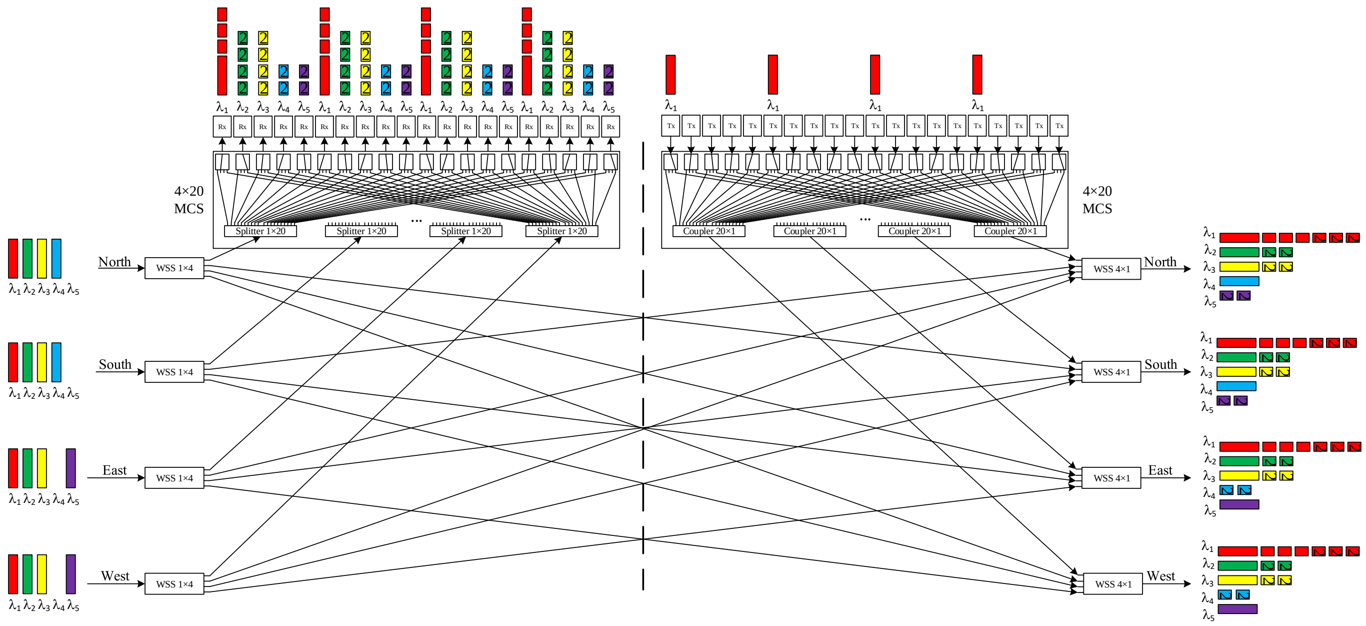

(c) Colorless, directionless and contentionless implemented with MCS

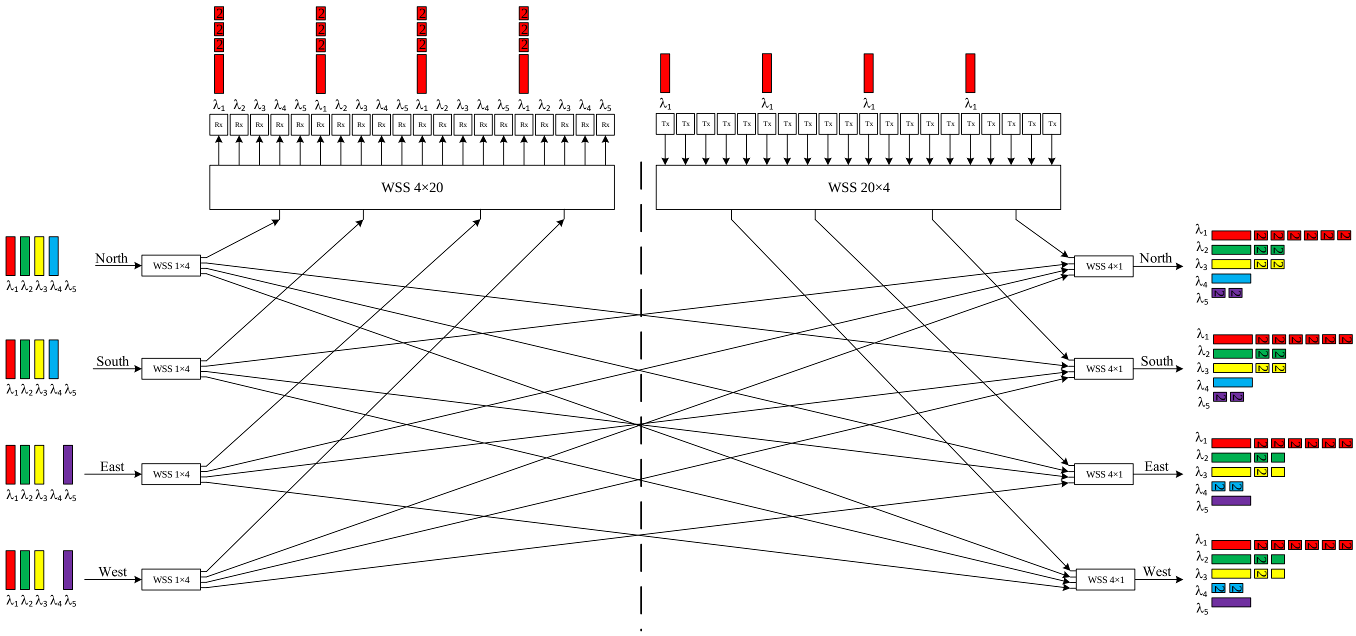

(d) Colorless, directionless and contentionless implemented with WSS

Figure 4.8 - A 4-degree (a) C (b) CD (c) CDC implemented with MCS (d) CDC implemented with WSS ROADM based on a R&S architecture with the crosstalk generation inside these structures.

4.5 In-Band Crosstalk Generated Inside a Multi-Degree ROADM

In this section, we present a summary of the number of interfering crosstalk signals, as a function of the ROADM degree N, considering a worst-case scenario: we assume that node 2 continues to communicate with all other nodes using the same wavelength and there is a total reuse of this wavelength. This means that, at the node 2, all signals carried by this wavelength that reach the node are dropped and new optical signals with equal wavelength are added and directed to the ROADM outputs.

Therefore, we present in table 4.1, the number of in-band crosstalk terms generated inside a multi-degree C, CD and CDC ROADM (implemented with MCSs and WSSs). We can conclude that, for a CDC ROADM implementation, the WSSs is the best choice in terms of in-band crosstalk generation, because all interfering signals are second order terms. For example, for an 8-degree CDC ROADM (N=8) implemented with WSSs 100% contentionless and based on a R&S architecture, we can predict by table 4.1 that, the number of in-band crosstalk terms that appear at the drop ports is seven $(N-1)$ second order terms and at each ROADM output is fourteen $[2(N-1)]$ second order terms.

Table 4.1 - Number of in-band crosstalk terms generated inside a N-degree C, CD and CDC ROADM.

	Architecture	Broadcast & Select				Route & Select			
	Local	Drop ports		Outputs		Drop ports		Outputs	
	Term order	1st	2nd	1st	2nd	1st	2nd	1st	2nd
ROADM	**C**	-	-	N–1	-	-	-	-	N–1
	CD	N–1	-	2(N–1)	-	N–1	-	N–1	N–1
	CDC - MCSs	N–1	-	2(N–1)	-	N–1	-	N–1	N–1
	CDC - WSSs	-	N–1	N–1	N–1	-	N–1	-	2(N–1)

4.6 Conclusions

In this chapter, we have investigated the impact of in-band crosstalk in a 3-degree C, CD and CDC ROADMs based on the B&S and R&S architectures and in 4-degree C, CD and CDC ROADMs based on the R&S architecture. For the CDC ROADMs, we studied two possible implementations for the add/drop structures, the MCSs and $N\times M$ WSSs.

In terms of the in-band crosstalk terms generation, the architecture R&S has a better performance than the architecture B&S. On the other hand, since in an architecture R&S, the signal passes through more WSSs, consequently through more filters, so the impact of filtering and the cost are higher in ROADMs based on this architecture.

With this study, we have concluded that CDC ROADMs based on MCSs are more vulnerable to the in-band crosstalk than CDC ROADMs implemented with $N\times M$ WSS. However, the implementation of add/drop structures with $N\times M$ WSSs is more expensive.

In section 4.5, we have summarized the number of in-band crosstalk signals, as a function of the ROADM degree, that arises in the add/drop structures implementations studied. Thus, we can predict, in terms of the number of interferers, the impact of in-band crosstalk in an optical network based on C, CD or CDC ROADMs. With this summary, we also have concluded that the number of in-band crosstalk terms in CD ROADMs is the same as in CDC ROADMs implemented with MCSs. The order of in-band crosstalk only changes if the add/drop structures of a CDC ROADM are based on $N\times M$ WSSs.

References

[1] I. Monroy and E. Tangdiongga, *Crosstalk in WDM Communication Networks*. Norwell, MA: Springer, 2002

[2] S. Tibuleac and M. Filer, "Transmission Impairments in DWDM Networks With Reconfigurable Optical Add-Drop Multiplexers," in *Journal of Lightwave Technology*, vol. 28, no. 4, pp. 557-598, February 2010.

[3] J. Simmons, *Optical Network Design and Planning*, Springer, 2ª ed., 2014.

[4] B. Collings, "Advanced ROADM technologies and architectures," *2015 Optical Fiber Communications Conference and Exhibition (OFC)*, Los Angeles, CA, pp. 1-3, March 2015.

[5] X. Wu, C. Lu, Z. Ghassemlooy and Y. Wang, "Evaluation of intraband crosstalk in an FBG-OC-based optical cross connect," in *IEEE Photonics Technology Letters*, vol. 14, no. 2, pp. 212-214, February 2002.

[6] L. Cancela, D. Sequeira, B. Pinheiro, J. Rebola and J. Pires, "Analytical tools for evaluating the impact of in-band crosstalk in DP-QPSK signals," *2016 21st European Conference on Networks and Optical Communications (NOC)*, Lisbon, pp. 6-11, June 2016.

[7] L. Cancela, J. Rebola, J. Pires, “Implication of in-band crosstalk on DQPSK signals in ROADM-based metropolitan optical networks”, *Optical Switching and Networking*, pp.134-144, January 2016.

[8] T. Zami, "High degree optical cross-connect based on multicast switch," *2014 Optical Fiber Communication Conference and Exhibition (OFC)*, San Francisco, CA, pp. 1-3, March 2014.

[9] R. Shankar *et al.* "Multi-degree ROADM based on wavelength selective switches: Architectures and scalability." *Optics Communications*, vol. 279 no.1, pp. 94-100, November 2007.

[10] S. Woodward *et al.* “ROADM-Node Architectures for Reconfigurable Photonic Networks”, *Optical Fiber Telecommunications VIB*, I. Kaminov, T. Li, and A. Willner, eds., Academic Press, 2013.

[11] W. Way, "Optimum architecture for M×N multicast switch-based colorless, directionless, contentionless, and flexible-grid ROADM," *2012 Conference on Optical Fiber Communication and the National Fiber Optic Engineers Conference (OFC/NFOEC)*, Los Angeles, CA, pp. 1-3, March 2012.

[12] L. Zong, H. Zhao, Z. Feng and Y. Yan, "Low-cost, degree-expandable and contention-free ROADM architecture based on M×N WSS," *2016 Optical Fiber Communications Conference and Exhibition (OFC)*, Anaheim, CA, pp. 1-3, March 2016.

[13] S. Thiagarajan, L. Blair and J. Berthold, "Direction-Independent Add/Drop Access for Multi-Degree ROADMs," *2008 Optical Fiber Communication Conference and the National Fiber Optic Engineers Conference (OFC/NFOEC)*, San Diego, CA, pp. 1-3, February 2008.

[14] Lumentum, TrueFlex® Reconfigurable Optical Add-Drop Multiplexer (ROADM) Portfolio, 2015. Available: https://www.lumentum.com/sites/default/files/technical-library-files/trueflexroadm-pb-oc-ae.pdf.

Chapter 5

Physical Impairments in an Optical Network Based on CDC ROADMs

5.1 Introduction

In this chapter, the performance of a *M*-QAM coherent receiver impaired by in-band crosstalk, ASE noise and optical filtering in an optical network composed by multi-degree CDC ROADMs is evaluated, using MC simulation, by calculating the BER with the DEC method and the OSNR penalty.

In section 5.2, a schematic model for the study of the physical impairments in an optical network based on CDC ROADMs is presented and explained. The generation of in-band crosstalk in the model is detailed in this section.

Properties and characteristics of the optical filters used in the simulation to model the WSSs inside the CDC ROADMs are presented and discussed in section 5.3. Subsections 5.3.1 and 5.3.2 present the optical passband and the optical stopband filters characteristics.

The 2×1 WSS is a basic component in the ROADM nodes, where a single in-band crosstalk interferer arises. The simulator validation, modeling this component, is performed in section 5.4 using MC simulation.

In section 5.5, we present the model considered for the add/drop structures of the CDC ROADMs nodes and the in-band crosstalk generated inside these structures is investigated.

The physical impairments (in-band crosstalk, optical filtering and ASE noise) are studied in section 5.6, considering a network based on CDC ROADMs and the QPSK modulation format. In subsection 5.6.1, the impact of the optical filtering and in-band crosstalk on the performance of an optical network with only one amplification stage at the end of the ROADMs cascade is studied. The impact of multiple amplification stages, at inputs and outputs of every CDC ROADMs, is analyzed in subsection 5.6.2.

Lastly, in section 5.7, the conclusions of this chapter are presented.

5.2 Schematic Model of an Optical Network with Multi-Degree CDC ROADMs

In this section, we present the schematic model of an optical network based on multi--degree CDC ROADMs, with coherent detection at the receiver, considered to study the network physical impairments, such as optical filtering, in-band crosstalk and ASE noise. The ROADM nodes are based on the R&S architecture. As we saw in the previous chapter, this architecture is the best architecture in terms of in-band crosstalk minimization. The key element of a R&S architecture is the WSS, used in both the routing and selecting sections of the ROADM. To implement the CDC properties [1], [2], the ROADM add/drop structures can be based on $N \times M$ WSSs [3], [4] or MCSs [5]. To model these structures, we use Super-Gaussian optical filters [6], [7]. Their respective characteristics are presented in section 5.3. The crosstalk generated inside of these structures is characterized in section 5.5, through analysis of the crosstalk level.

Notice that, nowadays, a cascade of ROADM nodes can represent a light-path of an optical signal inside a network with a generic topology (mesh, ring, etc.), since the moment the signal is added to the optical network until it is dropped. The signal referred in this work as a "primary" signal corresponds to the signal that is taken as a reference to the study the network physical impairments.

Figure 5.1 depicts the schematic model of an optical network with a cascade of M multi-degree ROADMs. The primary signal, represented in figure 5.1 by S_{in}, passes through an optical multiplexer with transfer function $H_{Mux}(f)$, designed for the fixed grid with 50 GHz channel spacing [8]. Note that all interfering signals that are routed through the ROADM node also pass through one identical optical multiplexer. This optical multiplexer simulates an optical channel of the fixed grid, spaced by 50 GHz.

Thus, a filtered primary signal, represented in figure 5.1 as $S_{in,f}$, enters the first ROADM node and the output of this ROADM, the signal called $S_{o,1}$, will be one of the inputs of the second ROADM node. This process is repeated until the primary signal reaches the M^{th} ROADM node. The signal generated from this ROADMs cascade, i.e., the output signal of the M^{th} ROADM, is denominated $S_{o,M}$. This signal, before entering the coherent receiver, passes through an optical demultiplexer, also designed for the fixed grid with 50 GHz channel spacing [8], and originates the signal S_{out} that will be detected by the coherent receiver [9].

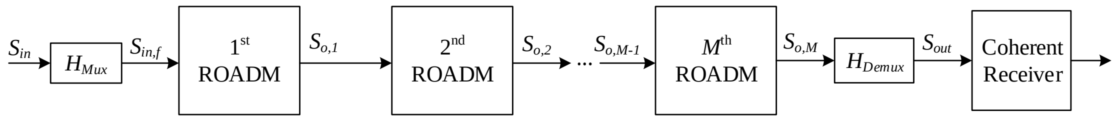

Figure 5.1 - Schematic model of an optical network based on a cascade of ROADMs.

Figure 5.2 also depicts the schematic model of figure 5.1, but with more detail regarding the crosstalk generation inside the ROADM nodes. The light-path of the primary signal, since it is added until it is dropped, is represented in figure 5.2 by the red line. To simplify, we only represent the output component for one ROADM direction, where the primary signal will be routed, and the connections from which the interfering signals arise. In the last ROADM, the signals at its inputs cannot all be dropped. However, as we study the CDC ROADM implementation and, in this implementation all ROADM inputs are connected with the same drop structure, all input signals are possible interfering signals. Consequently, this possible interference is represented in figure 5.2 as connections.

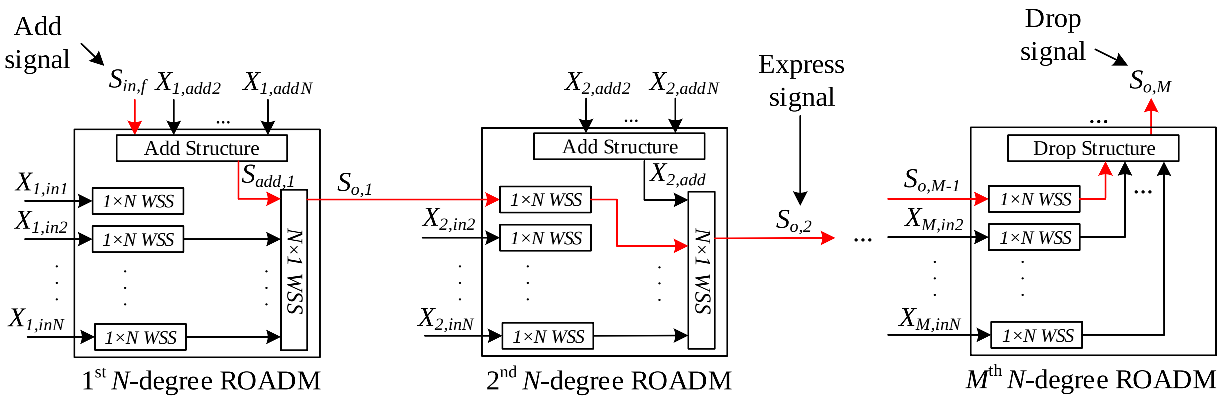

Figure 5.2 - Model of a cascade of M multi-degree CDC ROADMs based on the R&S architecture with detail on the in-band crosstalk signals generation.

Regarding the crosstalk generation in the model depicted in figure 5.2, the number of in-band crosstalk signals that arises in each ROADM node is determined by the ROADM degree and if the primary signal is added, expressed or dropped. In this chapter, we consider that all ROADM nodes in the same network have the same degree and all interfering signals have the same wavelength as the primary signal, so they are considered as in-band crosstalk signals. We also consider that, each ROADM node originates the maximum possible number of interferers, as described in the following paragraphs.

Therefore, in the first multi-degree CDC ROADM, where the filtered primary signal $S_{in,f}$ is added, it will be impaired by 2(*N*–1) in-band crosstalk signals. Half of them, i.e. *N*–1, come from the ROADM inputs, and are represented in figure 5.2 by the signals $X_{1,in2}$, …, $X_{1,inN}$. These interfering signals at the ROADM input, pass through a 1×*N* WSS (called route WSS) where they are blocked. The interfering blocked signals are routed for all ROADM outputs, except for one direction, hence arising *N*–1 interferers from the ROADM inputs. The other *N*–1 crosstalk signals arise from the add section. These signals, represented by $X_{1,add2}$, …, $X_{1,addN}$ in figure 5.2, pass through an add structure, where they are blocked. The filtered primary signal $S_{in,f}$ also passes through the add structure, where it is added to the blocked signals coming from the add structure and this addition, named signal $S_{add,1}$, is directed to one ROADM output. At the ROADM output, these signals are selected by one *N*×1 WSS (called the select WSS). The signal $S_{add,1}$ passes through this WSS and the interfering signals are blocked. Thus, the power spectral density (PSD) of the output signal at the first ROADM is given by

$$S_{o,1}(f) = S_{add,1}(f).\left|H_p(f)\right|^2 + X_{1,in}(f).\left|H_b(f)\right|^2 \tag{5.1}$$

where $S_{add,1}(f)$ is the PSD of the signal originated in the add section of the first ROADM, which is described by equation 5.2, if the add section is implemented with MCSs or by equation 5.3, if the add section is implemented with *N*×*M* WSSs. Note that, as we reported in chapter 3, inside the MCSs, the signals pass through one optical filter, while inside the *N*×*M* WSS, pass through two optical filters. The $H_p(f)$ and $H_b(f)$ are, respectively, the transfer functions of the passband and stopband optical filters inside the route and select WSSs. The signal $X_{1,in}(f)$ is the PSD of the in-band crosstalk generated in the inputs of the first ROADM, and is given by equation 5.4.

$$S_{add,1}(f) = S_{in,f}(f).\left|H_p(f)\right|^2 + \sum_{n=2}^{N} X_{1,addn}(f).\left|H_b(f)\right|^2 \tag{5.2}$$

$$S_{add,1}(f) = S_{in,f}(f).\left|H_p(f)\right|^4 + \sum_{n=2}^{N} X_{1,addn}(f).\left|H_b(f)\right|^4 \tag{5.3}$$

$$X_{1,in}(f) = \sum_{n=2}^{N} X_{1,inn}(f).\left|H_b(f)\right|^2 \tag{5.4}$$

The output signal of the first ROADM, called $S_{o,1}$, will correspond to one of the inputs of the second multi-degree CDC ROADM node. In this ROADM node, if the signal $S_{o,1}$ is an express signal, it passes through two WSSs, the route and select WSSs. In this situation, a total of 2*N*–3 in-band crosstalk signals are generated inside the ROADM. *N*–2 of these interfering signals are originated from the ROADM inputs, because one of the inputs is where the signal $S_{o,1}$ enters the node, and another ROADM input cannot be directed to its own output, since it is where the express signal $S_{o,1}$ will be directed. In figure 5.2, these signals are represented by the signals $X_{2,in2}$, …, $X_{2,inN}$. These crosstalk signals derived from the ROADM inputs are blocked by the route and select WSSs. The other *N*–1 interferers represented in figure 5.2 as $X_{2,add2}$, …, $X_{2,addN}$, are derived from the add section. These correspond to the maximum number of signals at the same wavelength that can be added in this node. These interferers coming from the add section are blocked by the add structure and the select WSS. Then, until the primary signal reaches its destination, the final ROADM, it passes through *M*–2 interconnect ROADMs as an express signal. The number of in-band crosstalk signals that are generated in each ROADM where the primary signal is expressed is the same as the one generated in the second ROADM node. Therefore, the PSD of the signal at the input of the last ROADM node represented in figure 5.2 by $S_{o,M-1}$ is given by

$$S_{o,M-1}(f) = \sum_{m=2}^{M-1} \left[S_{o,m-1}(f).\left|H_p(f)\right|^4 + X_{m,in}(f).\left|H_b(f)\right|^2 + X_{m,add}(f).\left|H_b(f)\right|^2 \right] \tag{5.5}$$

where $X_{m,in}(f)$ and $X_{m,add}(f)$ are the PSDs of the crosstalk signals generated in the ROADMs inputs and add section, respectively, of the M^{th} ROADM. These are described by equations 5.6, 5.7 and 5.8, respectively. In equation 5.6, the sum starts at 3 because, as we saw earlier, when the signal that carries the primary signal S_{in} is an express signal, there is one less in-band crosstalk signal (derived from the ROADM inputs) than when the primary signal is added. Concerning the crosstalk signals derived from the ROADM add structure, we present the case of the add section implemented with MCSs in equation 5.7 and the case where it is implemented with *N*×*M* WSSs in equation 5.8, respectively.

$$X_{m,in}(f) = \sum_{n=3}^{N} X_{m,inn}(f).\left|H_b(f)\right|^2 \tag{5.6}$$

$$X_{m,add}(f) = \sum_{n=2}^{N} X_{m,addn}(f).\,|H_b(f)|^2 \tag{5.7}$$

$$X_{m,add}(f) = \sum_{n=2}^{N} X_{m,addn}(f).\,|H_b(f)|^4 \tag{5.8}$$

Finally, when the primary signal reaches its destination, the *M^th^* multi-degree CDC ROADM node, the optical signal $S_{o,M-1}$ that contains the primary signal will be dropped. Consequently, it is impaired by *N*–1 in-band crosstalk signals derived from the ROADM inputs. These interfering signals are blocked by the route WSS and by the drop structure. The signal $S_{o,M-1}$ also passes by these two components, but through passband filters instead of stopband filters. If the drop structure is implemented with MCSs, the PSD of the dropped signal, named $S_{o,M}$ in figures 5.1 and 5.2, is given by equation 5.9. Otherwise, if the structure is implemented with *N*×*M* WSSs, the PSD of the dropped signal is given by equation 5.10. Notice that the crosstalk derived from the M^{th} ROADM inputs, denominated $X_{M,in}$, is described in the same way as in the first ROADM, as given by equation 5.4.

$$S_{o,M}(f) = S_{o,M-1}(f).\left|H_p(f)\right|^4 + X_{M,in}(f).\,|H_b(f)|^2 \tag{5.9}$$

$$S_{o,M}(f) = S_{o,M-1}(f).\left|H_p(f)\right|^6 + X_{M,in}(f).\,|H_b(f)|^4 \tag{5.10}$$

With the derivation of the previous equations, we can conclude that, when the CDC ROADM add/drop structures are implemented with *N*×*M* WSSs, the interfering signals pass through more stopband filters than when the implementation of the add/drop structures is based on MCSs. Consequently, the total crosstalk generated in a cascade of CDC ROADMs based on *N*×*M* WSSs is lower.

On the other hand, if the add/drop structures are implemented with *N*×*M* WSSs, the primary signal passes through two more passband optical filters than if these structures are implemented with MCSs. One when it is added and another when it is dropped. So, the optical filtering has more degrading effect in the network performance in CDC ROADMSs with add/drop structures implemented with *N*×*M* WSSs.

5.3 Characteristics of the Optical Filters

In the model depicted in figure 5.2, we have two types of optical filters inside the WSSs, one to model the passband filter, $H_p(f)$, and the other one to model the stopband filter, $H_b(f)$. The signals that pass through the WSS are filtered by the passband filter, while the signals that the WSS blocks are filtered by the stopband filter (or rejection filter).

The optical passband filter $H_p(f)$ is modeled by a 4th order Super-Gaussian optical filter [6], [8] with –3 dB bandwidth (B_0) equal to 41 GHz, usually used for the 50 GHz channel spacing [8]. The same filters are used to model the optical multiplexer H_{Mux} and demultiplexer H_{Demux} [8].

The optical stopband filter $H_b(f)$ is modeled by the inversion of the transfer function of the optical passband filter and by setting the blocking amplitude *A*, in dB. The transfer functions of these two optical filters are given, respectively, by [10]

$$H_p(f) = \; e^{-\left[\left(\frac{f}{B_0}\right)^{2n} \cdot \frac{\ln 2}{2}\right]} \tag{5.11}$$

$$H_b(f) = \; 1 - (1 - a). e^{-\left[\left(\frac{f}{B}\right)^{2n} \cdot \frac{\ln 2}{2}\right]} \tag{5.12}$$

where *n* is the order of the Super-Gaussian filter, *a* is the blocking amplitude of stopband filter $H_b(f)$ in linear units, $a = \; 10^{\frac{A\,[dB]}{20}}$ and *B* is a bandwidth initially set for the stopband filter. These transfer functions are represented in figure 5.3. Figure 5.3 (a) shows the transfer function used to model the passband filter $H_p(f)$, the optical multiplexer $H_{Mux}(f)$ and demultiplexer $H_{Demux}(f)$, given by equation 5.11. Figure 5.3 (a) shows that the passband filter is nearly "flat-top". Hence, inside their passband, the 4th order Super-Gaussian filter does not introduce significant amplitude distortion. At the passband edges, near the –3 dB bandwidth, amplitude distortion will occur. This distortion will be enhanced by the filters cascading effect along the optical nodes, which is studied in subsection 5.3.1. In figure 5.3 (b), we can observe the transfer function of the stopband filter $H_b(f)$, given by equation 5.12, with different blocking amplitudes (i) *A* = –20 dB, (ii) *A* = –30 dB, (iii) *A* = –40 dB and (iv) *A* = –50 dB.

Figure 5.4 depicts the power spectrum of a 50-Gb/s NRZ QPSK signal in three different scenarios: signal without blocking (black curve), signal blocked with one stopband filter with $A = -20$ dB (blue curve) and $A = -50$ dB (red curve). From this figure, we can see that, the signal that experiences higher blocking amplitude has higher signal power concentrated in the band edges than in the center frequency (red curve). On the other hand, when the signal experiences lower blocking amplitudes, the power of the blocked signal is similarly spread through the stopband.

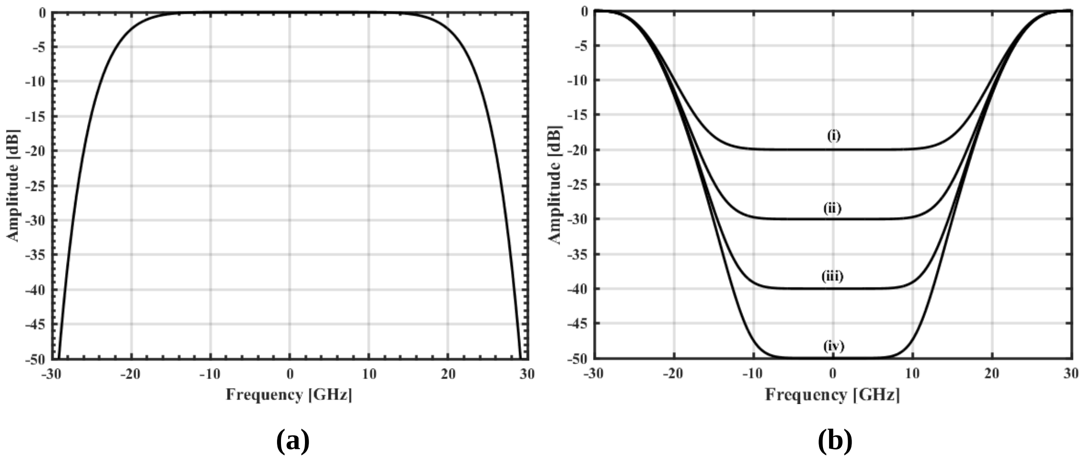

Figure 5.3 - Transfer function used to model the (a) optical Super-Gaussian 4th order passband filter $H_p(f)$, optical multiplexer $H_{Mux}(f)$ and demultiplexer $H_{Demux}(f)$, with B_0 = 41 GHz and (b) optical stopband filters $H_b(f)$ with different blocking amplitudes (i) –20 dB (ii) –30 dB (iii) –40 dB and (iv) –50 dB and $B_0 \sim$ 48 GHz.

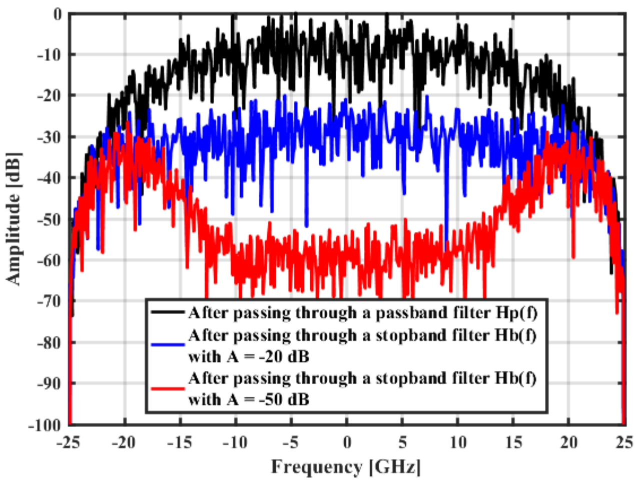

Figure 5.4 - Power spectrum of a 50-Gb/s NRZ QPSK signal for three scenarios: i) signal after passing the optical passband filter $H_p(f)$ (black curve) ii) after passing one stopband filter $H_b(f)$ with $A = -20$ dB (blue curve) and iii) after passing one stopband filter $H_b(f)$ with $A = -50$ dB (red curve).

5.3.1 Optical Passband Filter Properties

Regarding the optical passband filter $H_p(f)$ characteristics, it is important to understand the impact of a cascade of passband filters, since it will resemble the scenario in a real network environment where the signal passes through a cascade of several nodes along its light-path. When the primary signal S_{in} passes through several passband filters, the passband width will narrow. This effect is known as passband narrowing [11].

This effect has a great impact on the network performance [2], [11], mainly in networks based on ROADM nodes implemented with a R&S architecture, since in these type of networks, the optical signal undergoes more WSSs. At each ROADM based on this architecture, one optical signal passes always through two WSSs inside the ROADMs. For example, if a signal has passed through 16 ROADMs nodes until reaches its destination, it passes at least through 32 WSSs, two WSSs in each ROADM node. The passband narrowing, in this case, is depicted in figure 5.5 by the purple curve. We can observe in figure 5.5, that the -3 dB bandwidth B_0 narrowed approximately 14.4 GHz after passing through 32 filters in comparison with one filter [B_0 passes from 41 GHz (blue curve) to 26.6 GHz (purple curve)]. This narrowing is in accordance with the one presented in [12], where the passband narrowing is approximately 13.3 GHz after passing through 30 passband filters. Figure 5.5 also depicts the transfer functions after 8 and 16 cascaded passband filters.

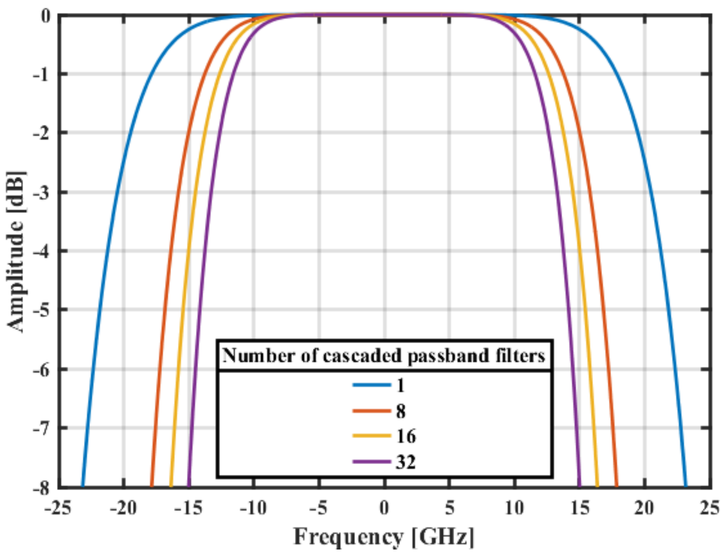

Figure 5.5 - Passband narrowing of the optical filter $H_p(f)$ for a 4th Super-Gaussian filter with B_0 equal to 41 GHz after passing through several passband filters.

Figure 5.6 (a) depicts the signal power as a function of the number of passband filters that the signal passes. We can observe that the signal power, initially set to 0 dBm, decreases 0.55 dB in the first filter. The signal power continues decreasing with the number of the passband filters that the signal passes and after 20 filters, the signal power is –1 dBm. This means that, after 20 cascaded filters, the signal power penalty due to the filtering is 1 dB. This power loss due to the narrowing of the passband filter can be compensates along the optical network by the OAs. In figure 5.6 (b), we can observe the filtering effect on a 50-Gb/s NRZ QPSK signal. In particular, the black curve represents the PSD of the optical signal after one filtering and the red curve after passing 32 passband optical filters. The narrowing of the signal PSD after 32 passband filters is clearly visible in this figure.

Figure 5.7, depicts the eye diagram of a QPSK signal after passing one passband filter (red curve) and after passing through 32 passband filters (black curve). From this figure, we can observe the amplitude distortion introduced by a cascade of 32 passband filters. Noticeably, the aperture of the eye diagram after 32 passband filters is smaller, about 1.5, than after one filter, where the aperture is around 2. This amplitude distortion introduced by the cascaded passband filters is not compensated by the optical network, and will originate a penalty due to the optical filtering. We evaluate the impact of the optical filtering on the performance of the coherent receiver in subsection 5.6.1.

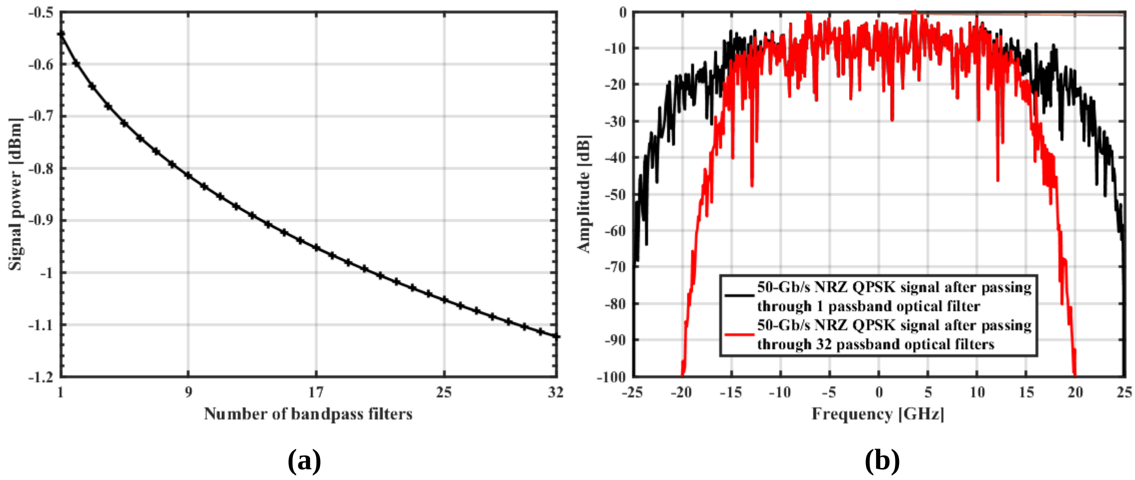

Figure 5.6 - (a) 50-Gb/s NRZ QPSK signal power as a function of the optical passband filters that the signal passes (b) Power spectrum of the same signal i) after one filtering (black curve) and ii) after passing through 32 passband filters (red curve).

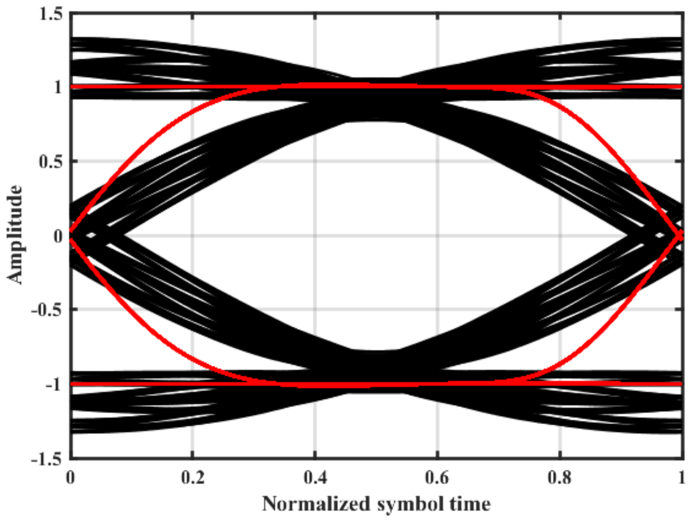

Figure 5.7 - Eye diagram of a NRZ QPSK signal after one passband filter (red curve) and after passing through 32 passband filters (black curve).

5.3.2 Optical Stopband Filter Properties

Regarding the stopband optical filter, the bandwidth B is set to 41 GHz, however, its –3 dB bandwidth B_0 changes slightly with the blocking amplitude. This change is shown in table 5.1, where the difference of –3 dB bandwidths between the minimum and maximum blocking amplitudes, –20 dB and –50 dB, is approximately 0.6 GHz. So, the –3 dB bandwidth B_0 of the stopband filter is approximately 48 GHz.

Another characteristic of these filters is the isolation floor bandwidth. This parameter represents the frequency bandwidth that the transfer function of the filter is exactly the blocking amplitude. As we can see in figure 5.3 (b) and in third column of the table 5.1, this bandwidth narrows with the blocking amplitude.

Table 5.1 – B_0 and isolation floor bandwidth of the stopband filter as a function of the blocking amplitude.

Characteristics of stopband optical filter $H_b(f)$		
Blocking Amplitude [dB]	B_0 [GHz]	Isolation floor bandwidth [GHz]
-20	~ 47.5	~ 13.9
-30	~ 47.9	~ 11.7
-40	~ 48.0	~ 10.4
-50	~ 48.1	~ 8.4

Another feature of the stopband filter is that the isolation floor bandwidth also changes with the cascade of stopband filters that the signal passes. Figure 5.8 (a) depicts, the 50-Gb/s NRZ QPSK signal power evolution as a function of the number of cascaded stopband filters: one stopband filter with A = –40 dB, two stopband filters each with A = –20 dB and four stopband filters each with A = –10 dB. The signal power is initially set at 0 dBm. Figure 5.8 (b) depicts the transfer functions of the cascaded stopband filters in these three cases. From figure 5.8 (b), we can conclude that the isolation floor bandwidth of an optical stopband filter with A = –40 dB is narrower than with two or four cascaded stopband filters. Thus, the signal power blocked is higher with the increase of the number of stopband filters, as shown in figure 5.8 (a) where an 8 dB difference can be observed. However, using stopband filters with poorer isolation floor amplitudes will lead to higher crosstalk.

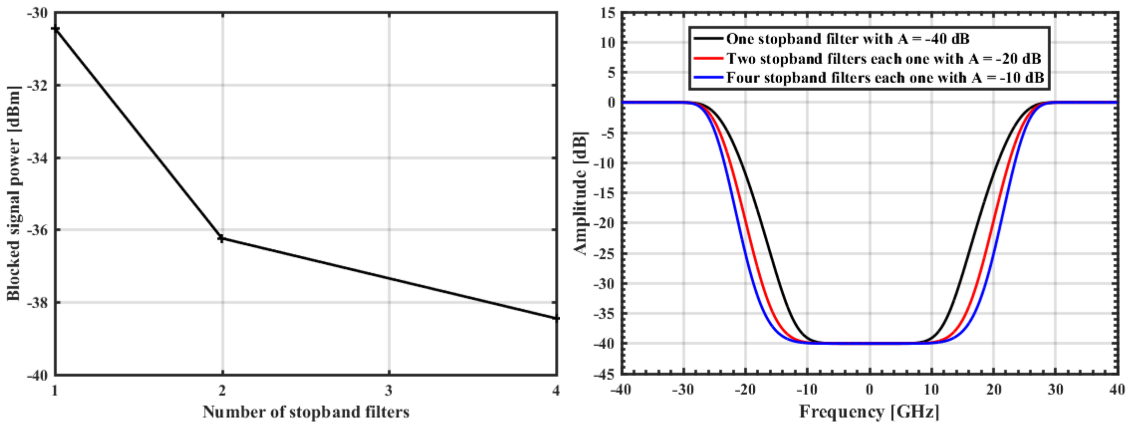

(a) **(b)**

Figure 5.8 - (a) 50-Gb/s NRZ QPSK signal power as a function of the number of optical stopband filters that the signal passes. (b) Transfer functions of the cascaded stopband filters for: one filter with A = –40 dB (black curve), two filters each one with A = –20 dB (red curve) and four filters each one with A = –10 dB (blue curve).

Figure 5.9 shows the power spectrum of a 50-Gb/s NRZ QPSK signal before (black spectrum) and after (red spectrum) one stopband filter with A = –40 dB, figure 5.9 (a), and four stopband filters each one with A = –10 dB, figure 5.9 (b). Once more, we can conclude that a cascade of blocking filters has a better performance in signal blocking than a single filter. Figure 5.9 shows that the cascaded stopband filters removes the non--blocked power (which was not removed by the stopband filter with A = –40 dB) at the edges of the signal band.

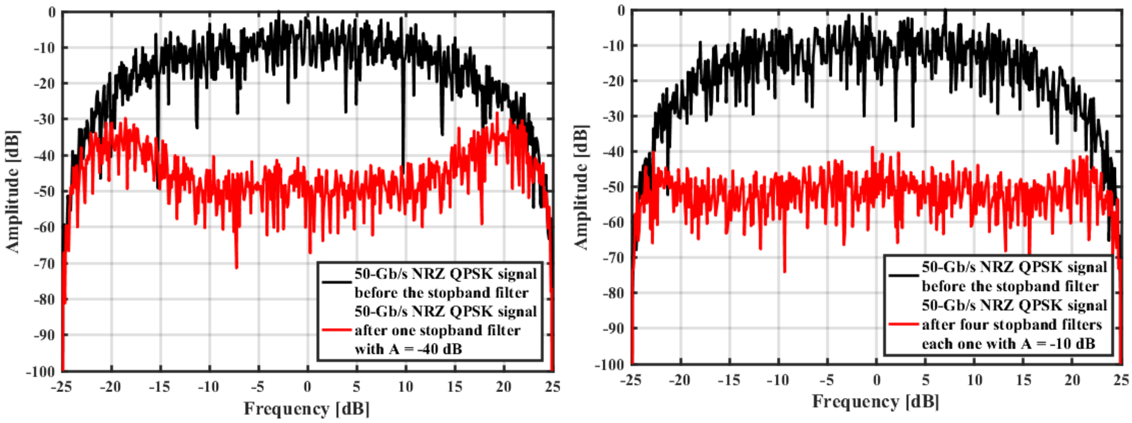

(a) **(b)**

Figure 5.9 - 50-Gb/s NRZ QPSK power spectrum before (black spectrum) and after passing (a) one stopband filter with A = –40 dB and (b) four stopband filters each one with A = –10 dB (red spectrum).

5.4 Simulator Validation for a Single Interferer

In this subsection, we validate the implementation of the simulator for a single in-band crosstalk signal, which corresponds to study the performance of the optical communication network considering that the interference is caused by an imperfect 2×1 WSS before the coherent detection. For studying this scenario, we consider the parameters shown in table 5.2 and the simulation model depicted in figure 5.10. This model considers a 2×1 WSS, where one of the inputs is the primary signal $S_{in}(f)$, that passes through a passband filter $H_p(f)$, and the other input is the in-band crosstalk signal $X_1(f)$, that passes through a stopband filter $H_b(f)$. The output signal of the WSS is the signal $S_0(f)$, which is impaired by the addition of ASE noise generated in an OA, which function is to compensate the losses inside the WSS and (de)multiplexer.

Initially, we simulated the path of the primary signal without the crosstalk impairment to find the reference OSNR, i.e., the OSNR required to reach the BER of 10^{-3} in presence of ASE noise only. Figure 5.11 depicts the BER as a function of the required OSNR for two modulation formats: QPSK (blue line) and 16-QAM (red line) for a baud rate of 25 Gbaud. The BER is estimated between 10^{-2} and 10^{-4}, and the required OSNR obtained for a BER of 10^{-3}, i.e., the reference OSNR is 10.3 dB, for QPSK and 15.9 dB, for 16-QAM.

Table 5.2 - Parameters used in the simulator validation.

Signals modulation format	QPSK	16-QAM
Transmitted signal power	1 mW	
Baud rate	25 Gbaud	
Bit rate	50-Gb/s (per polarization)	100-Gb/s (per polarization)
B_0 of passband filter	41 GHz	
B_0 of stopband filter	~ 48 GHz	
Blocking amplitude	[–27.5, –7.5] dB	[–27.5, –12.5] dB
Target BER	10^{-3}	
N_s	256	512
N_a	64	
MC stopping criteria	1000 counted errors	

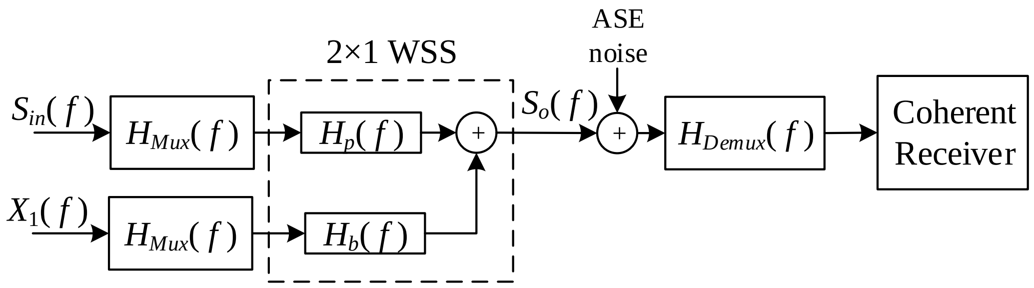

Figure 5.10 - Simulation model of the optical network considering one 2×1 WSS.

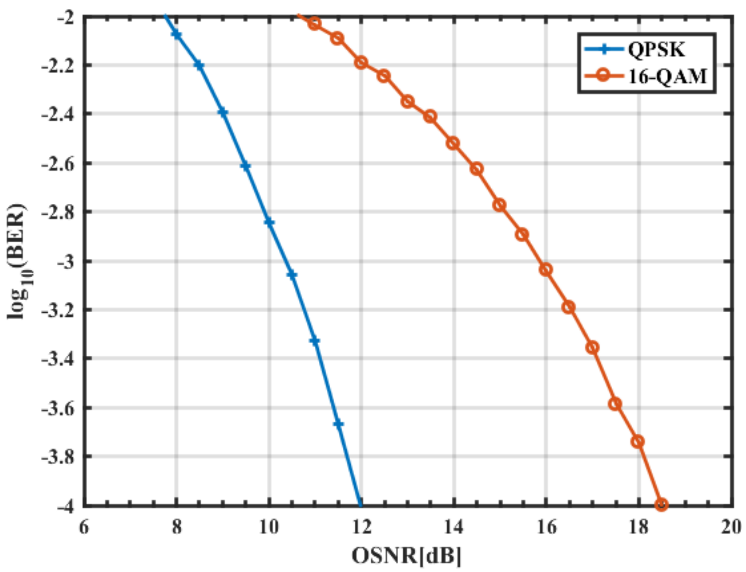

Figure 5.11 - BER as a function of the required OSNR for a 25 Gbaud NRZ QPSK (blue line) and 16-QAM (red line) signal using the simulation model presented in figure 5.10 without the crosstalk impairment.

After obtaining the reference OSNR, the OSNR penalty due to the in-band crosstalk is estimated for the optical network presented in figure 5.10. In this type of networks, we only have one interfering signal. The total crosstalk level, X_c, is defined by [8]

$$X_c = \frac{P_x}{P_0} \tag{5.13}$$

where P_x is the average power of the interfering signal after the blocking filter and P_0 is the average power of the filtered primary signal. In the case of multiple interferers, the power P_x represents the total power of all crosstalk signals that impair the primary signal [8]. In this simulation model, the crosstalk level X_c is mainly defined by the blocking amplitude of the stopband filter. For example, for one in-band crosstalk signal with 0 dBm of average power, after one stopband filter with A = –30 dB, the power P_x is approximately equal to –30 dBm as can be viewed in figure 5.8 (a) and, consequently, X_c is approximately –30 dB.

Throughout this work, we assume always that the crosstalk signals have the same characteristics as the primary signal: same modulation format, baud rate and OSNR level, but with different arbitrary transmitted symbols, different phases and a time misalignment between the two signals. In a real scenario, the crosstalk signals can have mixed modulation formats, baud rates, OSNR levels, etc. [8]. Furthermore, in a real scenario, the WSSs filter shapes, both passband and stopband, can change in each component that the signal passes along the optical network. In this study, we assume that the WSSs inside the ROADMs are equal, i.e., the passband and stopband filters are equal in all network nodes.

Figure 5.12 depicts the BER as a function of the required OSNR for (a) QPSK and (b) 16-QAM signals impaired by one in-band crosstalk signal, considering stopband filters with blocking amplitudes set to –30, –20 and –10 dB. The OSNR penalty due the in-band crosstalk can be estimated from the results plotted in figure 5.12. It corresponds to the difference between the OSNR required to reach a target BER of 10^{-3}, with and without crosstalk. For example, in figure 5.12 (a), for a BER of 10^{-3} and A = –20 dB (yellow line), the OSNR penalty due to the in-band crosstalk, represented as δ_{XT}, is approximately 0.4 dB. For a blocking amplitude of –10 dB, the OSNR penalty is approximately 3.3 dB.

From figure 5.12, we also conclude that for a stopband filter with a blocking amplitude of –30 dB (orange line), the OSNR penalty is low. For a blocking amplitude of –10 dB and a 16-QAM modulation format (purple line in figure 5.12 (b)), the system cannot reach a BER of 10^{-3}, stabilizing in a BER of approximately $10^{-2.1}$. This is called a BER floor. Hence, we can conclude that the 16-QAM modulation format is less tolerant to in-band crosstalk than the QPSK, as previously reported in the literature [13].

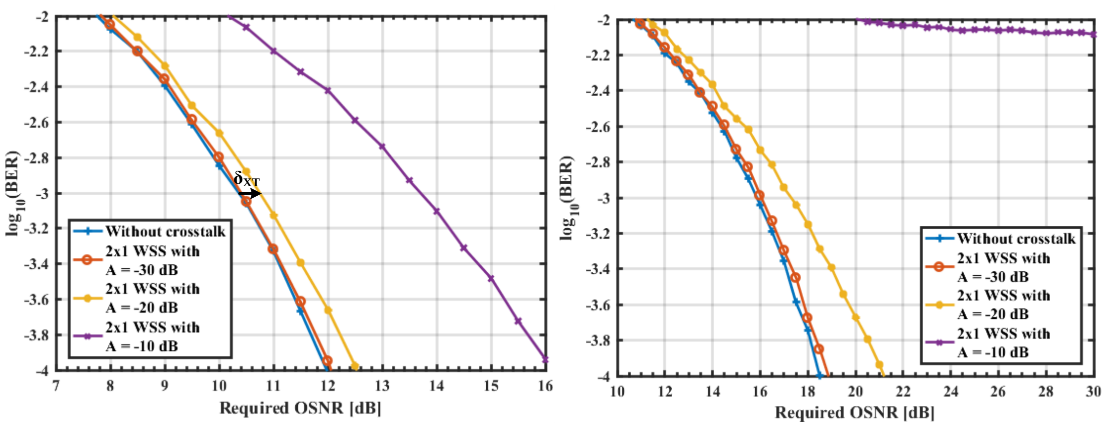

(a) **(b)**

Figure 5.12 - BER as a function of the required OSNR for one 2×1 WSS with different blocking amplitudes, for 25 Gbaud NRZ (a) QPSK and (b) 16-QAM signals.

Figure 5.13 depicts the OSNR penalty as a function of the crosstalk level, X_c, for a single in-band interferer for QPSK (blue line) and 16-QAM (red line) modulation formats. The crosstalk level was obtained by varying the blocking amplitude of the stopband filter between [–27.5, –7.5] dB for QPSK and [–27.5, –12.5] dB for 16-QAM. Similar results of OSNR penalty have been found in the works [13], for both modulation formats, and [14], for the QPSK modulation format. The crosstalk levels associated with a 1 dB OSNR penalty are –15.3 dB, for QPSK, and –20.6 dB, for 16-QAM. For example, for a crosstalk level of –20 dB, the OSNR penalty is 0.4 dB, for the QPSK modulation format, while it is 1.25 dB for the 16-QAM modulation format. Due to the agreement of our results with the results presented in [13], [14], we can consider that our simulator is validated for the case of a single interferer.

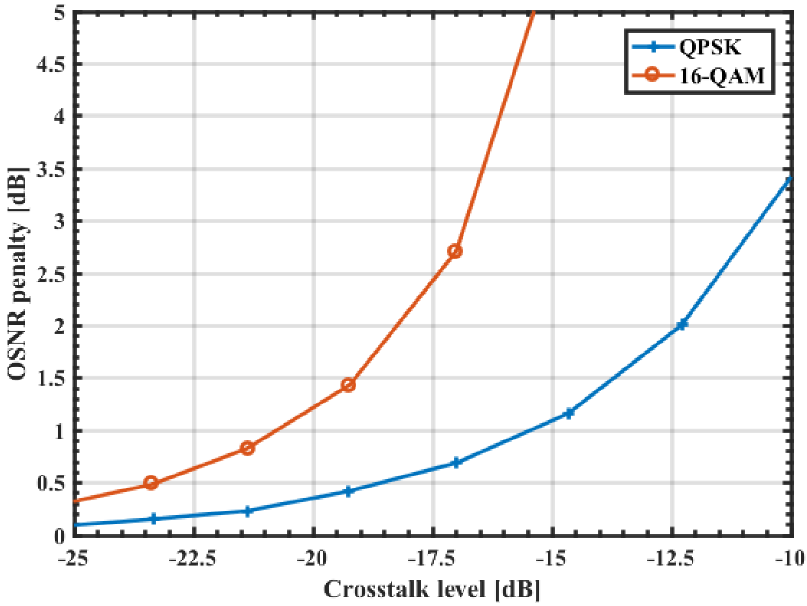

Figure 5.13 - OSNR penalty as a function of the crosstalk level for a single in-band crosstalk signal for QPSK (blue line) and 16-QAM (red line) modulation formats with a symbol rate of 25 Gbaud.

5.5 Add/Drop Structures Modeling in CDC ROADMs

After studying the impact of in-band crosstalk considering a single interferer and with the simulator validated in the previous section, we will in this section study the impact of the add/drop structures implemented with MCSs or $N\times M$ WSSs (several interferers) on the crosstalk level considering only one ROADM.

The simulation model for the add/drop structure with MCSs is depicted in figure 5.14. In this case, there is only one filtering stage. When the add/drop ROADM structure is implemented with $N\times M$ WSSs, the model assumes that the signals pass through two filtering stages, as illustrated in figure 5.15.

For this study, we consider add/drop structures with 2, 4, 8 and 16 inputs. In these types of structures, 1, 3, 7 and 15 in-band crosstalk signals can, respectively, arise. As previously stated, inside the add/drop structures, the primary signal passes through an optical passband filter and the interfering signals through optical stopband filters. After that, all signals are added and originate the output signal denominated $S_0(f)$. This output signal, plus the ASE noise originated in an OA, passes through the optical demultiplexer and is detected by the coherent receiver.

The crosstalk level generated in both models is shown in figure 5.16 as a function of the number of add/drop structure inputs, for the blocking amplitudes: –20, –30, –40 and –50 dB, considering a 50-Gb/s NRZ QPSK primary signal impaired by interferers with identical characteristics. From this figure, we can conclude that with an add/drop structure implemented with *N*×*M* WSSs, the total crosstalk level generated is low (below –20 dB). In the worst case, i.e., with a blocking amplitude of –20 dB and 16 inputs (dashed blue line), we estimate a crosstalk level of –23.5 dB. For the same case, but with add/drop structures implemented with MCSs (blue line), the total crosstalk level is –7 dB. It corresponds to a difference of 16.5 dB in terms of the crosstalk level. So, we conclude that, for add/drop structures implemented with MCSs, the total crosstalk level generated inside of them is much higher than for structures based on *N*×*M* WSSs.

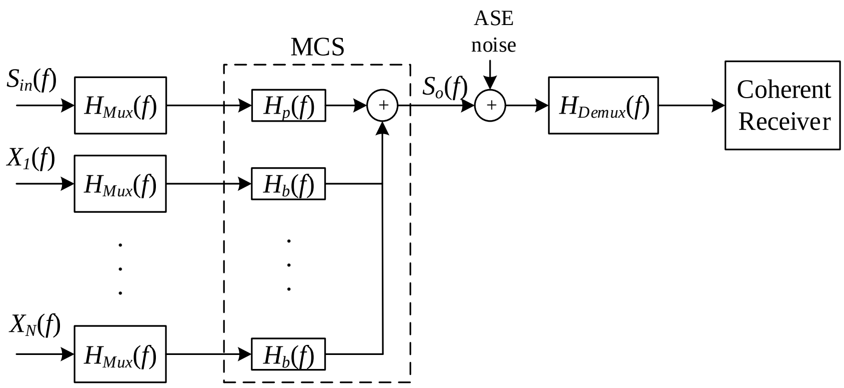

Figure 5.14 - Simulation model of an add/drop structure based on MCS.

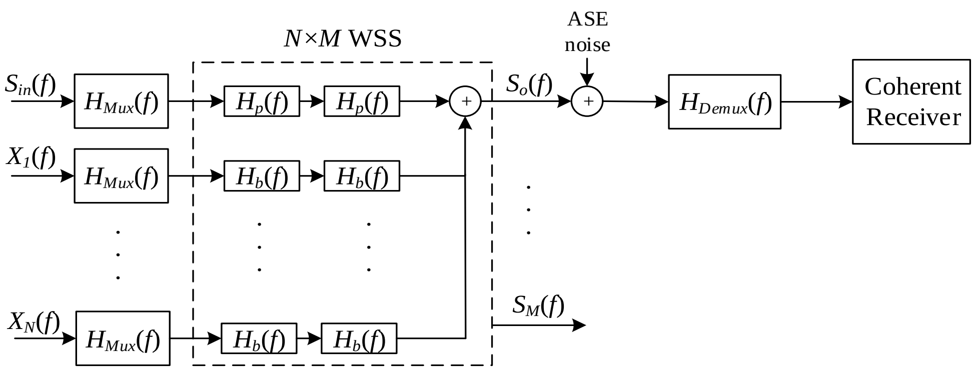

Figure 5.15 - Simulation model of an add/drop structure based on *N*×*M* WSS.

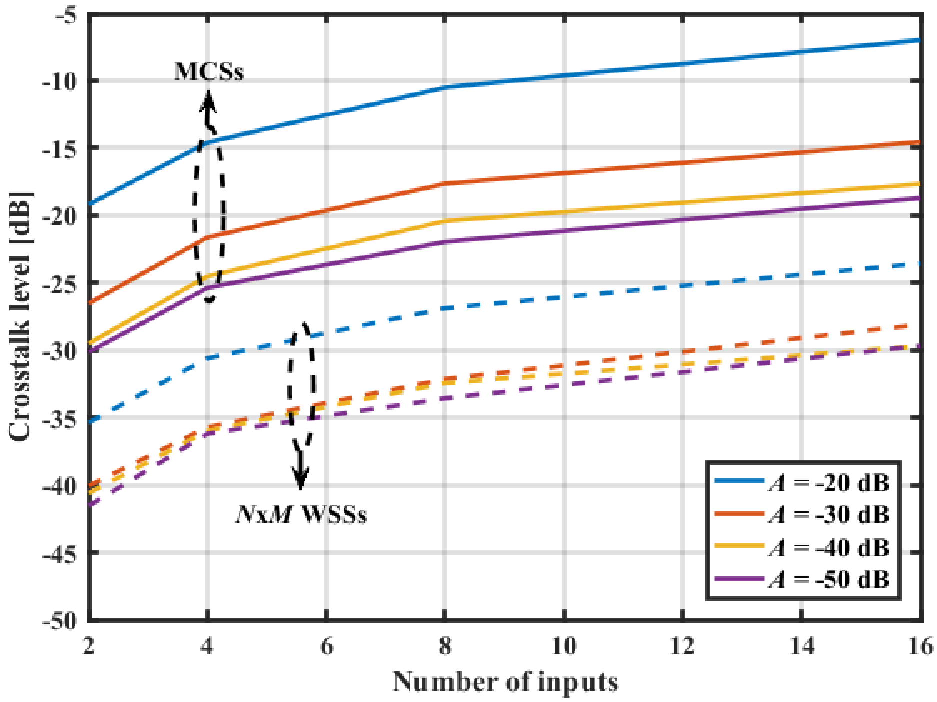

Figure 5.16 - Crosstalk level as a function of the number of inputs for –20 dB, –30 dB, –40 dB and –50 dB blocking amplitudes considering the add/drop structures based on MCSs or N×M WSSs.

5.6 Impact of In-Band Crosstalk, Optical Filtering and ASE Noise in a Multi-Degree CDC ROADMs Cascade

In this section, the impact of in-band crosstalk, optical filtering and ASE noise in a cascade of multi-degree CDC ROADMs based on the R&S architecture with add/drop structures implemented with N×M WSS and MCSs is studied. The main goal of this study is to discover the maximum number of ROADMs nodes that one optical signal can pass until the degradation on the optical network performance caused by these physical impairments is considerable.

For this study, we consider 2, 4, 8 and 16 ROADM degrees and a maximum number of network nodes of 32. Nowadays, the common ROADM degree is 8 [2] and the optical signal can transit through 24 or more nodes in a typical network [15]. We vary the blocking amplitudes of the stopband filters, that model the WSSs or the MCSs inside of the ROADMs nodes.

5.6.1 Impact of Optical Filtering and In-Band Crosstalk on a ROADM Cascade with Only One Amplification Stage

In this subsection, in order to analyze the impact of the optical filtering and in-band crosstalk in our network model, we consider the simulation model with only one amplification stage, i.e., one addition of ASE noise, at the end of the ROADMs cascade to set the OSNR level. We start this analysis by considering only the effect of optical filtering with no crosstalk in the system. Figure 5.17 shows the simulation model used in this study and table 5.3 the parameters used in the MC simulator.

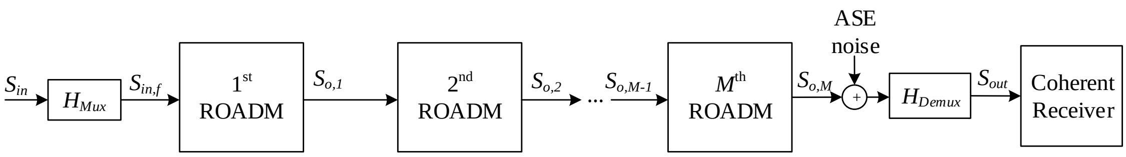

Figure 5.17 - Simulation model to study the optical filtering effect on an optical network composed by *M* cascaded ROADMs.

Table 5.3 - Parameters used in the simulator to study the physical impairments.

Signals modulation format	QPSK
Transmitted Signal power	1 mW
Baud rate	25 Gbaud
Bit rate	50-Gb/s (per polarization)
B_0 of passband filter	41 GHz
B_0 of stopband filter	~ 48 GHz
Blocking amplitudes	[–50, –40, –30, –20] dB
Number of ROADMs	[2, 4, 8, 16, 32]
Degree of ROADMs	[2, 4, 8, 16]
Target BER	10^{-3}
N_s	256
N_a	64
MC stopping criteria	1000 counted errors

In this case, the primary signal S_{in} passes through 2 to M^{th} ROADMs nodes and, for each case, we estimate the OSNR required to reach the target BER of 10^{-3} and assess the OSNR penalty due to the optical filtering that the primary signal suffers until it reaches the final ROADM. In the simplest case, the primary signal passes through two nodes, it is added on the first ROADM and dropped in the second ROADM node.

Figure 5.18 depicts the BER as a function of the required OSNR for a signal that passes through 2, 4, 8, 16 and 32 nodes. The OSNR difference between the case when the primary signal passes 2 nodes, our reference case, and the other cases, represents the penalty due to the optical filtering. This penalty is represented in figure 5.18 by δ_F, for the case of 32 nodes and is about 1.2 dB, which is in accordance with the results presented in subsection 5.3.1. Table 5.4 shows the OSNR required to reach a BER of 10^{-3} and the corresponding OSNR penalties estimated for the different number of ROADMs nodes.

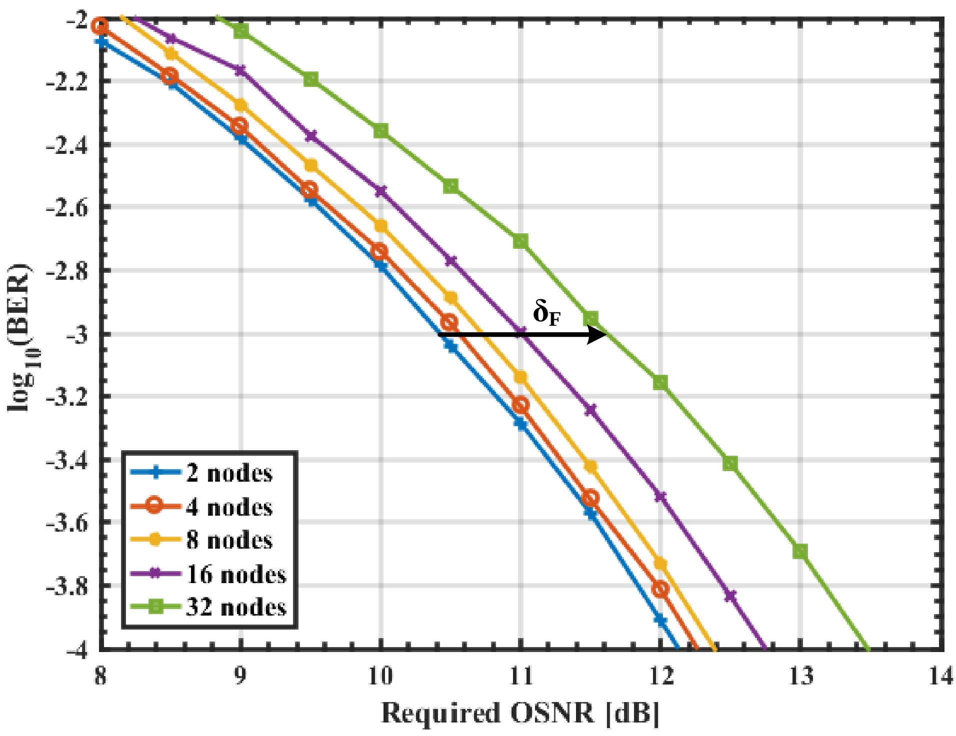

Figure 5.18 - BER as a function of the required OSNR for a 50-Gb/s NRZ QPSK signal that passes through a cascade of several ROADMs nodes.

Table 5.4 - OSNR required for a BER = 10^{-3} and the respective OSNR penalty due to the optical filtering inside the ROADMs nodes.

Number of ROADMs	OSNR for a BER = 10^{-3} [dB]	OSNR penalty [dB]
2	10.4	0
4	10.5	0.1
8	10.7	0.3
16	11	0.6
32	11.6	1.2

Now, after having evaluated the optical filtering penalty and the OSNR to reach a BER of 10^{-3} without the crosstalk impairment, we can add the in-band crosstalk signals, and estimate the OSNR penalty due to in-band crosstalk in the case of a network composed by several ROADMs. For this study, we use the model depicted in figure 5.19. As we can observe from this figure, the interfering signals arise from the ROADM inputs and from the add structure of the ROADMs represented, respectively, by $X_{m,in}$ and $X_{m,add}$, and depend on the ROADM degree as shown analytically in section 5.2 (see figure 5.2 and corresponding conclusions). The add/drop structures can be implemented with MCSs or $N \times M$ WSSs. We start by investigating the total crosstalk level imposed for both add/drop structures.

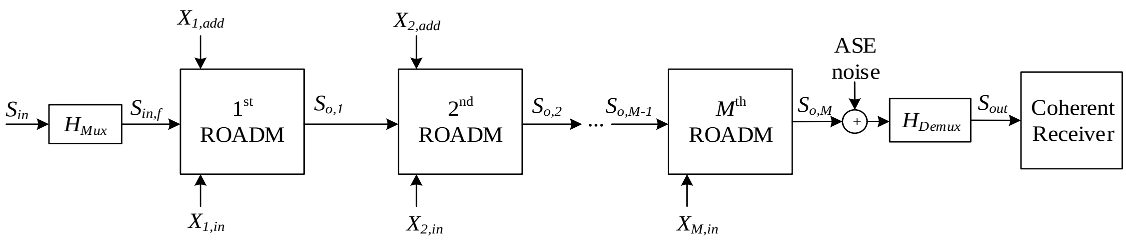

Figure 5.19 - Simulation model of an optical network composed by M ROADMs impaired by ASE noise and in-band crosstalk.

Figure 5.20 depicts the total crosstalk level as a function of the number of ROADMs nodes with add/drop structures implemented with MCSs and for the blocking amplitudes of −30 dB, figure 5.20 (a), and −20 dB, figure 5.20 (b). Figure 5.21 exhibits the same study, but with the add/drop structures implemented with $N \times M$ WSSs, for the blocking amplitudes of −30 dB, in figure 5.21 (a), and of −20 dB, in figure 5.21 (b).

Notice that from figures 5.20 and 5.21, as expected the crosstalk level increases with the increase of the ROADMs degree. For an optical network based on 2-degree ROADMs in both implementations of add/drop structures and also for both blocking amplitudes studied, the crosstalk level is practically constant along the network nodes. It is because in these type of networks, in the first ROADM node, the number of interfering signals is higher than in the other nodes, where the signal is expressed or dropped.

For a blocking amplitude of –30 dB, either with add/drop structures implemented with MCSs or $N\times M$ WSSs, the crosstalk level does not increase with the increase of the number of ROADMs nodes due to the good filtering isolation. In ROADMs with add/drop structures based on MCSs, the crosstalk level even decreases at the first node, since in this implementation, the interfering signals generated in the add section, when the primary signal is added, only pass through one stopband filter. In the remaining express network nodes, the interfering signals that are generated are blocked at least two times.

Another interesting feature about the crosstalk level, for a blocking amplitude of –30 dB, especially when the add/drop structures are implemented with $N\times M$ WSSs, see figure 5.21 (a), is that in the last ROADM node, the crosstalk level decreases. This is because the interfering signals are blocked once in the ROADM inputs and twice in the drop structures, as can also be concluded from Equation 5.10.

Regarding a blocking amplitude of –20 dB, we can observe in figures 5.20 (b) and 5.21 (b), a higher crosstalk level when the add/drop structures are implemented with MCSs due to the smaller optical stopband filtering cascading. In both cases of the add/drop structures, the crosstalk level grows almost linearly with the number of ROADM nodes, except for the case of a network composed by 2-degree ROADMs.

Table 5.5 shows the crosstalk level estimated at the end of the 32 ROADMs nodes, with add/drop structures implemented with MCSs and $N\times M$ WSSs and for the blocking amplitudes of –30 dB and –20 dB. As we can observe in table 5.5, the crosstalk level generated with a blocking amplitude of –30 dB, for a network based on 16-degree ROADMs with 32 nodes and for both add/drop structures implementations, is considerably low (–17.2 and –29.4 dB). This means that, in these cases, the in-band crosstalk will practically not lead to the network performance degradation. When we decrease the blocking amplitude of the stopband filters (–40 dB and –50 dB), the total crosstalk level will be even smaller.

For a blocking amplitude of –20 dB, the total crosstalk levels obtained are significantly high at the end of the network with 32 ROADM nodes. For example, in a network composed by 32 16-degree CDC ROADMs nodes, the crosstalk level is –5.2 dB, for add/drop structures based on MCSs, and –13.4 dB, for add/drop structures based on *N*×*M* WSSs.

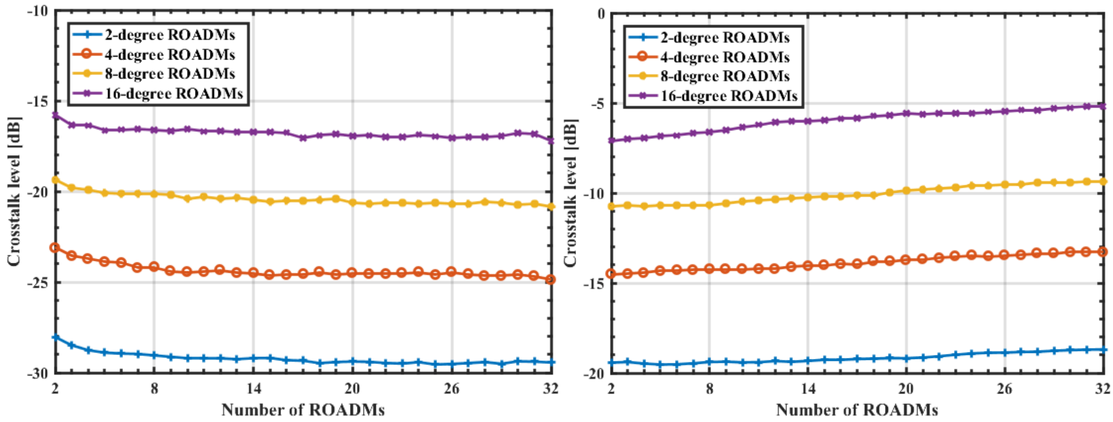

(a) **(b)**

Figure 5.20 - Crosstalk level as a function of the number of ROADM nodes, for a 50-Gb/s NRZ QPSK signal and add/drop structures implemented with MCSs, for stopband filters with blocking amplitudes of (a) –30 dB and (b) –20 dB.

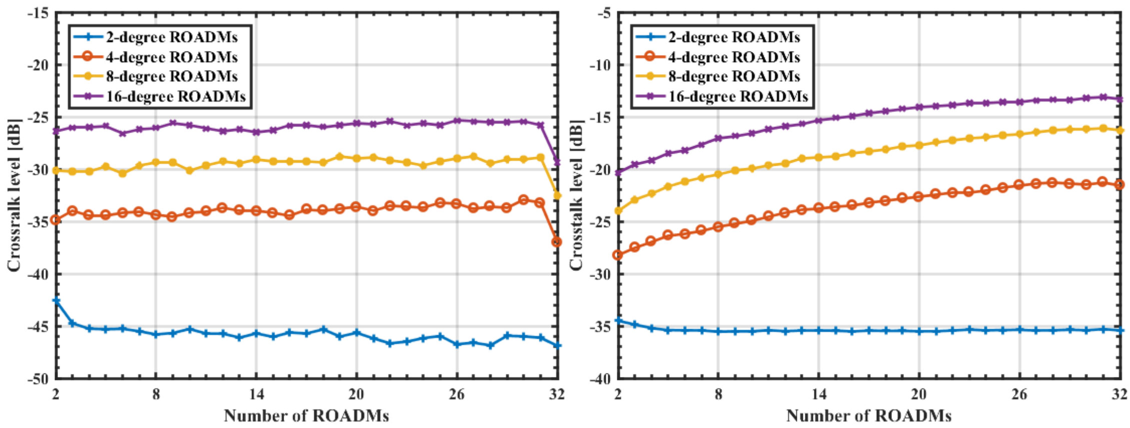

(a) **(b)**

Figure 5.21 - Crosstalk level as a function of the number of ROADM nodes, for a 50-Gb/s NRZ QPSK signal and add/drop structures implemented with *N*×*M* WSSs, for stopband filters with blocking amplitudes of (a) –30 dB and (b) –20 dB.

Table 5.5 - Crosstalk level at the end of an optical network with 32 CDC ROADMs.

	Crosstalk level [dB]			
	A = –30 dB		A = –20 dB	
ROADM degree	MCSs	*N*×*M* WSSs	MCSs	*N*×*M* WSSs
2-degree	–29.4	–46.9	–18.7	–35.4
4-degree	–24.9	–37.0	–13.3	–21.6
8-degree	–20.8	–32.6	–9.4	–16.3
16-degree	–17.2	–29.4	–5.2	–13.4

After studying the crosstalk level evolution along optical networks based on CDC ROADMs nodes, we investigate the OSNR penalty at a BER of 10^{-3} due to in-band crosstalk signals on those networks.

Figure 5.22 depicts the OSNR penalty as a function of the number of ROADMs nodes for a blocking amplitude of –20 dB and add/drop structures implemented with (a) MCSs or (b) $N\times M$ WSSs. As we can observe from this figure, when the add/drop structures are implemented with MCSs, the OSNR penalty is greater than when they are implemented with $N\times M$ WSSs. As previously analyzed in figures 5.20 and 5.21, the total crosstalk level generated in networks with ROADMs nodes with add/drop structures based on MCSs is much higher. For 16-degree ROADMs and add/drop structures implemented with MCSs, the OSNR penalty is greater than 5 dB, and is not represented in figure 5.22 (a). Note that with add/drop structures implemented with MCSs and 4-degree nodes, the OSNR penalty after the signal passes through only two nodes is 1.3 dB, higher than at the end of 32 ROADMs with 2, 4 and 8-degree with add/drop structures implemented with $N\times M$ WSSs.

When we have add/drop structures implemented with $N\times M$ WSSs, the number of ROADMs associated with a 1 dB OSNR penalty is 15 for 16-degree ROADMs and 28 for 8-degree ROADMs. The 2 and 4-degree ROADMs provide penalties below 0.5 dB at the end of 32 nodes. As an example of the improvement achieved using $N\times M$ WSSs in the add/drop structures of a CDC ROADM considering the following scenarios: at the end of an optical network with 32 4-degree CDC ROADMs nodes (red curve in figure 5.22) with add/drop structures based on MCSs, the OSNR penalty due to the in-band crosstalk is 3 dB, while if the add/drop structure is implemented with $N\times M$ WSSs, the OSNR penalty is 0.4 dB. There is an OSNR improvement of 2.6 dB.

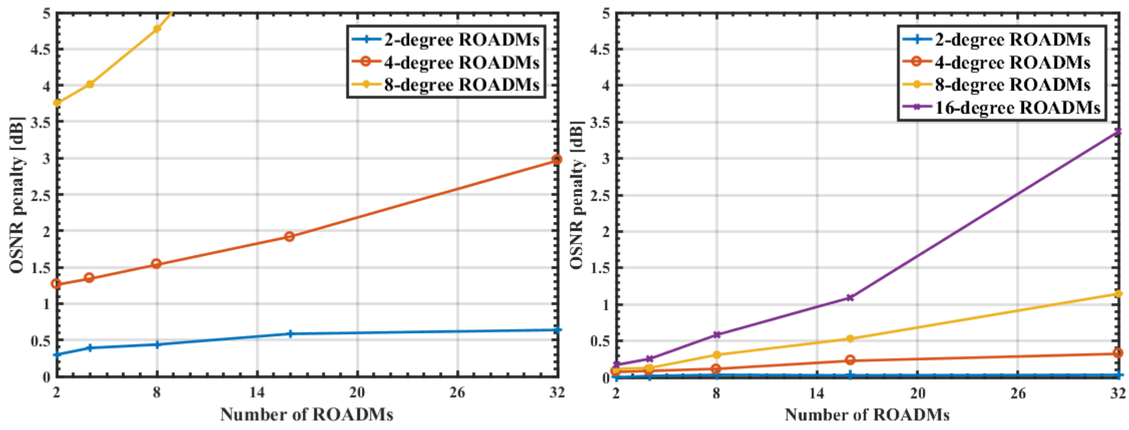

(a) **(b)**

Figure 5.22 - OSNR penalty as a function of the number of ROADMs nodes, for several ROADMs degrees, for a blocking amplitude of −20 dB and with the add/drop structures implemented with (a) MCSs or (b) $N \times M$ WSSs.

5.6.2 Impact of ASE Noise and In-Band Crosstalk on a ROADM Cascade with Amplification Stages at ROADM Inputs and Outputs

In this subsection, we analyze the impact of the ASE noise and in-band crosstalk on a network composed by a cascade of ROADMs in a more realistic scenario. In such scenario, there are optical amplifications stages at the inputs of the ROADMs to compensate for the path losses, and at the ROADMs outputs to compensate the losses inside the ROADMs nodes. Figure 5.23 shows the simulation model used for this study, similar to the one illustrated in figure 5.2, but considering amplification at the ROADMs inputs and outputs. For this study, we use the same simulation parameters presented in table 5.3.

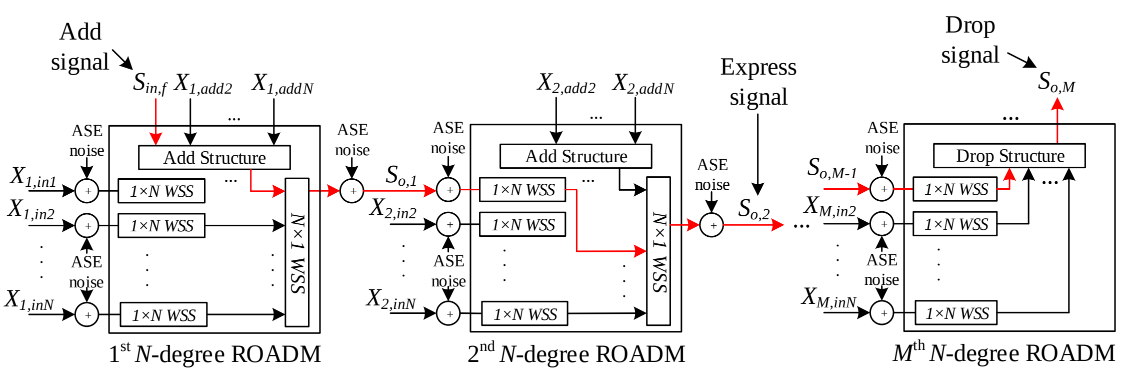

Figure 5.23 - Simulation model of a cascade of M multi-degree CDC ROADMs based on the R&S architecture with the in-band crosstalk signals generation and the ASE noise addition.

Figure 5.24 depicts the BER as a function of the required OSNR to reach a BER of 10^{-3}, without in-band crosstalk, for several ROADMs nodes and degrees. From figure 5.24, we conclude that the amplification, simulated by the addition of ASE noise in every ROADMs inputs and outputs, has a great impact in the network performance in terms of the required OSNR. For example, the difference of the required OSNR for 2 and 32 ROADMs with 8-degree (yellow curve) is about 9.5 dB.

Note that this required OSNR is measured at the output of each OA. Remark that in subsection 5.6.1, the required OSNR only changed with the number of ROADMs nodes due to the impact of the optical filtering. In the simulation model used in this subsection, the required OSNR changes with the number of ROADMs nodes and their respective degree due to the ASE noise accumulation. This leads to higher OSNRs requirements than the ones shown in figure 5.18.

Figure 5.25 depicts the OSNR penalty as a function of the number of ROADMs nodes for a stopband filter with blocking amplitude of −20 dB and add/drop structures implemented with (a) MCSs or (b) $N\times M$ WSSs in a network based on the simulation model depicted in figure 5.23. In this case, the total crosstalk level generated in the network is the same as the one studied in subsection 5.6.1, since the number of in-band crosstalk signals generated along the optical network and the filter blocking amplitudes are the same.

However, by comparison of figures 5.22 and 5.25, the OSNR penalty due to the in-band crosstalk obtained in this case is lower than the penalty previously obtained. For example, in the previous study, the number of CDC ROADMs implemented with $N\times M$ WSSs, that can be reached associated with the 1 dB OSNR penalty is 15, for 16-degree ROADMs, and 28, for 8-degree ROADM. In this subsection, figure 5.24 shows that, for 16-degree ROADMs, the number of nodes reached is 19 nodes and, for 8-degree ROADMs, the 1 dB OSNR penalty is not reached at the end of 32 nodes. This latter conclusion holds also for ROADMs based on MCSs, as can be observed by comparing figures 5.22 (a) and 5.24 (a).

Note that in [8], the OSNR penalty of 1 dB at BER of 10^{-3} due to in-band crosstalk in a cascade of WSSs, for QPSK modulation format, are also significantly low, less than 1 dB for a cascade of 30 WSSs with blocking amplitude of −35 dB.

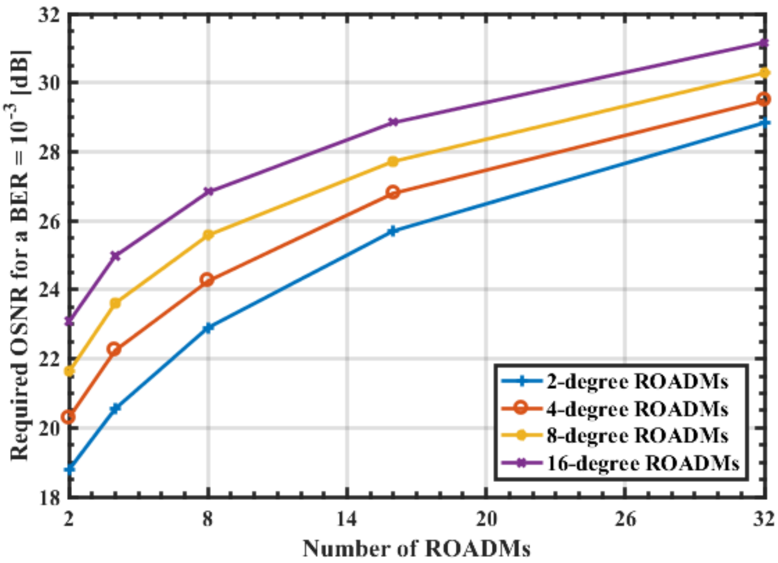

Figure 5.24 - Required OSNR as a function of the number of ROADMs for the degrees: 2, 4, 8 and 16, for a network without in-band crosstalk.

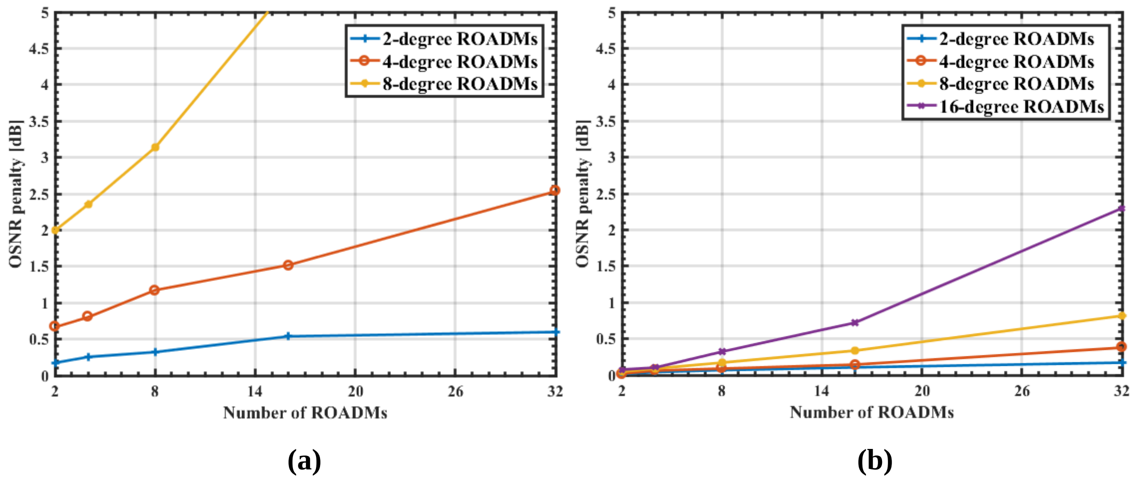

Figure 5.25 - OSNR penalty as a function of the number of ROADMs nodes for a blocking amplitude of –20 dB and with add/drop structures implemented with (a) MCSs or (b) *N*×*M* WSSs in a network with amplification at ROADMs inputs and outputs.

Remember that, in this network, the increase of the number of ROADMs, besides leading to a higher number of interferers, also leads to a substantial increase of the required OSNR due to the higher ASE noise power at the nodes inputs and outputs. To prove that the ASE noise has the highest contribution to the network performance degradation, we plot the signal power evolution as a function of the number of 16-degree ROADMs nodes, for three cases: only the signal, the signal plus the ASE noise and the signal plus ASE noise and in-band crosstalk. These results are plotted in figure 5.26, for add/drop structures implemented with MCSs in figure 5.25 (a) and with $N\times M$ WSSs in figure 5.25 (b), for the blocking amplitudes of –20 dB and –30 dB.

Figure 5.26 shows that, for A = –30 dB, the contribution of in-band crosstalk to the total signal power is practically negligible, and that is the reason why this case has not been studied in the previous figures of this subsection.

When the in-band crosstalk is relevant, for A = –20 dB, figure 5.26 shows that the ASE noise power is dominant on the total signal power over the in-band crosstalk power. Hence, the impact of crosstalk on the network performance degradation is reduced, as shown in figure 5.25, in comparison with the results presented in subsection 5.6.1. As expected, this impact is higher for add/drop structures implemented with MCSs, as shown in figure 5.26 (a).

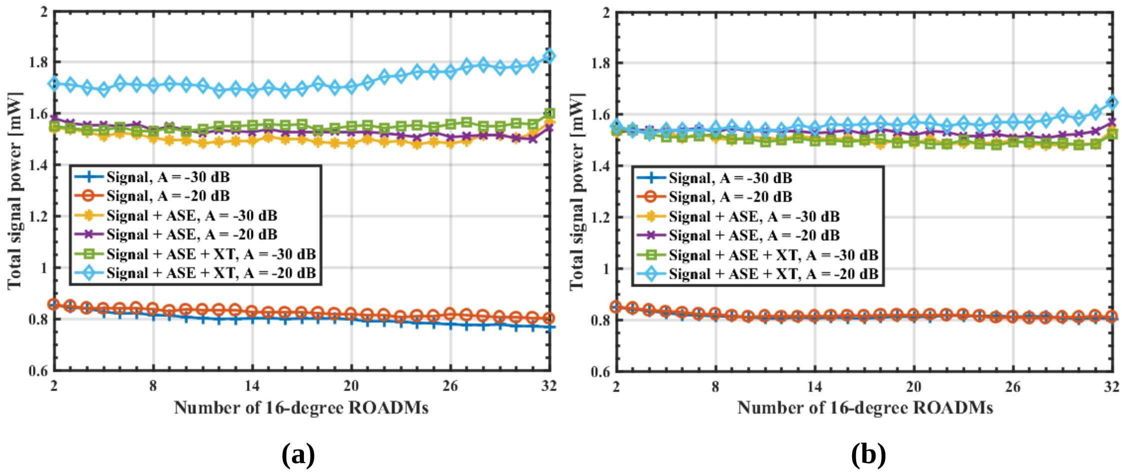

Figure 5.26 - Total signal power as a function of the number of 16-degree CDC ROADMs nodes with add/drop structures implemented with (a) MCSs or (b) $N\times M$ WSSs for the blocking amplitudes of –20 dB and –30 dB.

5.7 Conclusions

In this chapter, the impact of in-band crosstalk, ASE noise and optical filtering in the performance of an optical network with cascaded CDC ROADMs has been studied and analyzed. Firstly, we have described analytically the in-band crosstalk signals that are generated along the optical network with cascaded CDC ROADMS with add/drop structures based either on $N\times M$ WSSs or MCSs and the PSD of the signal at the output of the network has been derived.

The characteristics of the optical filters used to model the WSSs have been presented and discussed. The effect of the passband narrowing due to the filter cascading was studied, as well as the associated power penalty. A good agreement has been observed with the results shown in [11]. A study of the filtering cascading effect in the stopband filters has also been performed. We have concluded that, cascaded stopband filters remove the power at the signal band edges more efficiently than a single stopband filter.

The validation of the MC simulation model implemented in Matlab has been done for the case of a single interferer through modeling of a 2×1 WSS. This validation was done by comparing the OSNR penalties due to the in-band crosstalk obtained in our MC simulator with the results shown in [12] for the QPSK and 16-QAM modulation formats and in [13] for the QPSK modulation format.

The modeling of the add/drop structures in CDC ROADMs was presented and the total crosstalk level generated inside these structures was analyzed. The add/drop structures implemented with N×M WSSs generate a significantly lower crosstalk level than the structures implemented with MCSs. For the worst-case studied, components with 16 inputs and blocking amplitude of −20 dB, a crosstalk level of −23.5 dB, for N×M WSSs, and −7 dB, for MCSs, has been estimated.

Then, the performance of the optical network with one ASE noise addition at the network output was evaluated and was observed that the OSNR penalty due to the optical filtering at the end of 32 ROADMs nodes is 1.2 dB. In the presence of in-band crosstalk, for the blocking amplitudes of −50 dB, −40 dB and −30 dB, the OSNR penalty is very low. Only with a blocking amplitude of −20 dB, we can observe the network performance degradation. This degradation is higher in networks where the add/drop structures of CDC ROADMs are implemented with MCSs.

In a more realistic scenario, with amplification at every ROADM inputs and outputs, the system degradation becomes mainly influenced by to the ASE noise accumulated along the network nodes. In a network composed by 16-degree CDC ROADMs, where more ASE noise and in-band crosstalk are added to the primary signal at the network nodes, the total number of nodes that a signal can pass until the 1 dB OSNR penalty due to the in-band crosstalk is reached, with one amplification stage at the end of the network is 15 nodes, while with amplification at the ROADM inputs and outputs is 19 nodes. This is caused by the dominance of the accumulated ASE noise power over the in-band crosstalk power on the network performance degradation.

References

[1] B. Collings, "Advanced ROADM technologies and architectures," *2015 Optical Fiber Communications Conference and Exhibition (OFC)*, Los Angeles, CA, pp. 1-3, March 2015.
[2] J. Simmons, *Optical Network Design and Planning*, Springer, 2ª ed., 2014.
[3] N. Fontaine, R. Ryf and D. Neilson, "N×M wavelength selective crossconnect with flexible passbands," *2012 Optical Fiber Communication Conference and the National Fiber Optic Engineers Conference (OFC/NFOEC)*, Los Angeles, CA, pp. 1-3, March 2012
[4] H. Yang, B. Robertson, P. Wilkinson and D. Chu, "Low-cost CDC ROADM architecture based on stacked wavelength selective switches," in *IEEE/OSA Journal of Optical Communications and Networking*, vol. 9, no. 5, pp. 375-384, May 2017.
[5] W. Way, "Optimum architecture for M×N multicast switch-based colorless, directionless, contentionless, and flexible-grid ROADM," *2012 Conference on Optical Fiber Communication and the National Fiber Optic Engineers Conference (OFC/NFOEC)*, Los Angeles, CA, pp. 1-3, March 2012.
[6] F. Heismann, "System requirements for WSS filter shape in cascaded ROADM networks," *2010 Conference on Optical Fiber Communication and the National Fiber Optic Engineers Conference (OFC/NFOEC)*, San Diego, CA, pp. 1-3, March 2010.
[7] X. Zhou and C. Xie, *Enabling Technologies High Spectral-efficiency Coherent Optical Communication Networks*. New Jersey: John Wiley & Sons, 2016.
[8] M. Filer and S. Tibuleac, "Generalized weighted crosstalk for DWDM systems with cascaded wavelength-selective switches," *2012 Conference on Optical Fiber Communication and the National Fiber Optic Engineers Conference (OFC/NFOEC)*, Los Angeles, CA, pp. 1-3, March 2012.
[9] B. Pinheiro, J. Rebola and L. Cancela, "Impact of in-band crosstalk signals with different duty-cycles in M-QAM optical coherent receivers," *2015 20th European Conference on Networks and Optical Communications (NOC)*, London, pp. 1-6, July 2015.
[10] I. Monroy and E. Tangdiongga, *Crosstalk in WDM Communication Networks*. Norwell, MA: Springer, 2002
[11] Y. Hsueh *et al*., "Passband Narrowing and Crosstalk Impairments in ROADM-Enabled 100G DWDM Networks," in *Journal of Lightwave Technology*, vol. 30, no. 24, pp. 3980-3986, December 2012.
[12] T. Rahman *et al*., "On the Mitigation of Optical Filtering Penalties Originating From ROADM Cascade," in *IEEE Photonics Technology Letters*, vol. 26, no. 2, pp. 154-157, January 2014.
[13] P. Winzer, A. Gnauck, A. Konczykowska, F. Jorge and J. Dupuy, "Penalties from in-band crosstalk for advanced optical modulation formats," *2011 37th European Conference and Exhibition on Optical Communication (ECOC)*, Geneva, pp. 1-3, September 2011.
[14] L. Cancela, D. Sequeira, B. Pinheiro, J. Rebola and J. Pires, "Analytical tools for evaluating the impact of in-band crosstalk in DP-QPSK signals," *2016 21st European Conference on Networks and Optical Communications (NOC)*, Lisbon, pp. 6-11, June 2016.
[15] M. Filer and S. Tibuleac, "N-degree ROADM architecture comparison: Broadcast-and-select versus route-and-select in 120 Gb/s DP-QPSK transmission systems," *2014 Optical Fiber Communication Conference and Exhibitions (OFC)*, San Francisco, CA, pp. 1-3, March 2014.

Chapter 6

Conclusions and Future Work

In this chapter, the main conclusions of this dissertation are presented, as well as some suggestions for possible future work.

6.1 Final Conclusions

In this dissertation, the performance of an optical network based on multi-degree CDC ROADMs impaired by in-band crosstalk, ASE noise and optical filtering has been investigated considering QPSK signals.

In Chapter 2, the simulator model of the optical network used in the Matlab software has been described. Details regarding the optical components (transmitter, fiber, coherent receiver and amplifier) have been presented. Additionally, the MC simulator developed to assess the optical network performance impaired by in-band crosstalk and ASE noise has been described.

Chapter 3 was dedicated to the study of the ROADMs nodes evolution. The ROADMs characteristics, components, typical add/drop structures and advantages and disadvantages of the ROADMs architectures have been discussed. Regarding the ROADMs architectures, it has been concluded that the B&S architectures is the cheapest implementation, but is more vulnerable to crosstalk since the signal passes through less optical filtering than with a R&S architecture. The ROADMs add/drop structures have evolved from fixed and colored to CDC structures. This type of add/drop structures allows that any wavelength, arising from any ROADM degree can be routed in the CDC ROADM. To achieve this evolution, a key component has been the WSS as well as the new technology, LCoS.

In chapter 4, an investigation about the number of in-band crosstalk signals that is generated inside multi-degree C, CD and CDC ROADMs has been performed. Firstly, we have investigated the impact of in-band crosstalk in terms of the number of interferers in 3-degree ROADMs nodes based on B&S and R&S architectures. With this study, we concluded and demonstrated that the R&S architecture has a better performance in terms of in-band crosstalk generation, mainly because this architecture is based in WSSs. Then, we have increased the ROADM degree to investigate the same impact in 4-degree ROADMs and have generalized the conclusions regarding the in-band crosstalk impact for an arbitrary ROADM degree. We have concluded that, for CDC ROADMs with add/drop structures implemented with MCSs, the number of in-band crosstalk terms that appears at the outputs and drop ports is the same as in CD ROADMs. For a R&S architecture, we have concluded that N–1 first order and N–1 second order terms appear at the ROADMs outputs, and N–1 first order terms appear at the drop ports, of a N-degree ROADM. With the use of WSSs in the add/drop structures of a CDC ROADM based on a R&S architecture, the crosstalk robustness improves, since these in-band crosstalk terms are second order terms.

The study of the physical impairments in an optical network with cascaded CDC ROADMs based on the R&S architecture and add/drop structures implemented with MCSs and $N \times M$ WSSs has been investigated in chapter 5. The ROADMs with add/drop structures implemented with $N \times M$ WSSs, as the interfering signals pass through more filters, have a better performance than the structures implemented with MCSs in terms of blocking the interfering signals.

Next, the simulator validation was made in a scenario considering only a single interferer. The validation was made by comparison of the system performance degradation due to the in-band crosstalk, for QPSK and 16-QAM modulation formats, obtained with our simulator and with the results found in the literature. Then, we have investigated the total crosstalk level originated in add/drop structures implemented with MCSs and $N \times M$ WSSs. As expected, the crosstalk level increases with the increase of the number of structures inputs and for add/drop structures implemented with $N \times M$ WSSs, the total crosstalk level generated is lower than in structures based on MCSs.

Then, the degradation of the optical network performance due to the in-band crosstalk and filtering was investigated and our results have shown that for a BER = 10^{-3}, the OSNR penalty due to the optical filtering is 1.2 dB. Thus, the total crosstalk level originated in a network with cascaded multi-degree CDC ROADMs, for both add/drop structures implementations, and several blocking amplitudes has been investigated. With the blocking amplitudes of –50 dB, –40 dB and –30 dB, the crosstalk level originated is very low and, consequently, the OSNR penalty becomes negligible. With a blocking amplitude of –20 dB, the degradation is higher in a network where the add/drop structures of CDC

ROADMs are implemented with MCSs. For CDC ROADMs with add/drop structures based on $N \times M$ WSSs, the number of cascaded ROADMs nodes, that leads to a 1 dB OSNR penalty due to the in-band crosstalk is 28, for 8-degree ROADMs, and 15, for 16-degree ROADMs.

In a more realistic scenario, with amplification at the ROADMs inputs and outputs, the system degradation is principally due to the ASE noise accumulation, making the in-band crosstalk impact lower than in networks with one amplification stage. By comparing with the previous case study, for CDC ROADMs with add/drop structures based on $N \times M$ WSSs, the number of cascaded ROADMs nodes, for a 1 dB OSNR penalty degradation is 19 for 16-degree ROADMs, while previously it was 15 cascaded ROADMs. For 8-degree ROADMs, the OSNR penalty does not reach 1 dB at the end of a network composed by 32 nodes.

6.2 Future Work

For future investigation, we propose the following topics that were not addressed in this work:

- Analysis of the impact of in-band crosstalk in an optical network based on multi-degree CDC ROADMs nodes, where the interfering signals have different modulation formats than the primary signal;
- Study the impact of in-band crosstalk on the performance of optical networks considering a more realistic model for the WSSs;
- Investigation of the in-band crosstalk impact on the performance of an optical network with Nyquist pulse shaped signals;
- Study of the influence of the fiber effects in each links span in the results presented in this work;
- Study of the impact of the in-band crosstalk on CDC ROADMs-based flexible grid optical networks.